Synthesis of Redox-cycling Therapeutic Agents

by

Xiaoqing Cai

A Dissertation Presented in Partial Fulfillment
of the Requirements for the Degree
Doctor of Philosophy

Approved July 2011 by the
Graduate Supervisory Committee:

Sidney Hecht, Chair
Ian Gould
Hilairy Hartnett

ARIZONA STATE UNIVERSITY

August 2011

ABSTRACT

Cellular redox phenomena are essential for the life of organisms. Described here is a summary of the synthesis of a number of redox-cycling therapeutic agents. The work centers on the synthesis of antitumor antibiotic bleomycin congeners. In addition, the synthesis of pyridinol analogues of α-tocopherol is also described.

The bleomycins (BLMs) are a group of glycopeptide antibiotics that have been used clinically to treat several types of cancers. The antitumor activity of BLM is thought to be related to its degradation of DNA, and possibly RNA. Previous studies have indicated that the methylvalerate subunit of bleomycin plays an important role in facilitating DNA cleavage by bleomycin and deglycobleomycin. A series of methylvalerate analogues have been synthesized and incorporated into deglycobleomycin congeners by the use of solid-phase synthesis. All of the deglycobleomycin analogues were found to effect the relaxation of plasmid DNA. Those analogues having aromatic C4-substituents exhibited cleavage efficiency comparable to that of deglycoBLM A_5. Some, but not all, of the deglycoBLM analogues were also capable of mediating sequence-selective DNA cleavage.

The second project focused on the synthesis of bicyclic pyridinol analogues of α-tocopherol. Bicyclic pyridinol antioxidants have recently been reported to suppress the autoxidation of methyl linoleate more effectively than α-

tocopherol. However, the complexity of the synthetic routes has hampered their further development as therapeutic agents. Described herein is a concise synthesis of two bicyclic pridinol antioxidants and a facile approach to their derivatives with simple alkyl chains attached to the antioxidant core. These analogues were shown to retain biological activity and exhibit tocopherol-like behaviour.

ACKNOWLEDGMENTS

First and foremost, I would like to express my sincere gratitude to my advisor, Professor Sidney Hecht for his continuous support in my graduate research and study. I am very grateful for his unique "hands-off" training, which helps me to learn how to think and do research independently and creatively. In addition, his immense knowledge, strict attitude and enthusiasm in research have been of great value to me and will benefit me greatly during my career and life.

I would also like to thank my committee members, Professor Gould and Professor Hartnett for their time and support.

I also owe my gratidue to many talented chemists and biochemists in the Hecht laboratory. The thesis would not have been possible without their assistance. I would like to thank Dr. Jun Lu for helping me to get started when I first joined the group. I thank Dr. Yoshitsugu Akiyama for his assitance in my bleomycin project. I am grateful to Paul Zaleski and Dr. Omar Khdour for their assistance with the biological assays. I thank Ryan Nangreave for his patience and kindness whenever I need his help with my English. Warm thanks to all my other collegues, present and past, for helpful discussions, encouragment and friendship.

Last but not the least, especial thanks to my mother who always believes in me and encourages me to pursue my dream as a woman chemist. To her, I dedicate this thesis.

TABLE OF CONTENTS

LIST OF FIGURES

LIST OF SCHEMES

CHAPTER 1

INTRODUCTION

1.1 General introduction

1.1.1 Radicals and reactive oxygen species (ROS)

A radical is a species that possesses one or more unpaired electrons [1]. A molecule may lose or gain electrons singly or in pairs. One-electron transfer processes involve radicals. Two-electron transfers may involve either a simultaneous transfer of two electrons or two sequential one-electron transfers [2]. Both one-electron oxidations and one-electron reductions produce radicals [3]. Numerous oxydoreductases generate radicals as intermediates through their catalytic cycles, even though most biochemical oxidoreductions imply the exchange of two electrons [4].

Reactive oxygen species (ROS) include radicals, as well as other reactive singlet oxygen compounds [5]. The most important ROS are superoxide ($O_2^{\cdot -}$), hydroxyl radical (HO·), nitric oxide (NO·), and hydrogen peroxide (H_2O_2) [5,6]. The primary ROS formed *in vivo* are superoxide and hydrogen peroxide. Hydrogen peroxide is generated through nonenzymatic or enzymatic dismutation of superoxide [5]. However, the most reactive and harmful ROS is the hydroxyl radical, which can be formed from H_2O_2, but also via the reaction of superoxide with NO to produce peroxynitrite ($OONO^-$), the latter of which decomposes to form NO_2 and HO· (Figure 1.1) [7]. ROS play both harmful and beneficial roles

[9]. At low or moderate levels, ROS exert beneficial effects on cellular responses and immune functions; at high concentrations, they generate oxidative stress, a harmful process that can damage cell structures [10-20]. Oxidative stress plays a major part in the development of chronic and degenerative aliments such as cancer, arthritis, aging, autoimmune disorders, cardiovascular and neurodegenerative diseases [21-25].

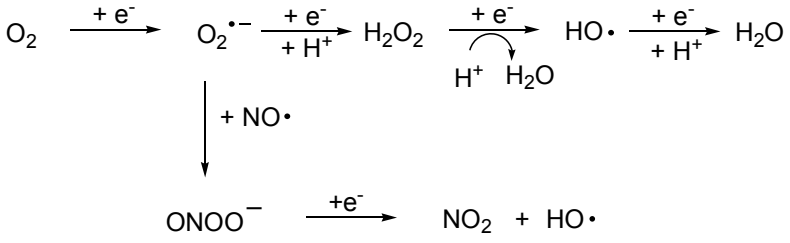

Figure 1.1. The formation of reactive oxygen species. (Modified from ref. 8)

1.1.2 Redox reactions in biological systems

Cellular redox phenomena are essential for the life of organisms. In biological systems, all processes that provide energy result from redox reactions [26,27]. Redox reactions are also important for intracellular radical production [28]. The major intracellular radical products are generated from the electron transport chain in mitochondria, endoplasmic reticulum and nuclear membrane(Figure 1.2) [29]. For instance, when cells use oxygen to generate energy, radicals are created as a by-product of ATP production by the mitochondria. Moreover, radicals are also

formed in endogenous and normal cell components, such as quinones (or precursors), flavins, organic thiols, orthocatechols, tetrahydrobiopterins and various other species [30]. The formed radicals can diffuse from the site of their production before their further oxidation or reduction

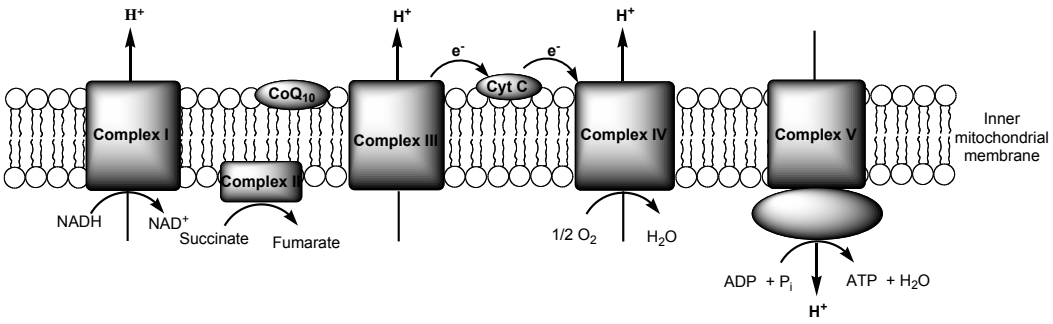

Figure 1.2. Mitochondrial electron transport chain.

to even-electron species. In addition, the metabolism of miscellaneous xenobiotics (drugs, phytochemicals, pollutants) also generates C, N, S, or O-centered radicals as a result of a one-electron exchange [30]. These organic radicals are likely to be rapidly reoxidized, and the ultimate product of such a one-electron chain reaction is superoxide anion ($O_2^{\cdot-}$). Finally, the redox reactions involving a metal complex (mainly iron, but also including copper, chromium, and vanadium) can also be important for radical production. Extensive evidence supports the idea that an iron ion can react with a peroxide, which can either be hydrogen peroxide or an organic hydroperoxide, to produce a HO· or RO· radical (Figure 1.3) [31-35].

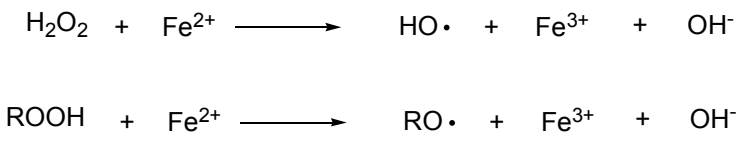

Figure 1.3. Metal-ion catalyzed redox decomposition of peroxides to produce radicals.

1.1.2 Redox cycling antitumor drugs

Extensive evidence supports the involvement of redox reactions and reactive oxygen species in the mechanism of many anticancer drugs. There are a number of antitumor drugs that are capable of redox cycling and can also interact directly with DNA. These interactions can involve noncovalent binding to the DNA minor groove, intercalation, alkylation, and DNA strand cleavage [36]. DNA is a polynucleotide that carries the genetic information, and thus is vital to the function of cells. Although DNA interactive agents are generally very toxic to normal cells as well as abnormal cells, some of them have been found to be effective against life-threatening diseases such as cancers.

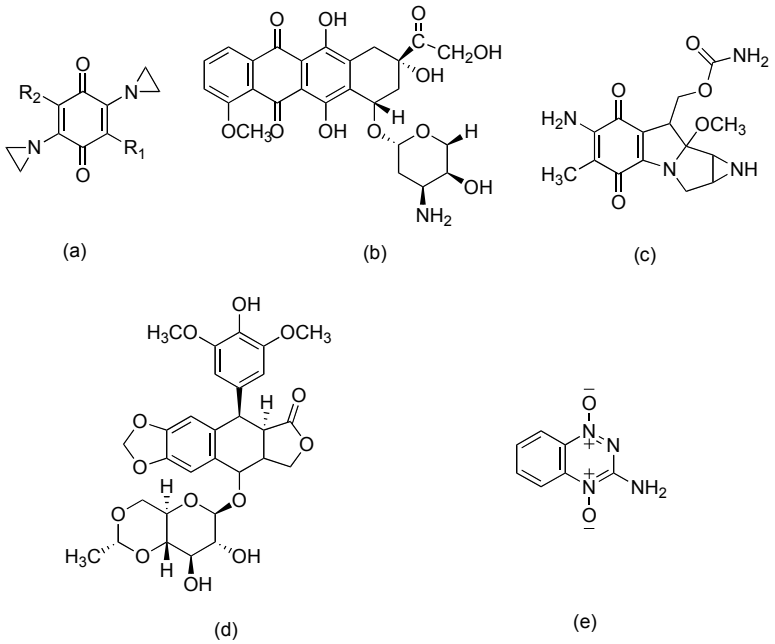

Figure 1.4. Structures of some redox cycling antitumor agents. (a) diaziridinylquinones, (b) adriamycin (doxorubicin), (c) mitomycin C, (d) etoposide, (e) tirapazamine.

Figure 1.4 shows several well known redox-cycling anticancer agents. There are many anticancer agents of this type containing quinones in their structures such as diaziridinylquinones (Figure 1.4a) and adriamycin (doxorubicin, Figure 1.4b). Figure 1.5 depicts the mechanism of action for quinone-containing antitumor agents. By virtue of their quinone structure, the antitumor agents can undergo a biochemical reduction by one or two electrons that is catalyzed by a flavoenzyme in the organism using NAD(P)H as the electron source [37]. Electrons are transferred from the NAD(P)H to the quinone of the antitumor agents leading to the formation of the semiquinone. The subsequent electron

transfer from the semiquinone to oxygen results in the production of superoxide. This redox cycle continues until the system becomes anaerobic. The formation of superoxide is the beginning of a cascade that generates H_2O_2, and subsequently hydroxyl radicals (HO·), which is the most reactive and harmful ROS (Figure 1.1). The reactive radicals generated can cause the oxidative cleavage of DNA backbone [38]. Doxorubicin (Figure 1.4a) belongs to the anthracyclines, a well-known class of DNA damaging agents. It is well established that this class of compounds possesses the capacity to undergo redox cycling with the generation of ROS [39]. The process is similar to that of diaziridinylquinones (Figure 1.5). However, other possibilities have also been proposed to account for the activity of doxorubicin and the mechanisms are still uncertain [40-43]. But it has been asserted that the redox-cycling process "is responsible for most if not all biological activity" [44].

Mitomycin C (Figure 1.4c) is the best known of all the aziridinylquinones and is a very potent DNA alkylating agent. Extensive research has been focused on its inter- and intra-strand cross-linking interaction with DNA [45-47]. Although redox cycling can participate and lead to ROS, it is generally claimed that this aspect exerts a minor influence on cancer cell lethality [48]. Etoposide (Figure 1.4d) is a semisynthetic analogue of the antitumor antibiotic podophyllotoxin. Etoposide can be metabolically activated by oxidation and demethylation to an *o*-quinone derivative [49]. Evidence supports the involvement

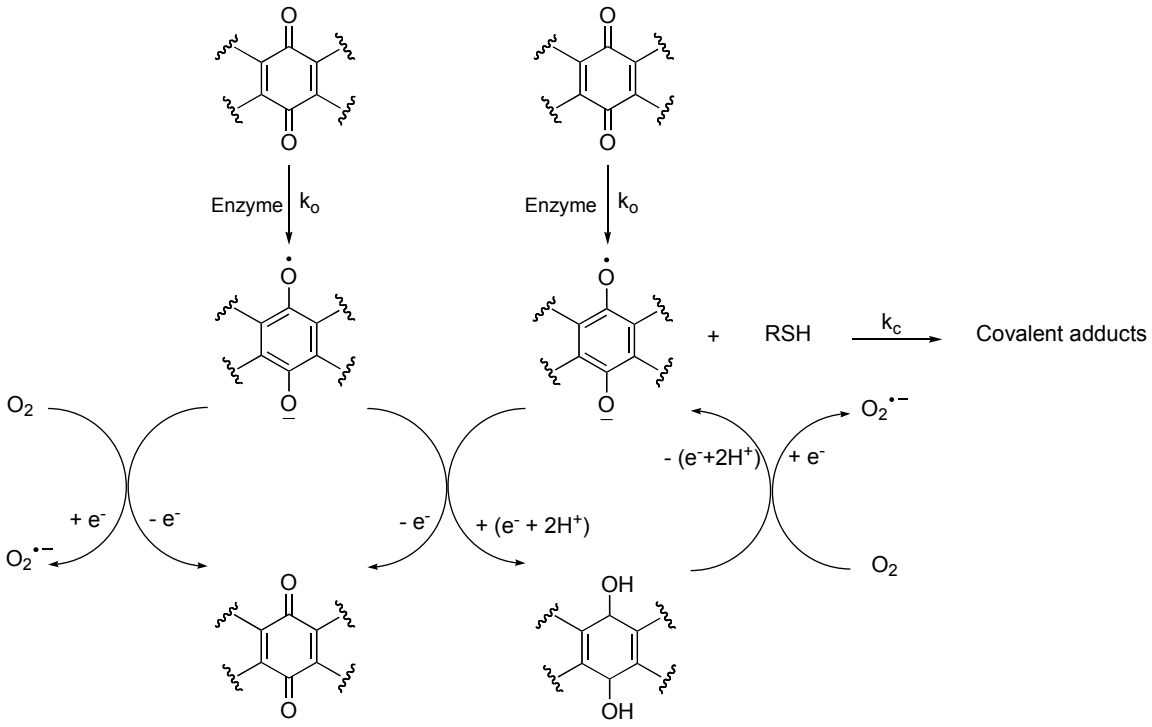

Figure 1.5. Redox cycling of quinone-containing antitumor agents initiated by a one-electron reduction and the subsequent pathways. (Adapted from ref. 37)

of ROS in the mechanism [50]. Tirapazamine (Figure 1.4e) is a bioreductively activated antitumor agent that selectively kills hypoxic cells in solid tumors [51]. One-electron reduction, possibly by enzymes such as NADPH-cytochrome p450 reductase or xanthine oxidase, produces its radical intermediate, which undergoes homolytic cleavage and generates hydroxyl radicals (Figure 1.6) [52].

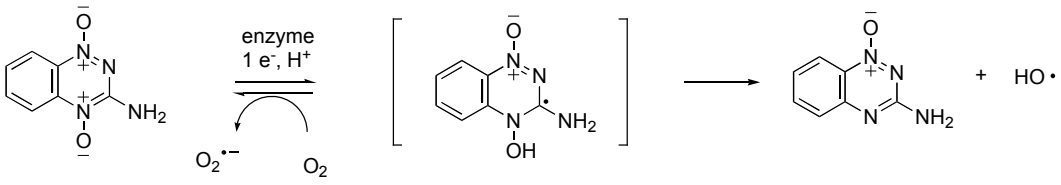

Figure 1.6. Mechanism for formation of hydroxyl radicals by tirapazamine.

1.1.3 Redox cycling antioxidants

Antioxidants are substances that can neutralize excess radicals and counteract oxidative stress in cells [53]. Therefore, antioxidants are widely used as ingredients in dietary supplements, and have also gained enormous attention as potential therapeutic agents to prevent radical damage in living systems [54]. Antioxidants are generally classified as enzymatic antioxidants (e.g., superoxide dismutase, catalase and glutathione peroxidase) and non-enzymatic antioxidants. This section deals with natural and synthetic non-enzymatic antioxidants [9]. Figure 1.7 shows several well-known small molecule antioxidants. α-Tocopherol (vitamin E, Figure 1.7a) is a lipophilic vitamin, and is perhaps the best-known natural antioxidant (discussed later in Section 1.3) [55]. The antixoidant activity of L-ascorbic acid (vitamin C, Figure 1.7b) results from its ability to donate electrons sequentially (Figure 1.8) [56]. Vitamin C is a cofactor in a variety of enzymatic

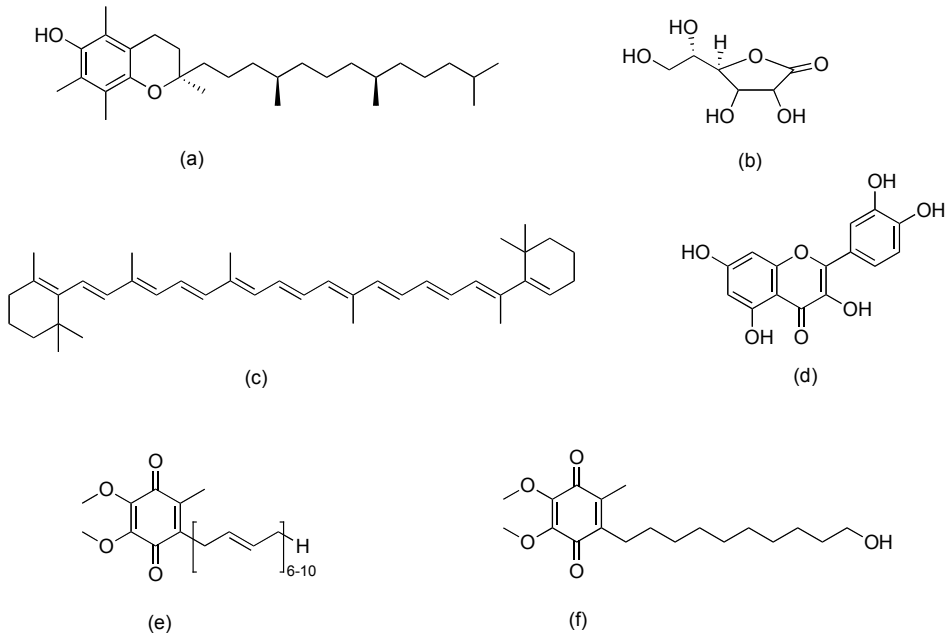

Figure 1.7. Structures of some redox cycling antioxidants. (a) α-tocopherol (vitamin E), (b) L-ascorbic acid (vitamin C), (c) β-carotene, (d) quercetin (flavonoid), (e) ubiquinone (coenzyme Q), (f) idebenone.

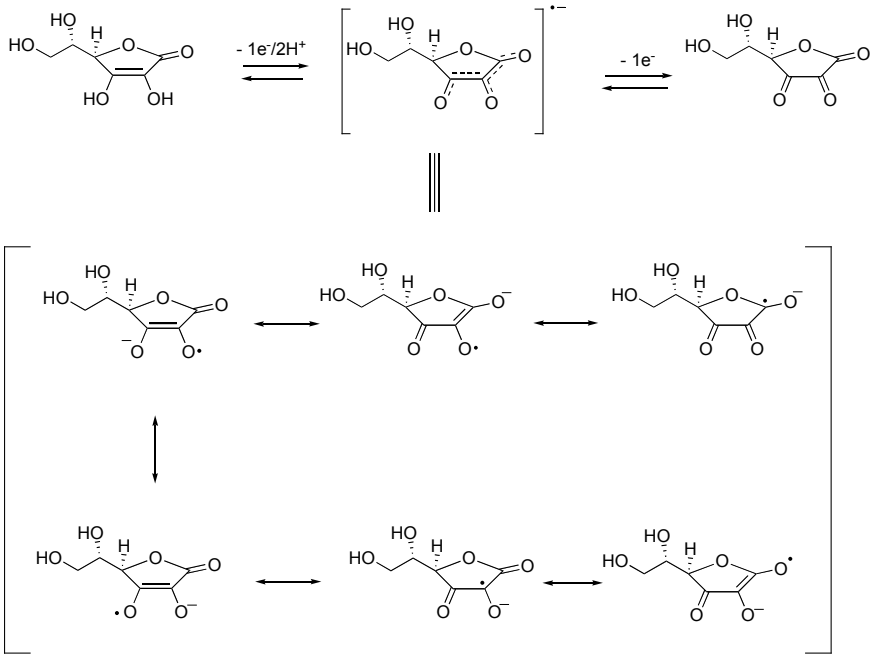

Figure 1.8. Two-electron oxidation of vitamin C.

reactions and also works synergistically with vitamin E to protect against radical damage [57]. β-Carotene (Figure 1.7c), which can be oxidatively cleaved in the human body, is a potent antioxidant and well known for its singlet oxygen quenching ability [58]. Quercetin (Figure 1.7d), the most abundant dietary flavonoid, is a strong antioxidant as a consequence of its structural features that enable radical scavenging. The catechol group in the B-ring is important for stabilizing the aroxyl radical [59]. Ubiquinone (coenzyme Q, Figure 1.7e) is a family of benzoqunones, which differ in the length of the lipophilic side chain. The antioxidative effect of ubiquinone resides in its electron-transport ability because ubiquinone can undergo a two-electron reduction to produce hydroquinone (Figure 1.9) [60]. Idebenone (Figure 1.7f), a synthetic analogue of coenzyme Q_{10}, is an experimental drug for the treatment of Alzheimer's disease and other neurological defects [61].

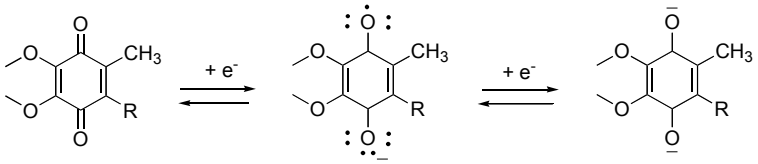

Figure 1.9. Two-electron reduction of ubiquinone.

1.2 Bleomycins: DNA damaging agents

1.2.1 Bleomycins

The bleomycins (BLMs) are a class of glycopeptide antibiotics that show antitumor properties and are used clinically for the treatment of several types of cancers [62]. Bleomycins were first isolated from a culture broth of the actinomycete *Streptomyces vericillus* in the early 1960's by Umerzawa et al. [63]. The structure of bleomycin with the assignment of the relative and absolute stereochemistry was determined through a series of chemical hydrolyses of the parent compound followed by X-ray crystallographic characterization by Umezawa et al. in 1977 [64]. This early structural identification contained a β-lactam, which was revised to its correct structure in 1978 [65]. The structures of BLM family members differ only by the nature of their C-termini (Figure 1.10). The clinically used anticancer drug Blenoxane, which is composed ~60% of bleomycin A_2 and ~30% of bleomycin B_2, with trace amounts of other bleomycin congeners, is used for the treatment of Hodgkin's lymphoma, carcinomas of the skin, head and neck, and testicular cancers [62,66].

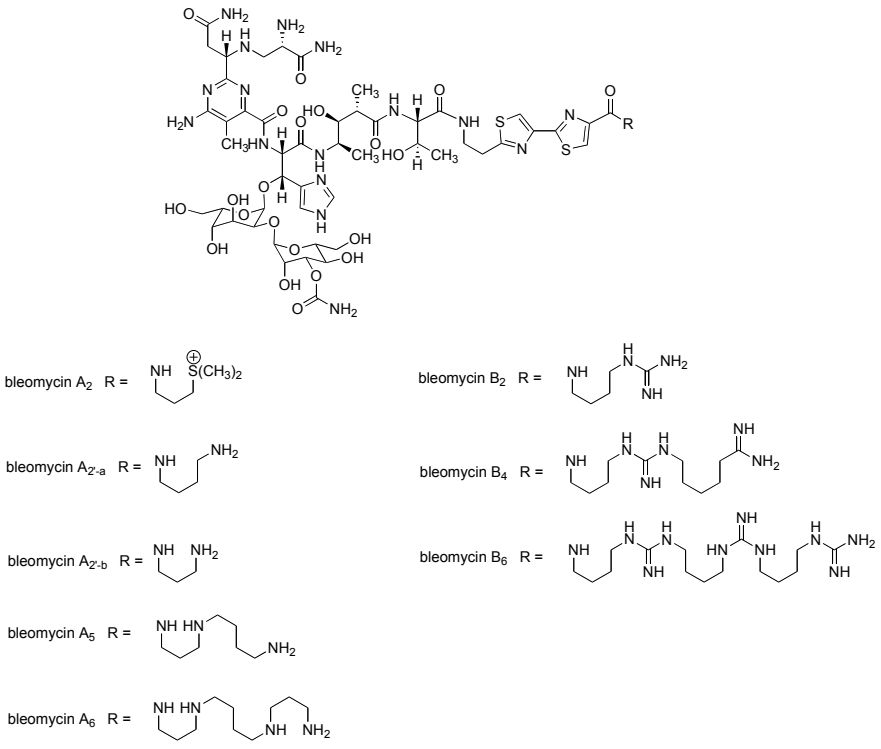

Figure 1.10. Bleomycin family members.

Bleomycin can selectively cleave DNA at 5'-GC-3' or 5'-GT-3' sites in the presence of a metal ion and oxygen [67]. More recently, it was found that bleomycin can also degrade some RNA, in both the presence and absence of Fe ion, and RNA may represent another therapeutic target [68-70]. Evidence has supported a mechanism in which Fe(II) forms a complex with bleomycin, which can interact with O_2 *in vivo* [71]. Other metals, such as copper, cobalt and manganese, have also demonstrated an ability to support BLM-mediated DNA cleavage [72-74].

Deglycobleomycin (Figure 1.11), lacking the carbohydrate moiety, cleaves DNA in a sequence selective manner similar to the natural bleomycin [75].

Despite a lower efficiency and a decreased double- to single-stranded cleavage ratio, deglycobleomycin is more readily accessible synthetically and therefore has been used successfully for understanding the essential structural elements necessary to perform sequence-selective oxidative DNA degradation [76], potentially leading to the development of improved antitumor BLMs.

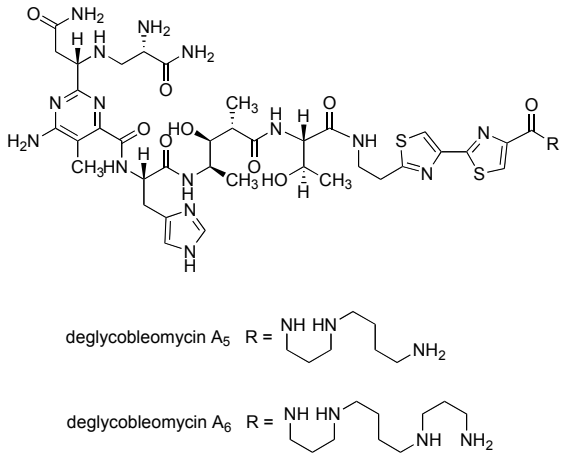

Figure 1.11. Structures of deglycobleomycin A_5 and A_6.

1.2.2 Structural domains in bleomycins

Bleomycin, exemplified by bleomycin A_5 and bleomycin A_6 in Figure 1.12, has four structural domains. The C-terminus domain consists of a bithiazole moiety and a positively charged polyamine C-substituent as in bleomycin A_5 and A_6. This domain plays an important role in DNA binding [77,78]. The linker region, which consists of L-threonine and methylvalerate organizes the metal binding domain and the DNA binding domain to facilitate productive DNA

binding and thereby enable cleavage [66,79,92(b),99,106(b)(c)]. The metal binding domain is composed of β-hydroxyhistidine and pyrimidoblamic acid moieties. This domain is responsible for the chelation of a metal ion cofactor and oxygen activation [80,81] and is likely also involved in the sequence selectivity of DNA cleavage [79,82]. The carbohydrate moiety participates in the metal ion binding [83,84], and also in cell surface recognition [85] and the cellular effects of the drug [86,87]. These four domains are discussed in detail below.

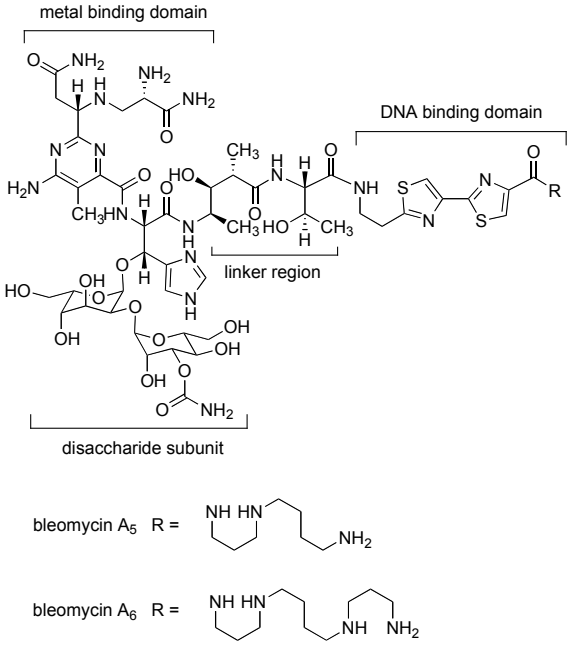

Figure 1.12. Functional domains of bleomycin A_5 and A_6.

1.2.2.1 DNA binding domain

The DNA binding domain consists of the bithiazole moiety and an alkyl substituent bearing a positively charged functional group. Several studies utilized fluorescence spectroscopy and proton magnetic resonance spectroscopy to

examine bleomycin binding to calf thymus DNA have demonstrated the interaction of bithiazole and the terminal amine moiety with various deoxyribodinucleotides [88], suggesting that this portion of the molecule was involved in the binding of bleomycin to DNA.

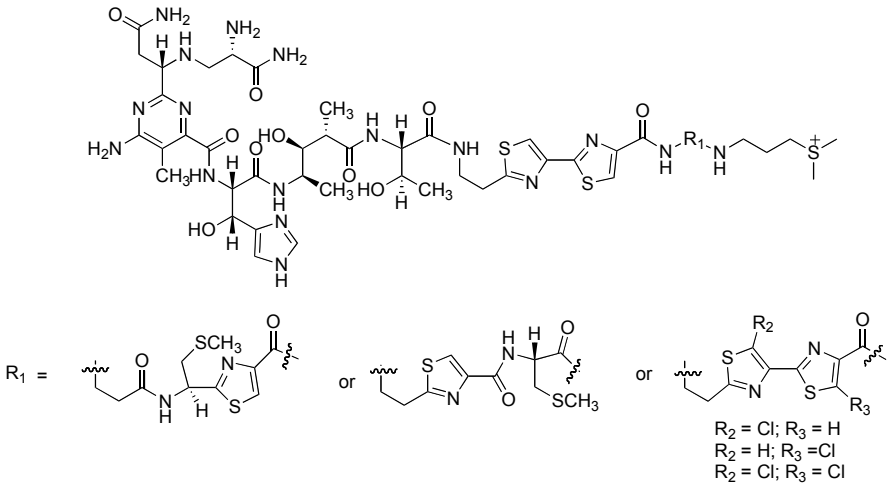

Figure 1.13. Deglycobleomycin congeners containing thiazole-modified analogues.

To better understand the role of the DNA binding domain in the sequence selectivity of DNA cleavage, bithiazole analogues have been synthesized and incorporated into bleomycin. Monothiazole bleomycin analogues (Figure 1.13), in which either of the two thiazole rings was replaced with *S*-methyl-L-cysteine, was found to lose DNA sequence selectivity. Presumably, it was resulted from inefficient DNA binding [89]. This result suggested that the DNA binding domain could provide a source of DNA affinity to support sequence-selective DNA cleavage. In addition, bleomycins containing chloro-substituted bithiazole

analogues (Figure 1.13), demonstrated DNA sequence selectivity in the presence of UV light. Additional studies confirmed that the metal binding domain could be responsible for the observed pattern of DNA cleavage [90(a)]. It has been found that EDTA-conjugated bithiazole analogues afforded strand scission in DNA with no sequence selectivity in the presence of Fe^{2+} [90(b)]. This argued that the bithiazole moiety and the metal binding domain could act in a cooperative manner to display selective DNA cleavage. Another line of evidence to support this conclusion is that modified bithiazoles were shown to yield different sequence selectivity (Figure 1.14). Hecht and coworkers showed that bleomycin containing a trithiazole moiety exhibited altered sequence selectivity from 5'-GC-3' to 5'-GT-3' [91]. Ohno and co-workers have also developed two deglycobleomycin analogues containing a distamycin moiety in the place of the bithiazole moiety that can shift the sequence selectivity to 5'-AT-3' rich regions [92].

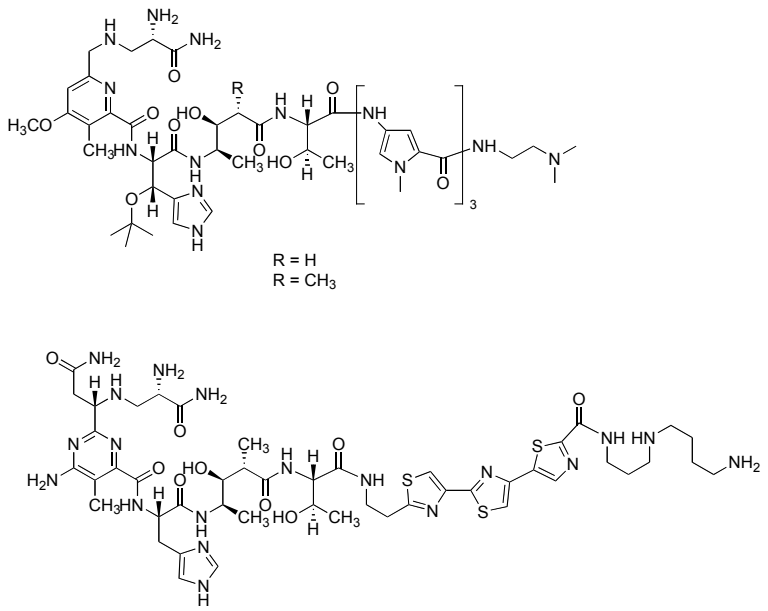

Figure 1.14. Deglycobleomycins that demonstrated alternative DNA cleavage patterns.

1.2.2.2 Linker region

The linker region consists of L-threonine and methylvalerate moieties. This domain of bleomycins was initially thought of as a tether that links the DNA binding domain and metal binding domain together. The role of this domain was not truly understood and investigated until almost ten years after the isolation of this natural product [62,93].

The early study of the linker region carried out by Umezawa et al. demonstrated that the specific stereochemistry of the substituents on the linker backbone was required to promote efficient DNA cleavage [62,92(b)]. Another early study of this region carried out by Boger et al. involved incorporating a linking peptide chain that lacked the peripheral substituents. This BLM congener

was found to exhibit 100 times less effective DNA cleavage than deglycoBLM, although sequence selectivity was still retained [94]. Hecht et al. also simplified the linker by removing or replacing the threonine with mono-, di-, or tetraglycine [95], as well as with tyrosine and methionine (Figure 1.15) [96]. They found that the cleavage efficiency decreased significantly and that sequence selectivity was affected as well. In addition, Boger et al. reported a systematic study of the role of the threonine moiety by replacing it with alanine, serine, valine and 2-(*R*)-aminobutyric acid (Figure 1.15) [97]. The efficiency of DNA cleavage was dramatically affected after the removal of the hydroxy group on the threonine. Increasing the steric bulk of the functionalities on threonine moiety also decreased DNA cleavage efficiency. These results suggested that the threonine subunit, especially the presence of hydroxyl group, is necessary to support the DNA cleavage activity of bleomycin.

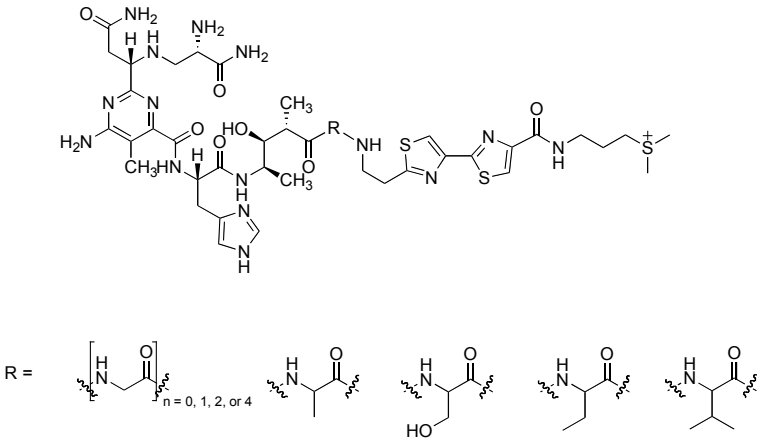

Figure 1.15. Deglycobleomycin congeners modified in the threonine moiety.

The role of the methylvalerate moiety has also been the subject of many studies. The initial experiments modifying the methylvalerate moiety showed that the absolute stereochemistry and the presence of the 3'-hydroxyl group on the methylvalerate moiety were both important to support the function of bleomycins [92]. It was suggested that the conformation of the methylvalerate moiety played a role in "making the flexible BLM molecule rather inflexible in the twisted minor groove of DNA" [92(a)]. By inverting the configuration of the C4 center, Ohno et al. demonstrated that the corresponding BLM analogues exhibited significantly decreased ability to degrade DNA [98]. It was concluded that the 4*R* configuration of the three consecutive asymmetric centers (2*S*, 3*S*, 4*R*) was of particular importance [99].

A more systematic study of the methylvalerate subunit was reported by the Boger laboratory regarding the effects of the C2- and C4-methyl groups and the C3-hydroxy group, as well as the length of the linker [99]. By synthesis and characterization of a series of BLM analogues containing modifications in the methylvalerate moiety of deglycobleomycin A_2 (Figure 1.16a), it was revealed that each of the substituents played a significant role in the DNA cleavage efficiency but had minimal impact on DNA sequence selectivity. The presence of a C3-hydroxy group had only a modest effect on the bleomycin activity, possibly through H-bonding with DNA. The more significant effect of the C4-methyl group is linked to the presence of the C2-methyl group. In contrast, the C2-

methyl group exhibited only a modest effect and its impact is not coupled to the presence of the C4-methyl group. These effects were explained by the conformation of the resulting BLM analogues after modification. This unique β-hydroxy-γ-amino acid is believed to orient BLM into a rigid and compact conformation essential for DNA interaction [76(a)]. Methyl substitutions at the C2- and C4-positions were suggested to stabilize the compact conformation to allow for efficient DNA interaction while alteration of that conformation could greatly diminish DNA cleavage [99]. Furthermore, it was suggested that the length of the linker is also important (C4 > C5 > C3 > C2). However this effect was examined in the absence of linker substituents.

Since the methylvalerate moiety may be responsible for a conformational bend in bleomycin required for efficient DNA cleavage, the Hecht laboratory has synthesized a number of conformationally constrained methylvalerate analogues and incorporated them into deglycoBLM A_5 congeners in order to probe the effects of conformational constraint on the native valerate moiety [100]. However, none of these analogues mimicked the conformation proposed for the natural valerate linker, they all exhibited diminished DNA cleavage activity and lacked sequence selectivity (Figure 1.16b). More recently, two deglycoBLM analogues modified in the methylvalerate moiety were selected from a 108-member deglycoBLM A_6 library, both of which contained phenylmethylvalerate moieties (Figure 1.16c). These two BLM congeners displayed potencies of supercoiled

DNA relaxation greater than that of the parent deglycobleomycin [96,101]. This suggested that increased steric bulk at the methylvalerate C4-position could alter the efficiency and pattern of DNA cleavage.

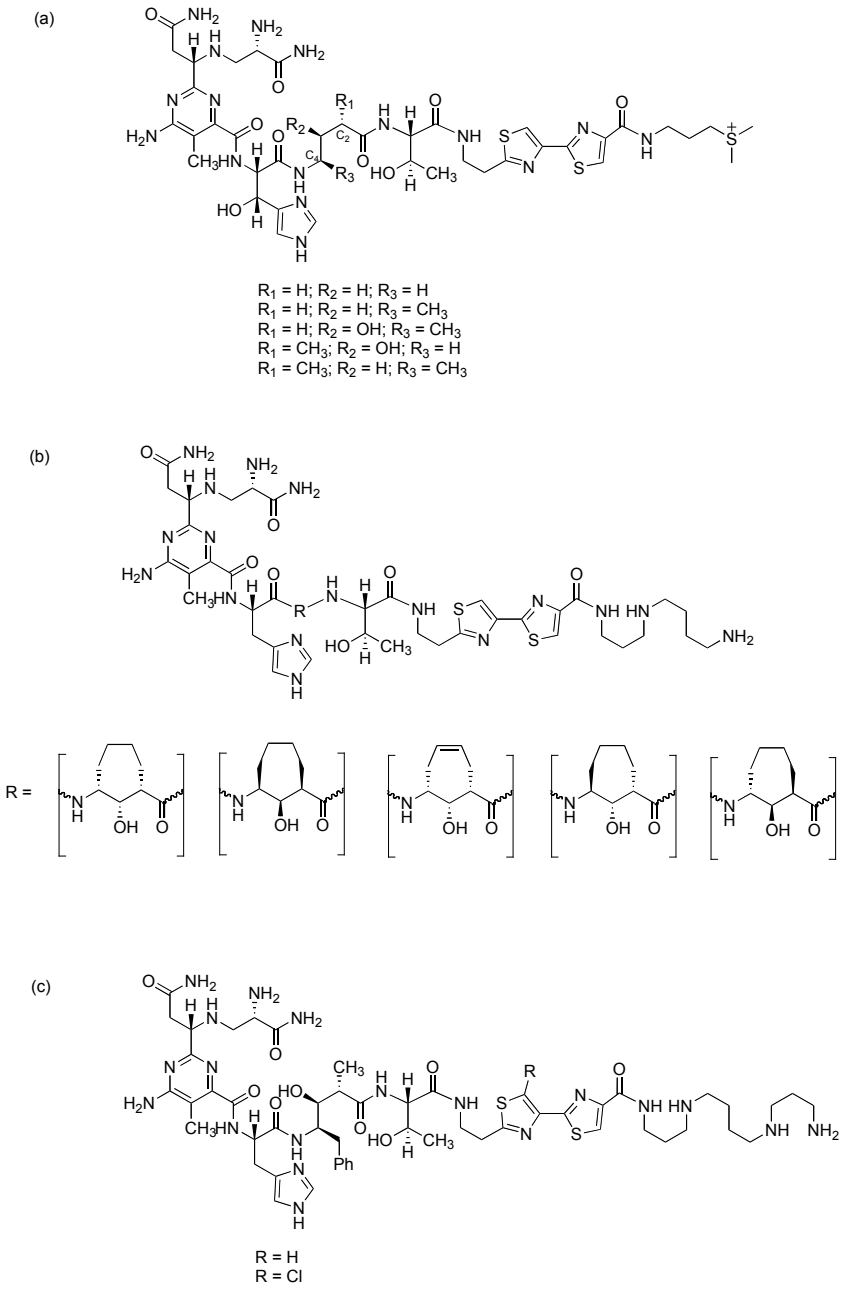

Figure 1.16. Deglycobleomycin congeners modified in the methylvalerate moiety.

1.2.2.3 Metal binding domain

The metal binding domain consists of the β-hydroxyhistidine and pyrimidoblamic acid moieties. This region is believed to be responsible for metal binding, oxygen activation and DNA cleavage selectivity. Based on the X-ray crystal structure of Cu(II)•P-3A, a putative biosynthetic precursor of bleomycin, the initial metal coordination model of bleomycin was proposed by Umezawa [102]. In this model, the P-3A copper complex adopts a square pyramidal geometry, in which the N1 of the 4-aminopyrimidine, N3 of imidazole, the deprotonated amide of histidine, and the secondary amine of the β-aminoalanine form the base of the pyramid with the primary amine of β-aminoalanine as the apex (Figure 1.17). Although lacking the carbohydrate moiety and the C5 methyl group in the pyrimidine ring, this model provided the first coordination geometry of the metal-binding domain. Based on this Cu(II)•P-3A model, a model for the Cu(II)•bleomycin structure was proposed, in which the carbamoyl oxygen from the carbohydrate formed the remaining coordination site (Figure 1.18) [103]. A number of biochemical and spectroscopic studies of the metal-bound complexes have since been described and support the proposed coordination geometry of bleomycin.

The metal binding domain is also important for the sequence selectivity of DNA cleavage [76(b),79,104]. The effect of the metal binding domain on DNA sequence selectivity is coupled with the DNA binding domain. It has been

demonstrated that analogues of the metal binding domain that lacked the bithiazole and C-terminus did not display DNA cleavage pattern [76]. However, when combined with the bithizole moiety, these analogues demonstrated sequence selective DNA cleavage [105(c)]. The sequence selectivity may result from hydrogen bonding between guanine in the DNA backbone and the 4-amino group as well as the N3 of the pyrimidine ring based on the structure of HOO-Co(III)•BLM A_2 [106]. This was further confirmed by the analogues lacking the 4-amino group or the analogues with the 4-amino group methylated [107]. The analogues were shown to have diminished selectivity for 5'-GC-3' and 5'-GT-3' sequences.

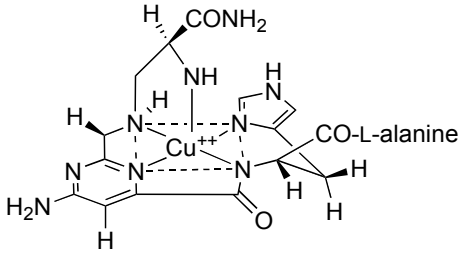

Figure 1.17. X-ray crystallographically determined structure of Cu(II)•P-3A.

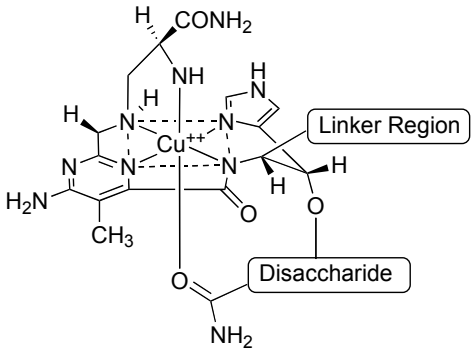

Figure 1.18. Proposed structure for Cu(II)•BLM complex.

Another part of the metal binding domain, the β-hydroxyhistidine moiety, has also been well studied. Removal of the imidazole ring resulted in decreased efficiency and loss of sequence-selective DNA cleavage [96]. The nitrogen atom of the amide (N^a) and the imidazole nitrogen atom (N^π) were both essential for metal coordination (Figure 1.19) [108]. The Boger laboratory prepared a number of analogues modified in the β-hydroxyhistidine moiety that provided some useful insights about this subunit [109]. It was found that removal of the β-hydroxy group from β-hydroxyhistidine did not significantly affect either the cleavage efficiency or the sequence selectivity. Additionally, the replacement of N^a with N-methylamide or ester resulted in sequence neutral DNA cleavage as well as diminished DNA cleavage efficiency [109]. This is presumably because this moiety was unable to coordinate the metal properly with the amide nitrogen atom. Modification of the imidazole ring nitrogen or replacement of the imidazole ring with a totally different ring system, such as oxazole, thiophene or pyrrolobenzene, resulted in less cleavage efficiency [96,101]. These results suggested that both the position and electronic nature of the N^π and N^σ are important for metal binding and sequence selectivity of DNA cleavage (Figure 1.19).

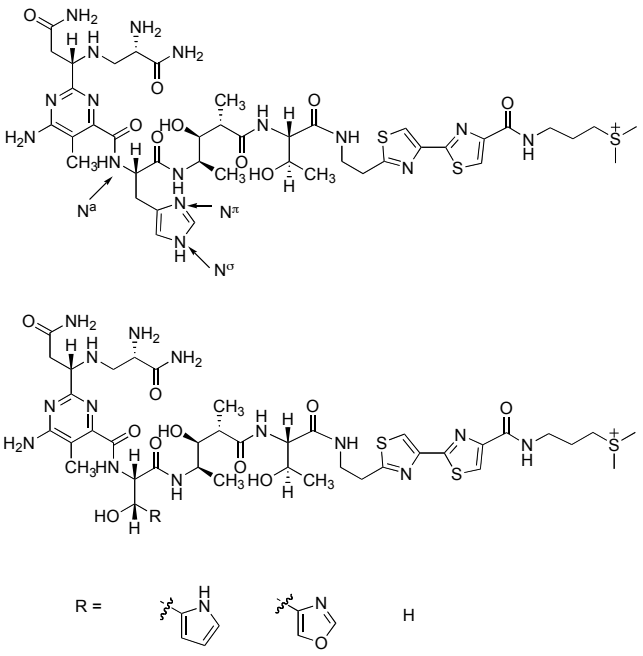

Figure 1.19. Deglycobleomycins congeners modified in the β-hydroxyhistidine moiety.

1.2.2.4 Carbohydrate moiety

The carbohydrate moiety is comprised of L-gulose and carbamoyl-D-mannose. Of all the functional domains of bleomycin, the carbohydrate moiety is the least well understood [76a]. The carbohydrate moiety may participate in metal ion binding [83,84], as well as in cell surface recognition [85], and the cellular effects of the drug [83,111]. The C3 carbamoyl group on the mannose moiety has been postulated to provide an additional axial ligand for metal coordination [111]. It is also suggested that the disaccharide moiety together with C2-acetamido side chain of pyrimidoblamic acid act as a "shield" to protect the activated meal-oxo species [112]. Removal of the carbohydrate moiety from bleomycin provided

deglycobleomycin, which has a lower DNA cleavage potency and a decreased ratio of double-strand cleavage to single-strand cleavage [45,76(b),104(b)]. Interestingly, removal of the mannose moiety has a minimal effect on DNA cleavage efficiency, whereas removal of the gulose resulted in a significant diminished DNA cleavage [113]. Recently, Hecht et al. applied a microbubble technique to demonstrate that the carbohydrate moiety could assist BLM in binding selectively to cancer cells [85]. The experiments showed the BLM A_5–microbubble conjugate adhered to cultured MCF-7 human breast carcinoma cells whereas no adhesion of the deglycoBLM A_5–microbubble conjugate was observed in cancer cells. In addition, the BLM A_5-microbubble was found to bind selectively to MCF-7 cells while there was no adhesion of the BLM A_5-microbubble conjugate to the "normal" breast cell line MCF-10A. These results support the concept that the carbohydrate moiety of BLM A_5 is required for tumor cell targeting.

1.2.3 Mechanism of action of bleomycins

The primary mechanism of action of BLM is generally believed to be the generation of single- and double-strand breaks in chromosomal DNA with a metal ion cofactor [114]. Ferrous ion is believed to form a complex with bleomycin, which can interact with O_2 *in vivo* (Figure 1.20). The pyrimidoblamic acid and β-hydroxyhistidine make up the Fe(II) binding domain that binds oxygen through a

single electron reduction [115,116]. The formed reactive species is termed "activated bleomycin" [71(d), 114(a)]. This ternary complex is believed to be responsible for DNA cleavage.

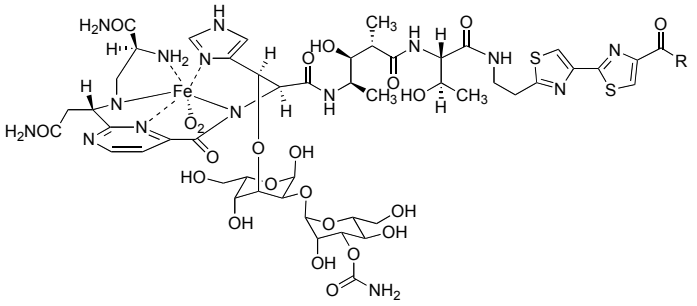

Figure 1.20. The proposed structure of Fe(II)•BLM complex interacting with O_2.

The formation of "activated bleomycin" has been studied theoretically for many years, and has resulted in a number of proposals. However, the actual structure of the "activated bleomycin" has not yet been observed experimentally and the detailed mechanism of the antitumor activity of bleomycin is still unknown. A possible catalytic cycle by which bleomycin degrades DNA is suggested in Figure 1.21 [114(c)]. In the first step, iron metal coordinates with bleomycin and binds one molecule of dioxygen [117]. The next step is activation of the ternary complex of bleomycin. In this step, a one-electron reduction is believed to occur either chemically or by a microsomal NAD(P)H-cytochrome p450 reductase-catalyzed reduction [116]. As mentioned above, the reactive species formed is termed "activated bleomycin"; it is believed to be the species

involved in DNA degradation. This species can degrade DNA while being oxidized to Fe(III)•BLM. In the final step, further reduction occurs to regenerate Fe(II)•BLM.

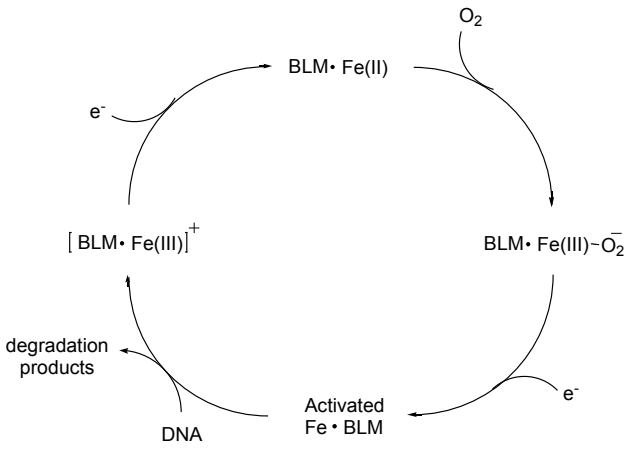

Figure 1.21. The catalytic cycle of the Fe•BLM complex.

There are two mechanisms proposed involving the activated bleomycin mediating DNA single-strand and double-strand degradation. Figure 1.22 shows the first proposed mechanism for oxidative DNA strand-scission by "activated bleomycin" [118]. This pathway starts from the homolytic abstraction of the C4'-hydrogen of deoxyribose generating a C4' radical species, which reacts with an oxygen molecule to form a hydroperoxyl radical. Following reduction of the hydroperoxide, this intermediate then undergoes a Criegee-type rearrangement that leads to the cleavage of the C3'-C4' bond of deoxyribose. The "cleaved" sugar is further decomposed by an anti-elimination, generating the base propenal, a 5'-phosphoronucleotide and a 3'-oligonucleotide.

At low oxygen concentration, bleomycin is believed to produce alkali-labile DNA lesions (Figure 1.23) [119]. After C4'-hydrogen abstraction to form a radical species on ribose, the resulting intermediate undergoes a one-electron oxidation to form a carbocation, which can immediately react with water to produce a C4'-hydroxyl nucleoside. Further collapse of this species results in a DNA strand scission product containing a terminal 3'-phosphate, and a 5'-phosphate [119].

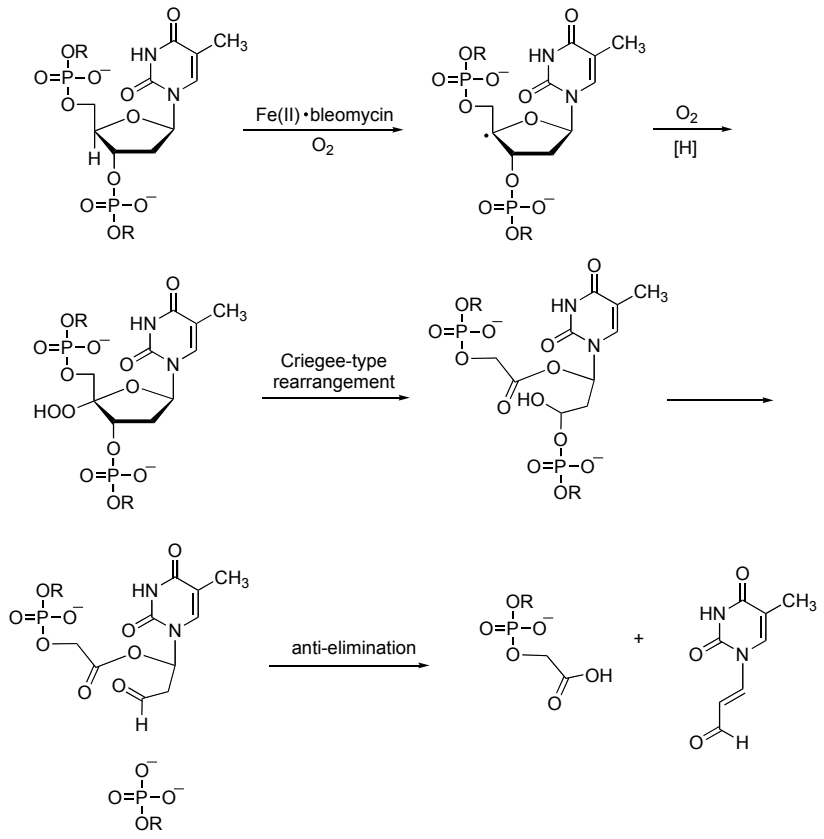

Figure 1.22. Proposed mechanism for oxidative DNA strand-scission by "activated bleomycin".

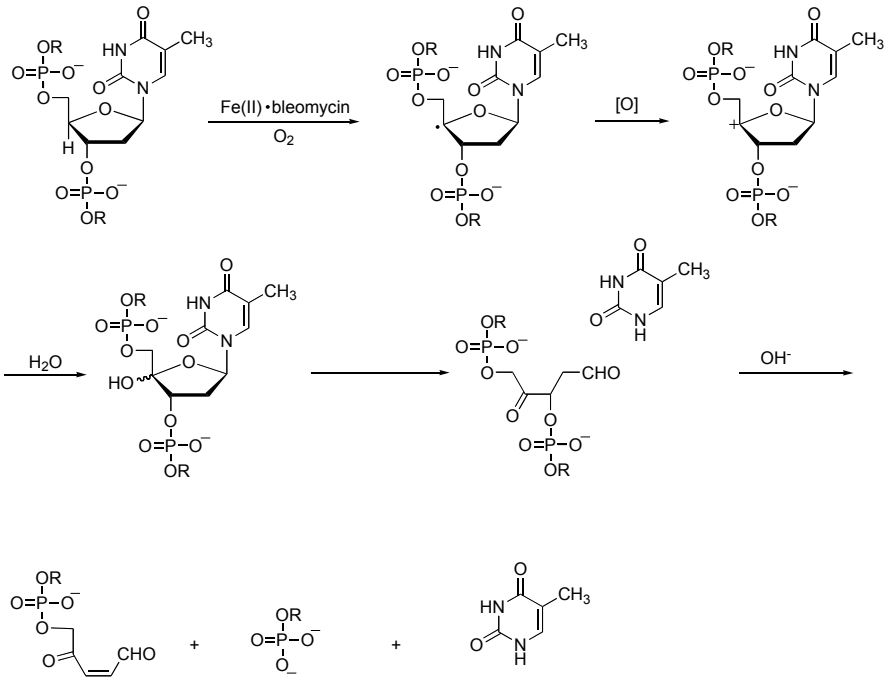

Figure 1.23. Proposed mechanism for the formation of alkali-labile lesions in DNA.

In addition to DNA, bleomycins have also been shown to degrade some RNA substrates [114(c),69(c)], including DNA-RNA heteroduplex [120], and different types of RNAs such as transfer RNA [69(a)], messenger RNA [121], and ribosomal RNA [69(b)]. The significance of RNA as a potential therapeutic target for bleomycin can be envisioned for several reasons. First, RNA is located in the cytoplasm, and therefore, should be much more easily accessible, whereas the majority of cellular DNA is located in the cell nucleus [122]. Moreover, there are several repair mechanisms by which certain bleomycin-induced DNA lesions can be repaired. However there is currently no evidence to support analogous robust mechanisms by which damaged RNA can be repaired.

Studies have suggested that the degradation of RNA oligonucleotides is substantially more complex than the degradation of DNA [69(c)]. The oxidative damage of RNA is believed to occur at both the C4' and C1' positions of the ribose sugar (Figure 1.24). However, C1'-hydrogen abstraction did not lead directly to strand scission. Furthermore, treatment of the rearranged aldehyde with 1,2-diaminobenzene resulted in the formation of a dinucleotide quinoxaline with release of the nucleobase, carbon dioxide, and the 5'-phosphate [123].

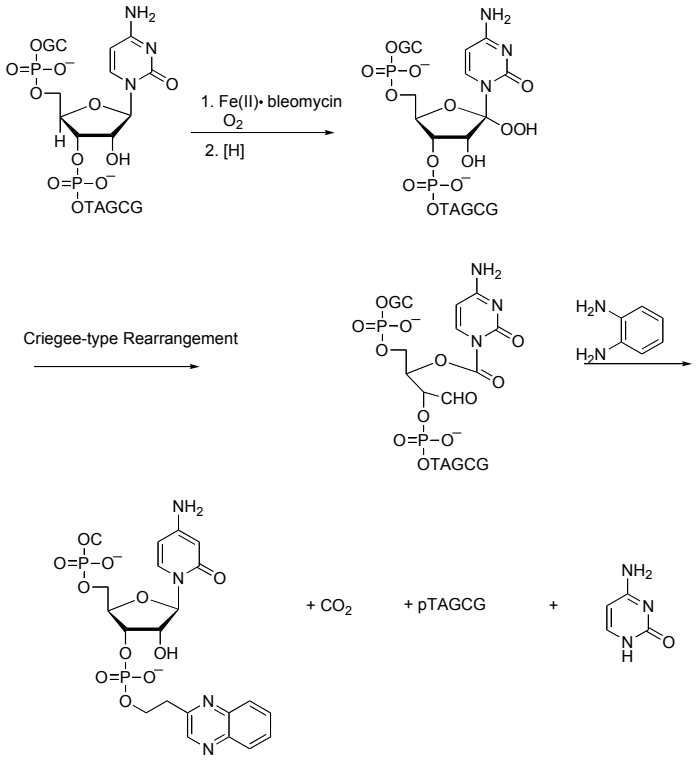

Figure 1.24. Degradation of chimeric octanucleotide by Fe(II)•BLM in the presence of 1,2-diaminobenzene.

1.3 α-Tocopherol and bicyclic pyridinol antioxidants

1.3.1 Vitamin E and α-Tocopherol

Vitamin E is a lipophilic vitamin having excellent antioxidant potency. The vitamin E family includes eight members: α-, β-, γ-, δ-tocopherol and α-, β-, γ-, δ-tocotrienol. The vitamin E family members have methylated hydroquinone moieties and an isoprenoid chain (Figure 1.25). Since the discovery of vitamin E several decades ago its roles in human health and its biological functions have been studied extensively [124].

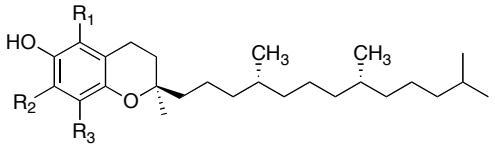

α-tocopherol: R_1=CH_3, R_2=CH_3, R_3=CH_3
β-tocopherol: R_1=CH_3, R_2=H, R_3=CH_3
γ-tocopherol: R_1=H, R_2=CH_3, R_3=CH_3
δ-tocopherol: R_1=H, R_2=H, R_3=CH_3

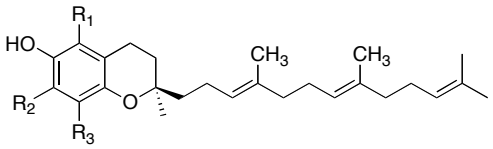

α-tocotrienol: R_1=CH_3, R_2=CH_3, R_3=CH_3
β-tocotrienol: R_1=CH_3, R_2=H, R_3=CH_3
γ-tocotrienol: R_1=H, R_2=CH_3, R_3=CH_3
δ-tocotrienol: R_1=H, R_2=H, R_3=CH_3

Figure 1.25. Structures of vitamin E family members.

α-Tocopherol (α-TOH) is not only the major component of vitamin E but also the most active form in human body (Figure 1.26). α-Tocopherol is known to react readily with a variety of radicals and thus can prevent membrane peroxidation in the cell [125]. In addition, α-tocopherol can prevent the radical

oxidation of low density lipoproteins (LDLs), which act as the major carrier of cholesterol in human body. Oxidation of LDLs is strongly implicated in the development of atherosclerosis diseases [126]. Because of its antioxidant capacity, α-TOH has been studied for the treatment of several diseases, such as cardiovascular disease [127], diabetes mellitus [128], dementia [129] and cancer [130]. α-Tocopherol is best known as a chain-breaking antioxidant that prevents lipid peroxidation by scavenging the lipid peroxyl radicals in the peroxidation chain [125(a)].

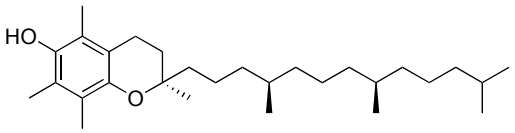

α-tocopherol
(α-TOH)

Figure 1.26. Structure of α-tocopherol (α-TOH)

Lipid peroxidation is a radical chain reaction, and has been studied extensively since the 1960s. The chain reactions of lipid peroxidation before quenching by any antioxidants is summarized as shown in Figure 1.27. Steps other than those shown in Figure 1.27 are possible, including the coupling of various radicals in the chain termination step to form several stable species, such as L–L, L–O–O–L, and L–O–L; but it is more common to show that the initiating radical (i.e., L•) undergoes dimerization in the chain termination step [131(a)].

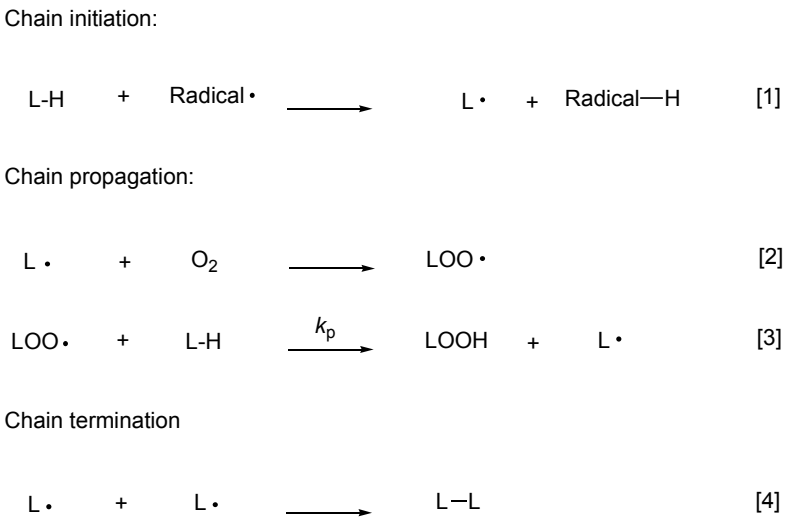

Figure 1.27. Chain reactions in lipid peroxidation before quenching by any antioxidants.

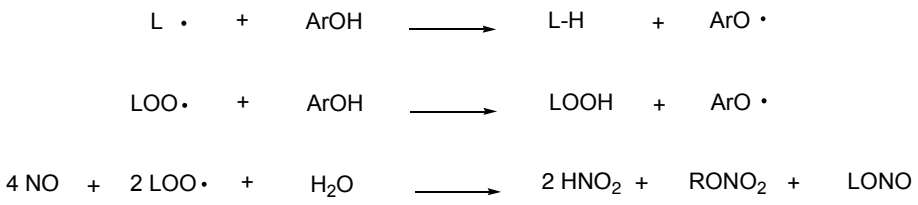

Figure 1.28. Inhibition of lipid peroxidation.

Inhibition of lipid peroxidation can, in principle, be accomplished in several ways (Figure 1.28). One involves suppressing the initiation step that produces the radical L• [131(a)(b)]. The chain reactions can also be interrupted when an antioxidant functions as a hydrogen atom donor to react with the peroxyl radical (LOO•) [131(b)]. A third way involves accelerating the chain termination sequence by introducing a new termination mechanism. For example, nitric oxide (NO) inhibits lipid peroxidation; the available data suggest its antioxidant activity results

from the chain termination [131(c)]. The last two quenching mechanisms are substantially similar, since in both case antioxidants react with the peroxyl radicals.

As mentioned above, α-tocopherol is generally believed to quench lipid peroxidation by transferring its phenolic hydrogen to the propagating peroxyl radical (Figure 1.29), since α-TOH reacts with LOO• at a rate ($k_q \sim 10^6$ $M^{-1}s^{-1}$) much faster than that of chain propagation ($k_p \sim$ 10–100 $M^{-1}s^{-1}$; Figure 1.27, Equation 3) [132]. The addition of oxygen to L• to form LOO• (Figure 1.27, Equation 2) is extrememly fast with rate constants on the order of 10^9 $M^{-1}s^{-1}$ [131(d),(e)]. Thus, the reaction of phenolic antioxidants with L• is normally neglected at low concentration of phenols and normal concentration of oxygen [139(b)]. However, it is probably overly simplistic to assert that any given antioxidant should act in only one fashion.

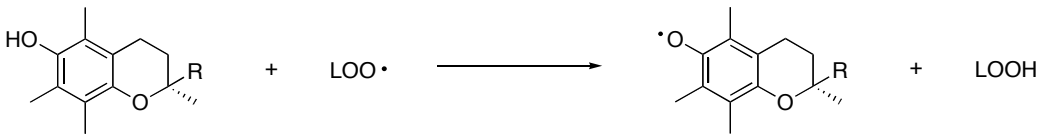

Figure 1.29. Quenching of lipid peroxidation by α-tocopherol.

After transferring a phenolic hydrogen atom to the peroxy radical (Figure 1.29) to quench the lipid peroxidation, the generated α-TOH radicals from the quenching step are stable because the unpaired electron on the oxygen atom can be

delocalized into the aromatic ring structure. Thus, they are insufficiently reactive to abstract H• from the methylene groups of the unsaturated fatty acyl moieties of membrane phospholipids [30]. Furthermore, due to the stability of the α-TOH radicals, α-TOH can be regenerated by cooperating with vitamin C and NADH (Figure 1.30) [133].

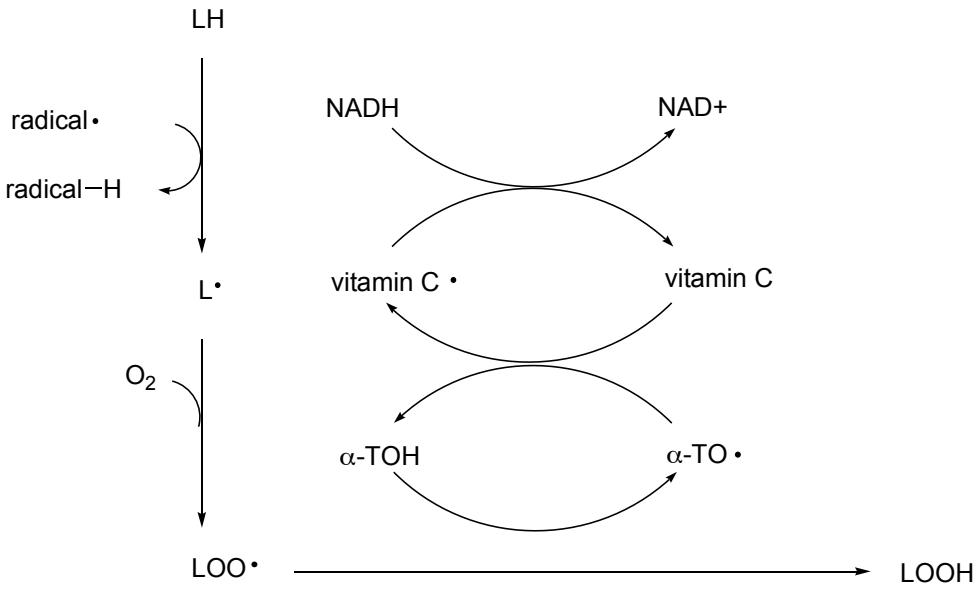

Figure 1.30. Regeneration of α-TOH by vitamin C and NADH [30].

1.3.2 Tocopherol-like analogues

Recently, considerable effort has been devoted to identifying synthetic antioxidants with activity superior to α-TOH [132(a),134]. Current research has been met with limited success due to the decomposition of compounds upon extended exposure to the atmosphere [135]. The ongoing goal includes compound

stability towards air oxidation as well as high reactivity with peroxyl radical. The bond dissociation enthalpy (BDE) of the phenolic O–H bond plays an important role in the antioxidant activity. Phenols that have lower O–H BDEs are generally better antioxidants. An increase in electron density of the aromatic ring leads to a lower BDE by stabilizing the electron deficient ArO• radical [136]. Another important parameter used in the design of new phenolic antioxidants is the ionization potential (IP), which indicates the electron transferring ability of phenols. With a lower IP value, it is easier for a phenol to lose electrons and be oxidized. An increase in IP suggests higher air-stability of the compounds [132(a),134(d),137]. Substitution with electron-donating groups (e.g., $–NH_2$) at positions *ortho* and *para* to the phenolic OH group can lower BDEs, and increase rates of H-atom transfer to peroxyl radicals. However, good electron-donating substituents also lead to a decrease in the IP of the phenol, making the substance less stable to air oxidation.

Porter, Pratt and coworkers first reported that incorporation of two nitrogen atoms at the 3- and 5-positions or one nitrogen atom at the 3-position of the phenolic ring significantly raises the IP, which improves the air stability of the compounds, and also lowers the O–H BDE to some extent [134(b),134(c),138]. 3-Pyridinols (e.g., **2** in Figure 1.31) exhibited a higher radical inhibition rate than 5-pyrimidinols (e.g., **1** in Figure 1.31). In addition, the same laboratory reported the fusion of an aliphatic ring to the free 5-position in the 3-pyridinol structures to

provide compounds **3** and **4** (Figure 1.31). Interestingly, compounds **3** and **4** were shown to be highly effective antioxidants, exhibiting 88-fold and 28-fold greater potency, respectively, than α-TOH in suppressing the autoxidation of methyl linoleate. It is suggested that improved stereo-electronic behavior increases the radical quenching rate [139].

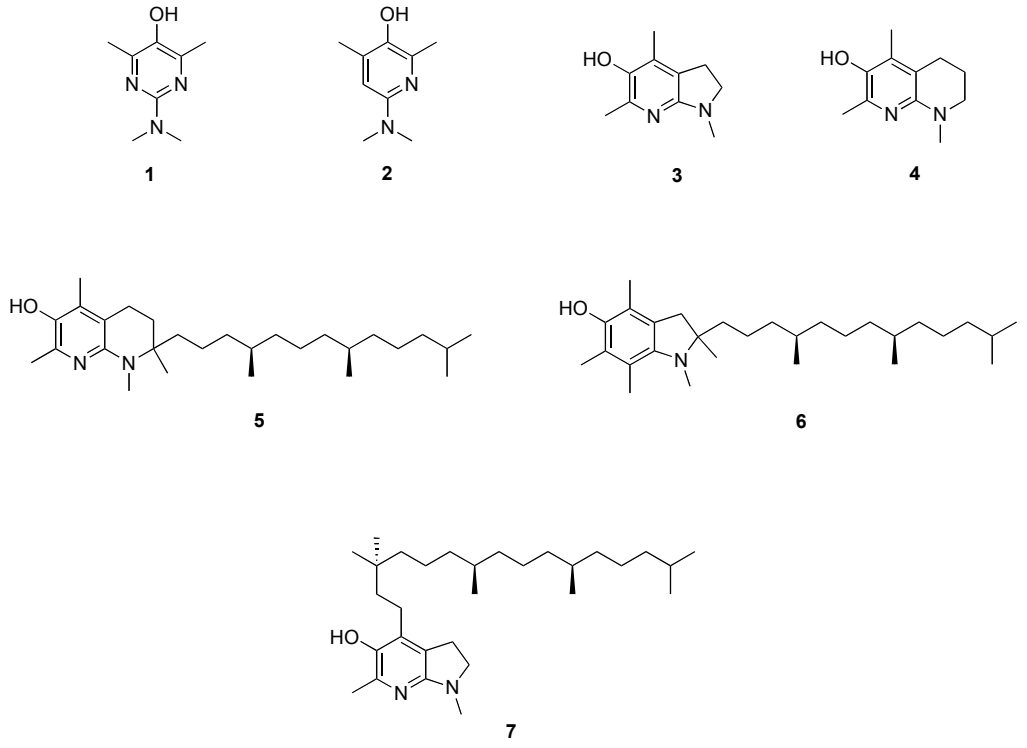

Figure 1.31. Structures of 5-pyrimidinol, 3-pyrimidinol and tocopherol-like analogues.

The bicyclic 6-amino-3-pyridinols (compounds **3** and **4**) have since been elaborated by the Porter laboratory and our laboratory by conjugating the pyridinol cores with the phytyl side chain of α-TOH (e.g., compounds **5**, **6** and **7**) [140]. The lipophilic phytyl group in α-TOH is believed to assist in the accumulation of the antioxidant in membranes, including mitochondrial

membranes, thereby protecting the cells and mitochondria from oxidative stress [141]. Although these analogues displayed promising biological profiles, the syntheses have not proven simple—all requiring 15 or more steps. The arduous approaches have therefore hindered the further development of these analogues. Thus, the development of simpler and more readily available analogues retaining biological activity has become an ongoing and important goal.

CHAPTER 2

SYNTHESIS OF DEGLYCOBLEOMYCIN A_6 ANALOGUES MODIFIED IN THE METHYLVALERATE MOIETY

2.1 Introduction

2.1.1 Solid-phase synthesis of deglycobleomycin A_6

In 1982, the Umezawa and Hecht laboratories independently reported the syntheses of bleomycins by solution-phase methods [142,143]. Their work gave an impetus to the study of the mechanism of action of bleomycins [76(a)], and initiated a wave of synthetic studies of bleomycins and their analogues within the synthesis community. These approaches have depended on the synthesis of the constituent amino acids, followed by the coupling of these amino acids to assemble the BLM scaffold. Despite the initial synthesis and the subsequent improvements, the synthesis of bleomycins remained an arduous process for synthetic chemists.

The pioneering work of Bruce Merrifield, which introduced solid phase peptide synthesis (SPPS), dramatically changed the strategy for peptide synthesis [144]. Merrifield's SPPS simplified the tedious and demanding steps of traditional solution-phase peptide synthesis. Nowadays, advances in solid phase synthesis have expanded from peptides to *O*-, *N*-, and *S*-linked glycopeptides [145], oligosaccharides [146], and even natural product-like small molecules [147].

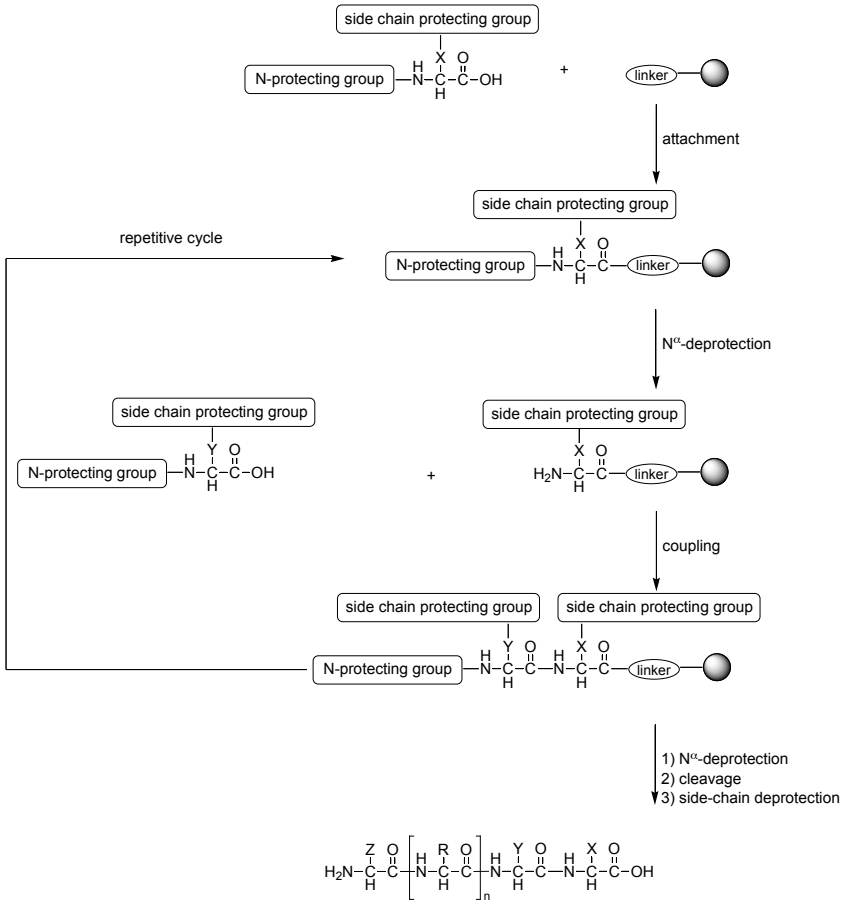

Scheme 2.1. Principles of solid phase peptide synthesis [148].

The principles of solid phase synthesis are illustrated in Scheme 2.1 [148]. Construction of a peptide chain on an insoluble solid support has obvious benefits. The coupling of amino acids is driven by employing excess reagents and the physical losses can be minimized since the peptide is bound to the solid support. Separation of the intermediate peptides from the reaction mixture can be achieved simply by filtration and washing the solid phase with solvents. The N-protected C-terminal amino acid residue of the target peptide is first attached to the solid support via its carboxylic acid group. The reactive functional groups at

the side chain of the amino acid should be masked with side chain protecting groups, which are not affected during the peptide coupling reactions. The terminal amino group of the attached amino acid is masked with N-protecting groups, which can be removed before the coupling of the next amino acid. The subsequent N-protected amino acid is added by activation of its α-carboxylic acid. After the coupling reaction is complete, the resin-bound product is removed from the reaction mixture by filtration and washing with excess solvent. This process (deprotection/coupling) is repeated until the desired peptide sequence is formed. In the final step, the peptide is released from the solid support and the side chain protecting group is removed simultaneously. Generally, the side chain protecting groups are chosen so that they can be removed under the same conditions used for cleavage of the target peptide from the solid support.

Two main strategies are used in solid phase peptide synthesis: the Boc/Bzl and the Fmoc/Boc approaches [148]. The Boc/Bzl method is based on the strategy of graduated acidolysis to achieve selectivity in the removal of N-protecting groups and side chain protecting groups [149]. The Fmoc/Boc method is based on an orthogonal protection strategy, which uses the base-labile N-Fmoc group for protection of the α-amino group and the acid-labile side chain protecting group and resin linkers [150]. Since this orthogonal strategy employs a different mechanism to remove the N-protecting groups and side chain protecting groups, it requires considerately milder conditions than those utilized in Boc/Bzl method.

The cleavage condition is more convenient and the operation is simplified, thus Fmoc-based SPPS is now generally the method of choice for the routine synthesis of peptides.

After two decades of effort in the synthesis of bleomycins (BLMs), deglycobleomycins and their analogues, a significant breakthrough occurred in 2000 when the Hecht laboratory first reported the solid phase synthesis of deglycobleomycin A_5 (Scheme 2.2) [151]. This methodology was improved and applied to the synthesis of bleomycin A_5 [69(e)] and deglycobleomycin A_5 analogue with a conformationally constrained methylvalerate [100]. This has permitted the facile synthesis of various (deglyco)BLM analogues [91,152]. In 2003, the successful construction of a 108-member deglycobleomycin A_6 library further confirmed the robustness of this methodology [96].

2.1.2 Synthesis of methylvalerate and its analogues

(2*S*, 3*S*, 4*R*)-4-Amino-3-hydroxy-2-methylpentanoic acid (methylvalerate) **2.1** is one of subunits of the linker region of bleomycin (Figure 2.1). This unique β-hydroxy-γ-amino acid has attracted the interest of several research laboratories due to the challenging preparation of three contiguous stereocenters at the backbone of this compound. In the first attempt of the synthesis of **2.1**, which was reported by Yoshioka et al., the corresponding ketone derivative **2.2** was reduced nonselectively with sodium borohydride to produce a mixture of four

stereoisomers [153]. The desired isomer (2*S*, 3*S*, 4*R*) was isolated as the minor isomer from the mixture in 12% yield (Scheme 2.3). The protocol

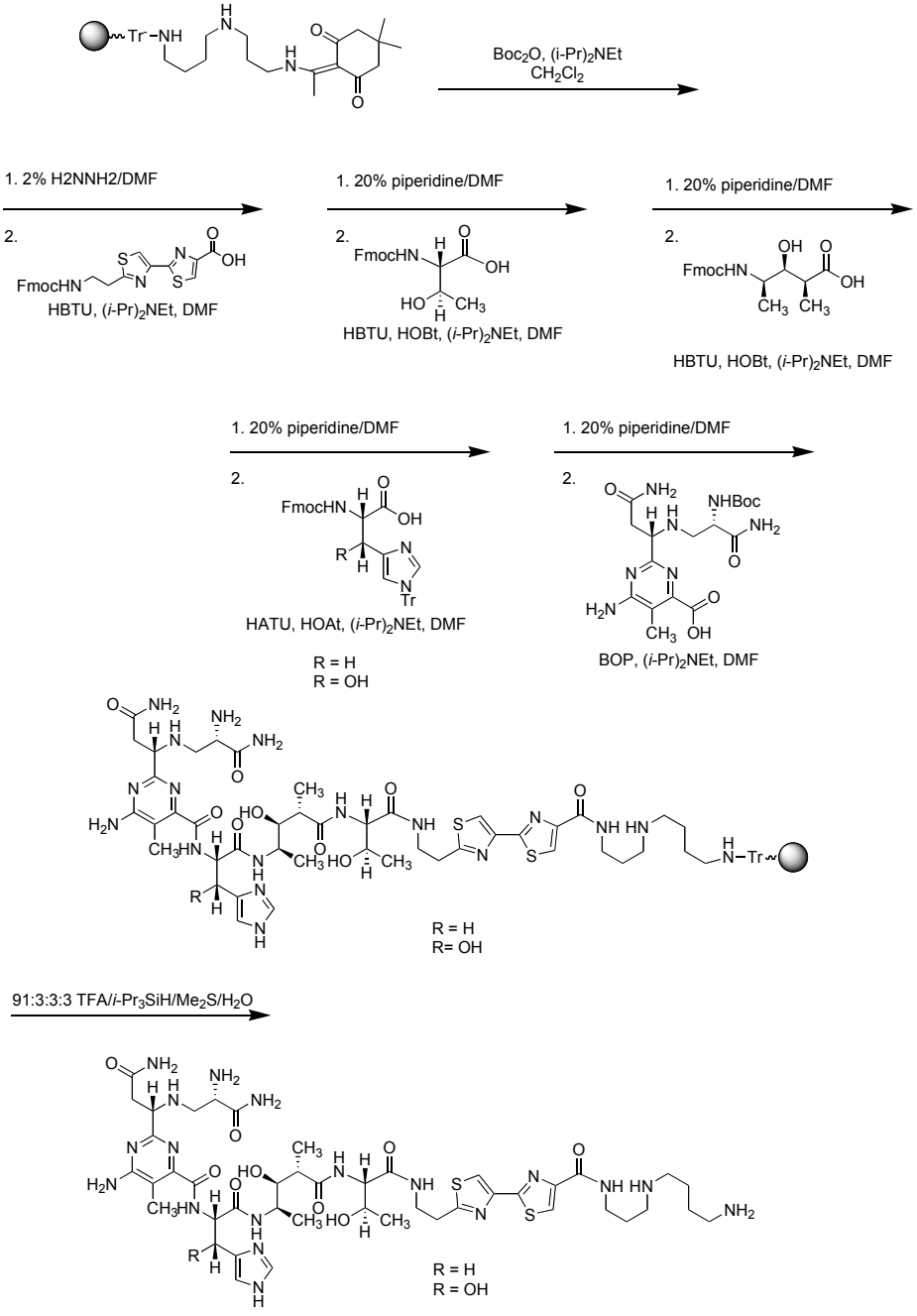

Scheme 2.2. The first reported solid phase synthesis of (deglyco)bleomycin A_5.

was improved by Hecht et al., in which the major isomer (2*R*, 3*S*, 4*R*) obtained was epimerized to the desired product via a cyclic lactam intermediate (Scheme 2.4) [154].

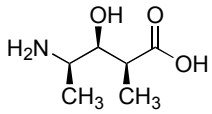

Figure 2.1. Structure of the methylvalerate moiety of BLM.

In order to improve the synthetic route, Ohgi described the first stereospecific approach to the methylvalerate moiety starting from 5-deoxy-L-arabino-γ-lactone, which could be obtained from L-rhamnose in four steps (Scheme 2.5) [155]. The 3'-hydroxyl group of compound **2.3** was mesylated selectively, followed by the formation of epoxide **2.4** under basic condition. Regioselective epoxide opening with lithium dimethylcuprate, followed by reductive debenzylation, and hydrolysis of lactam under acidic condition provided **2.1** as the HCl salt.

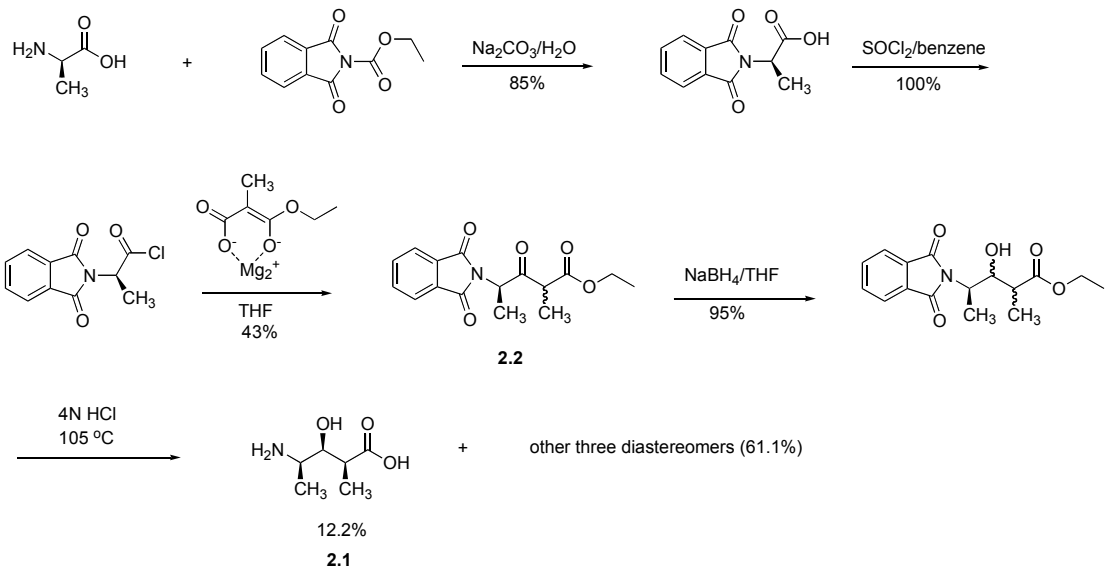

Scheme 2.3. Yoshioka's original synthesis of methylvalerate [153].

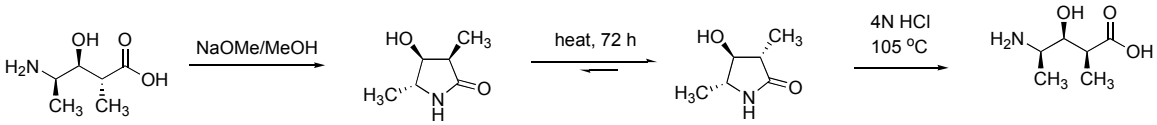

Scheme 2.4. Hecht's improvement on Yoshioka's synthesis [154].

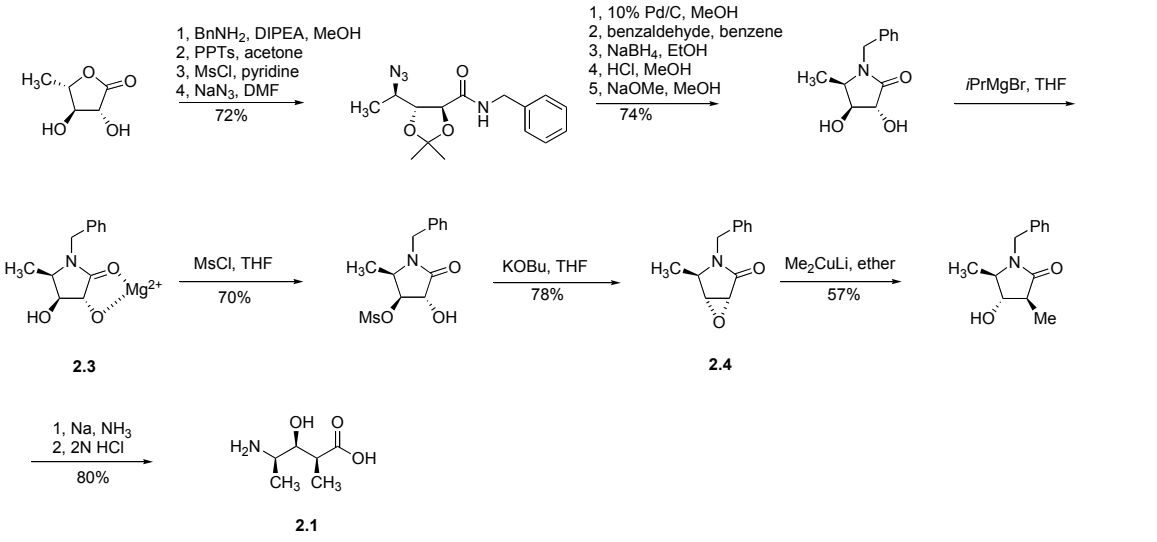

Scheme 2.5. Ohgi's stereospecific route to methylvalerate [155].

Seeking a more facile method, Ohno first employed a selective aldol reaction to generate the three consecutive stereocenters, giving isomers **2.5** and **2.6**, which were converted to methylvalerate **2.1** under acidic conditions (Scheme 2.6) [156]. A more stereocontrolled synthesis was reported by Dipardo and Bock using chiral enolates to mediate a highly stereo-controlled aldol reaction (Scheme 2.7) [157]. The aldol reaction provided the corresponding ketone **2.7**, which was reduced stereoselectively to **2.8** with zinc borohydride.

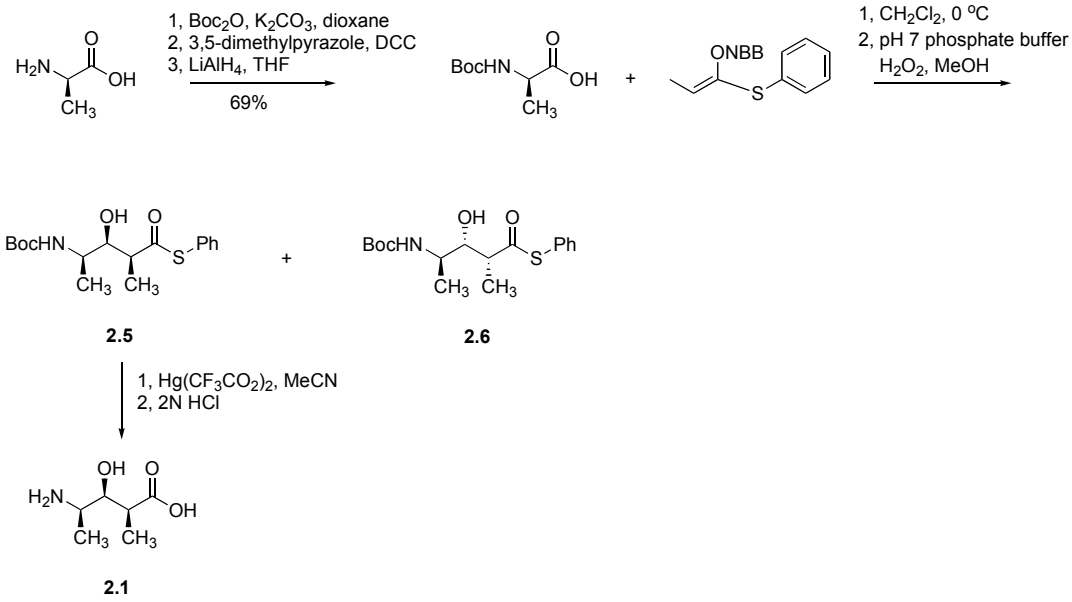

Scheme 2.6. Ohno's synthesis of methylvalerate [156].

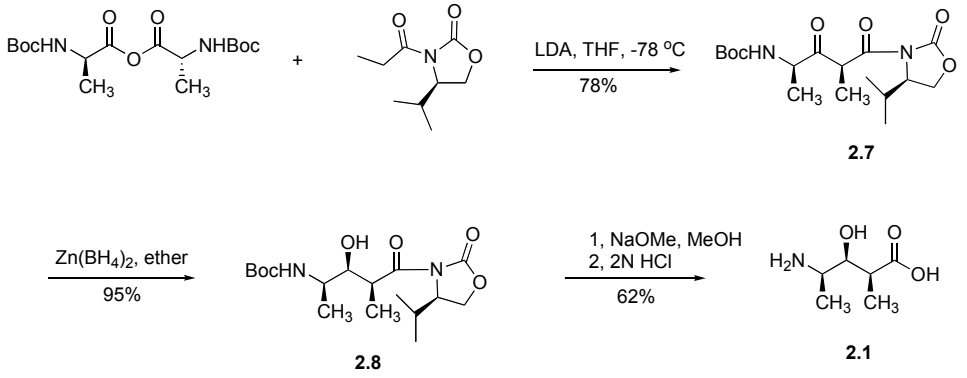

Scheme 2.7. Bock's synthesis of methylvalerate [157].

Ohno [158(a)], and later Boger [158(b)] further modified this method, in which the synthesis was simplied to three steps (Scheme 2.8) and in 61% total yield. In this method, Evans' chiral enolate was applied and proved highly efficient in mediating stereocontrolled aldol reaction [159]. This method works by temporarily creating a chiral enolate by appending a chiral auxiliary (Scheme 2.9). The pre-existing chirality from the auxiliary is then transferred to the aldol adduct by performing a diastereoselective aldol reaction. Upon subsequent removal of the auxiliary, the desired aldol stereoisomer is revealed. The synthesis of the proposed methylvalerate analogues (**2.9–2.20**) (Figure 2.2) was accomplished using Ohno and Boger's method.

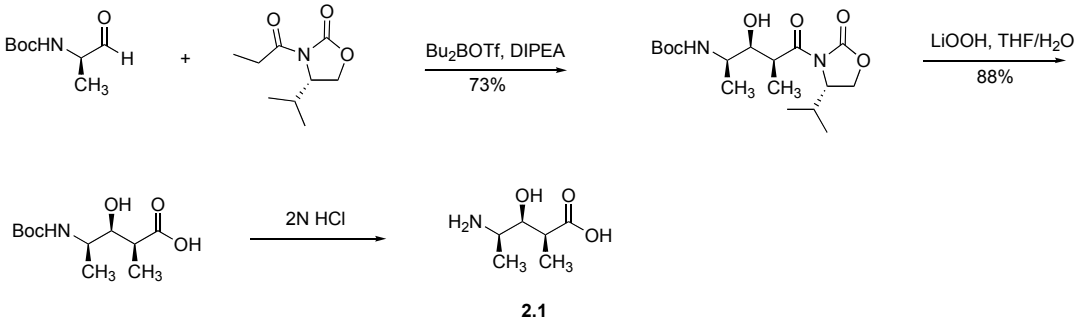

Scheme 2.8. Ohno's [158], and later Boger's [159] synthesis of methylvalerate.

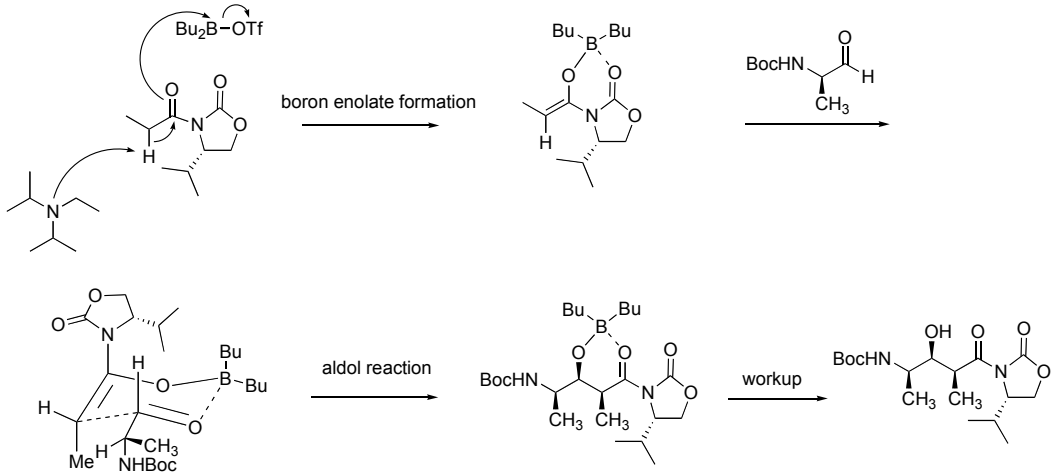

Scheme 2.9. Mechanism of Evans aldol reaction.

2.1.3 Design of methylvalerate analogues

Methyl substitutions at the C2 and C4-positions were suggested to stabilize the compact conformation to allow for efficient DNA interaction [99] while alteration of that conformation can greatly diminish DNA cleavage [100]. Additionally, it has been found that increased steric bulk at the methylvalerate C4-position can alter the efficiency and pattern of DNA cleavage [96,101]. Recently,

we have constructed a 108-member deglycoBLM A_6 library on a solid support. Two members of this library, both of which contained phenylmethylvalerate moieties, displayed potencies of supercoiled DNA relaxation greater than that of the parent deglycobleomycin [96,101]. To further investigate the effect of steric hindrance within the valerate moiety on the DNA cleavage efficiency of (deglyco) BLM, we designed a series of valerate analogues (Figure 2.2) to probe the effects of steric bulk at the C2- as well as C4-position, possibly allowing deglycoBLM to have better DNA cleavage efficiency.

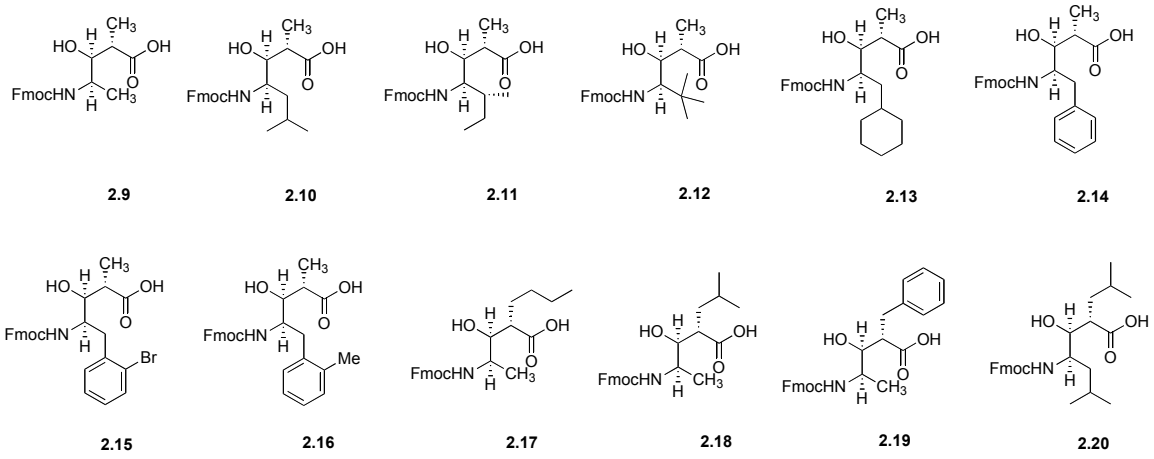

Figure 2.2. Fmoc-methylvalerate analogues prepared for incorporation into deglycobleomycin A_6 analogues.

2.2 Results

2.2.1 Analogues of methylvalerate to be incorporated into deglycobleomycin A_6

The designed analogues (Figure 2.2) involve modifications that introduce steric bulk at either the C2- or C4-position, or both of these two positions. Based on the native valerate moiety (**2.9**) of bleomycin, the methyl group was replaced with isobutyl, *sec*-butyl, and *tert*-butyl groups, to afford analogues **2.10**–**2.12**. The incorporation of **2.10** has been already reported, and exhibited a potency of relaxation of supercoiled plasmid DNA comparable to that of deglycobleomycin A_6 itself [96]. Analogues **2.11** and **2.12** were prepared; the steric alterations to the butyl group were hoped to affect the cleavage properties of BLM. Analogues **2.13**–**2.16** involve replacement of the methyl group at the C4-position with various cyclic substituents. Analogue **2.14** has already been prepared and incorporated into deglycoBLM A_6 previously; the resulting deglycoBLM analogue was shown to improve the DNA cleavage potency of deglycobleomycin [96]. The phenyl group of **2.14** was replaced with a cyclohexyl group affording **2.13.** With additional bromo and methyl groups, respectively, at the *ortho*-position of the phenyl ring of **2.14**, analogues **2.15** and **2.16** were designed to enhance the steric effects of the phenyl group in **2.14**. These modifications focused on probing the limit of effects of steric bulk at the C4-position of the methylvalerate moiety. Additionally, another three analogues containing n-butyl, isobutyl and phenyl groups at the C2-position (**2.17**–**2.19**) were prepared to probe the effect of steric bulk at this position, which has been less studied. Finally, analogue **2.10** with isobutyl groups at both the C2- and C4-positions was

prepared. This particular analogue was envisioned to provide a deglycoBLM analogue with additional steric bulk for biochemical evaluation.

2.2.2 Synthesis of Fmoc-methylvalerate moiety

The synthesis of Fmoc-methylvalerate analogues is shown in Scheme 2.10. The Weinreb amides were prepared from their corresponding Boc-protected amino acids [160,161]. Compounds **2.9a**–**2.16a** were treated with lithium aluminum hydride to afford their Boc protected aldehydes **2.9b**–**2.16b**; the resulting crude products were used for the next step without further purification. The aminoaldehydes were treated with the appropriate Z-boron enolate [92b,159] of chiral acyloxazolidinones **2.21**–**2.24**, giving products **2.9c**–**2.20c** in yields that varied from 66% to 95%. For the chiral acyloxazolidinones **2.21** [96], **2.22** [162] and **2.23** (Scheme 2.11) [163], the preparation was achieved in a single step from the corresponding acyl chlorides and lithiated oxazolidinone. Compound **2.24** was prepared by using 4-methylvaleric acid activated with pivaloyl chloride [164]. The chiral auxiliary was removed with lithium peroxide in 3:1 THF–H_2O at 0 ^{o}C. The Boc group was then removed with TFA and treated with *N*-(9-fluorenylmethoxycarbonyloxy)succinimide, which yielded the desired amino acid derivatives **2.9**–**2.20** in yields ranging from 14% to 95%.

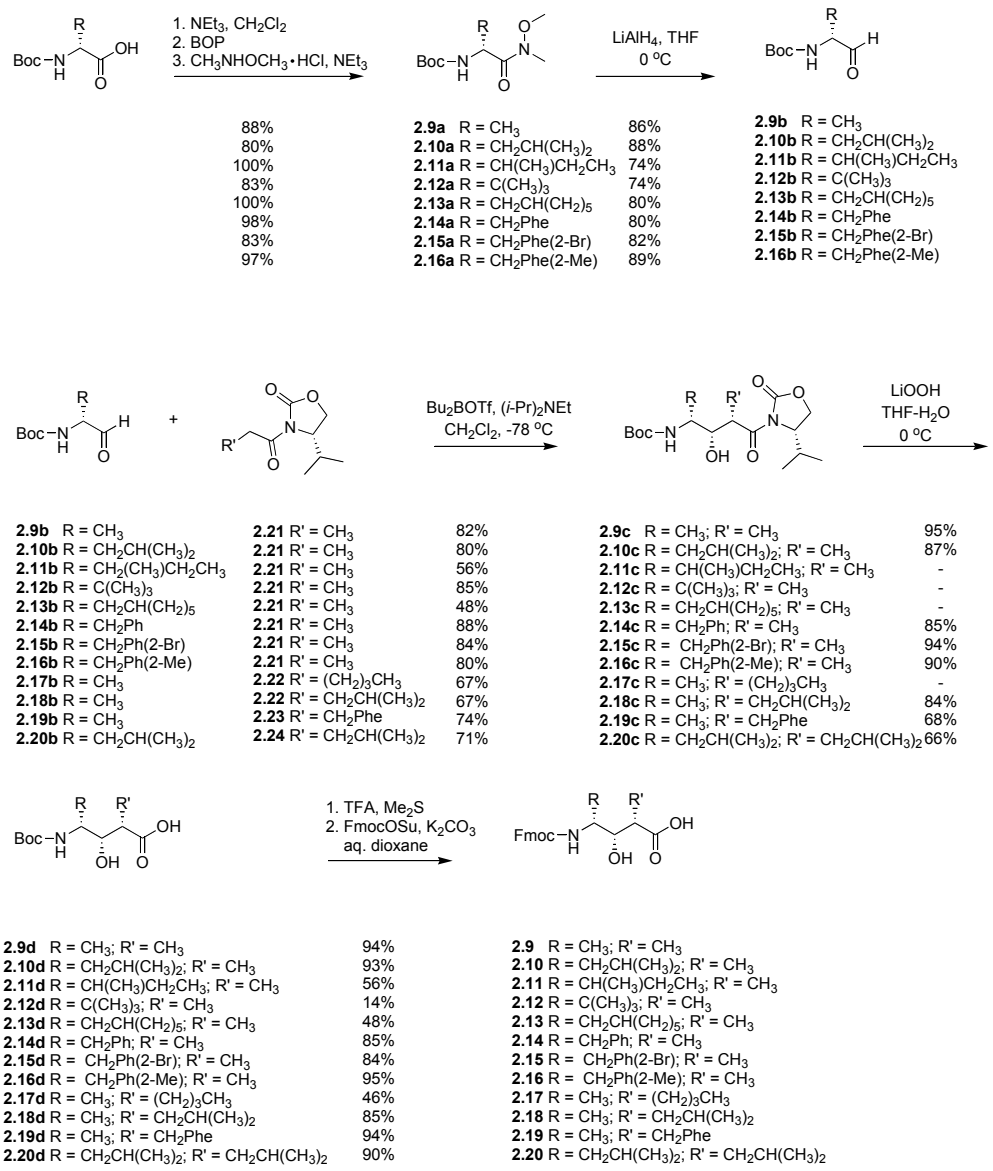

	2.9a R = CH_3	86%
88%	**2.10a** R = $CH_2CH(CH_3)_2$	88%
80%	**2.11a** R = $CH(CH_3)CH_2CH_3$	74%
100%	**2.12a** R = $C(CH_3)_3$	74%
83%	**2.13a** R = $CH_2CH(CH_2)_5$	80%
100%	**2.14a** R = CH_2Phe	80%
98%	**2.15a** R = $CH_2Phe(2\text{-}Br)$	82%
83%	**2.16a** R = $CH_2Phe(2\text{-}Me)$	89%
97%		

2.9b R = CH_3
2.10b R = $CH_2CH(CH_3)_2$
2.11b R = $CH(CH_3)CH_2CH_3$
2.12b R = $C(CH_3)_3$
2.13b R = $CH_2CH(CH_2)_5$
2.14b R = CH_2Phe
2.15b R = $CH_2Phe(2\text{-}Br)$
2.16b R = $CH_2Phe(2\text{-}Me)$

2.9b R = CH_3	**2.21** R' = CH_3	82%
2.10b R = $CH_2CH(CH_3)_2$	**2.21** R' = CH_3	80%
2.11b R = $CH_2(CH_3)CH_2CH_3$	**2.21** R' = CH_3	56%
2.12b R = $C(CH_3)_3$	**2.21** R' = CH_3	85%
2.13b R = $CH_2CH(CH_2)_5$	**2.21** R' = CH_3	48%
2.14b R = CH_2Ph	**2.21** R' = CH_3	88%
2.15b R = $CH_2Ph(2\text{-}Br)$	**2.21** R' = CH_3	84%
2.16b R = $CH_2Ph(2\text{-}Me)$	**2.21** R' = CH_3	80%
2.17b R = CH_3	**2.22** R' = $(CH_2)_3CH_3$	67%
2.18b R = CH_3	**2.22** R' = $CH_2CH(CH_3)_2$	67%
2.19b R = CH_3	**2.23** R' = CH_2Phe	74%
2.20b R = $CH_2CH(CH_3)_2$	**2.24** R' = $CH_2CH(CH_3)_2$	71%

2.9c R = CH_3; R' = CH_3	95%
2.10c R = $CH_2CH(CH_3)_2$; R' = CH_3	87%
2.11c R = $CH(CH_3)CH_2CH_3$; R' = CH_3	-
2.12c R = $C(CH_3)_3$; R' = CH_3	-
2.13c R = $CH_2CH(CH_2)_5$; R' = CH_3	-
2.14c R = CH_2Ph; R' = CH_3	85%
2.15c R = $CH_2Ph(2\text{-}Br)$; R' = CH_3	94%
2.16c R = $CH_2Ph(2\text{-}Me)$; R' = CH_3	90%
2.17c R = CH_3; R' = $(CH_2)_3CH_3$	-
2.18c R = CH_3; R' = $CH_2CH(CH_3)_2$	84%
2.19c R = CH_3; R' = CH_2Phe	68%
2.20c R = $CH_2CH(CH_3)_2$; R' = $CH_2CH(CH_3)_2$	66%

2.9d R = CH_3; R' = CH_3	94%
2.10d R = $CH_2CH(CH_3)_2$; R' = CH_3	93%
2.11d R = $CH(CH_3)CH_2CH_3$; R' = CH_3	56%
2.12d R = $C(CH_3)_3$; R' = CH_3	14%
2.13d R = $CH_2CH(CH_2)_5$; R' = CH_3	48%
2.14d R = CH_2Ph; R' = CH_3	85%
2.15d R = $CH_2Ph(2\text{-}Br)$; R' = CH_3	84%
2.16d R = $CH_2Ph(2\text{-}Me)$; R' = CH_3	95%
2.17d R = CH_3; R' = $(CH_2)_3CH_3$	46%
2.18d R = CH_3; R' = $CH_2CH(CH_3)_2$	85%
2.19d R = CH_3; R' = CH_2Phe	94%
2.20d R = $CH_2CH(CH_3)_2$; R' = $CH_2CH(CH_3)_2$	90%

2.9 R = CH_3; R' = CH_3
2.10 R = $CH_2CH(CH_3)_2$; R' = CH_3
2.11 R = $CH(CH_3)CH_2CH_3$; R' = CH_3
2.12 R = $C(CH_3)_3$; R' = CH_3
2.13 R = $CH_2CH(CH_2)_5$; R' = CH_3
2.14 R = CH_2Ph; R' = CH_3
2.15 R = $CH_2Ph(2\text{-}Br)$; R' = CH_3
2.16 R = $CH_2Ph(2\text{-}Me)$; R' = CH_3
2.17 R = CH_3; R' = $(CH_2)_3CH_3$
2.18 R = CH_3; R' = $CH_2CH(CH_3)_2$
2.19 R = CH_3; R' = CH_2Phe
2.20 R = $CH_2CH(CH_3)_2$; R' = $CH_2CH(CH_3)_2$

Scheme 2.10. Synthesis of analogues of methylvalerate.

2.2.3. Solid-phase synthesis of deglycoBLM analogues 2.26–2.36

The synthesis of deglycoBLM analogues **2.26–2.36**, is outlined in Scheme 2.12. The TentaGel amino functionalized resin (preloading of 0.48 mmol/g) was first attached with a hydrazine-labile Dde linker developed by Bycroft et al [165,166], followed by the treatment of di-Boc spermine in the presence of

Hünig's base in DMF [167]. The amino group was coupled immediately with the Fmoc-protected bithiazole in the presence of HBTU and Hünig's base in DMF. After the resin was washed successively with DMF, CH_2Cl_2 and MeOH, we assayed an aliquot of the resin using the Kaiser test to confirm the absence of free amino groups [168]. The coupling was quantified by Fmoc-cleavage with a solution of 20% piperidine in DMF and gave a loading of 0.12 mmol/g, corresponding to a 25% coupling efficiency. Fmoc cleavage was based on the dibenzylfulvene–piperidine adduct formed upon treatment of the resin with piperidine. The optical densities of 5540 M^{-1} at 290 nm and 7300 M^{-1} at 300 nm were used to calculate the loading from a known weight of dry resin. After the Fmoc group was removed from the dipeptide using a solution containing 20% piperidine in DMF, commercially available Fmoc-threonine was coupled to the free amine using HBTU, HOBt and Hünig's base in DMF. Fmoc analysis of the tripeptide indicated that the coupling had proceeded in 83% yield. Following by the removal of the Fmoc group from the resin-bound tripeptide, the synthesis of the tetrapeptide was accomplished by coupling with valerate analogues **2.10**–**2.20** (Figure 2.2), respectively, in the presence of HBTU, HOBt and Hünig's base in DMF. Fmoc analysis indicated the couplings had proceeded in yields varying from 80% to 98%. Following an additional treatment with piperidine solution, the commercial N^{α}-Fmoc-N^{im}-tritylhistidine was coupled to the resin using HATU, HOAt and Hünig's base [169,170], which provided the resin-bound pentapeptide

in 78% yield. Before the final coupling of the Boc-pyrimidoblamic acid moiety, the structure of the pentapeptide was verified by cleavage of a small sample from the resin with 2% hydrazine in DMF. The resulting solution was concentrated, and analyzed by MALDI-MS. After the molecular weight of the pentapeptide was confirmed, final Fmoc removal with 20% piperidine in DMF was followed by coupling with Boc-pyrimidoblamic acid by employing BOP and Hünig's base at 0 ^{o}C. This coupling was allowed to proceed over night in the absence of light to afford the fully protected deglycoBLM. Deprotection of the trityl and Boc groups was accomplished using a 90:5:5 TFA–Me_2S–triisopropylsilane solution [171]. The cleavage of the final products from the resin was achieved using a solution of 2% hydrazine in DMF. The crude deglycobleomycin analogues were purified by C_{18} reversed phase HPLC. The overall yields of the final coupling, deprotection and cleavage steps varied from 27% to 59%. The purified deglycobleomycin analogues were characterized by ^{1}H NMR spectroscopy and high resolution mass spectrometry.

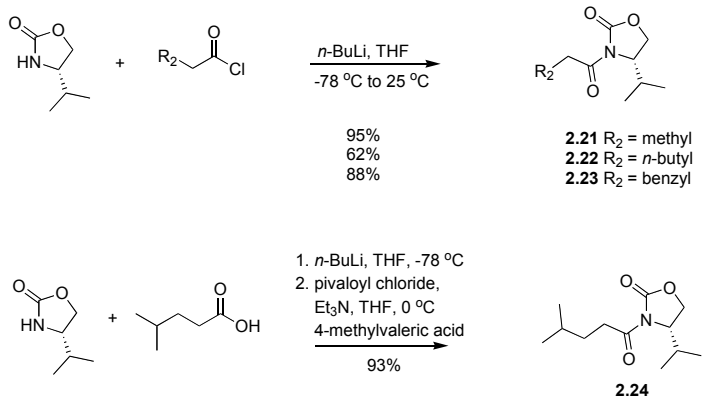

Scheme 2.11. Synthesis of chiral acyloxazolidinones.

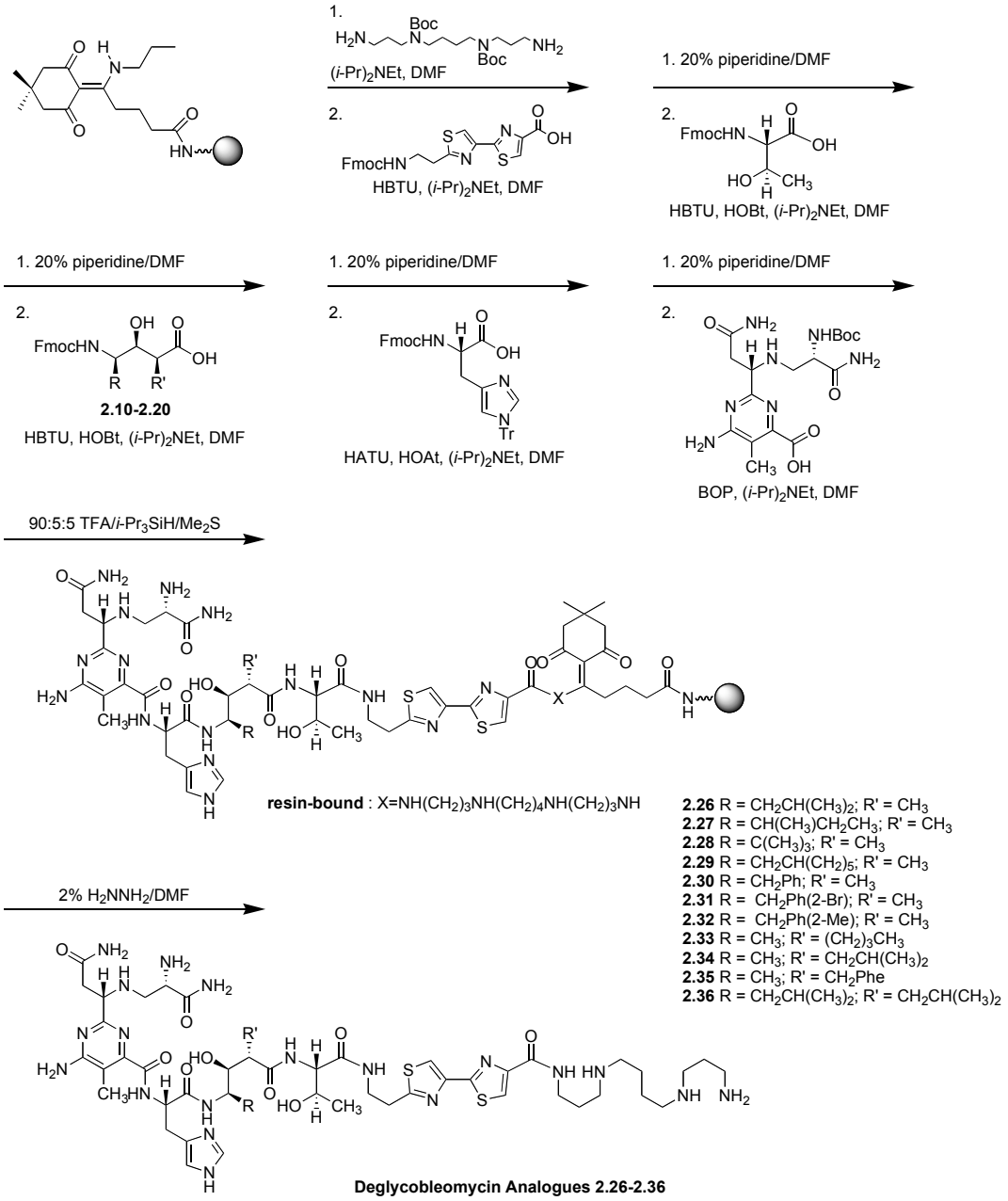

Scheme 2.12. Synthesis of deglycobleomycin analogues **2.26–2.36**.

2.2.4. Relaxation of supercoiled plasmid DNA by deglycoBLM analogues modified in the valerate moiety

All the deglycoBLM A_6 analogues were evaluated for their potency in relaxing supercoiled plasmid DNA. Figure 2.3 shows the image of agarose gel electrophoresis of plasmid DNA. A single nick at any site on the supercoiled circular (Form I) DNA results in a relaxed circular DNA, which is termed Form II DNA. The introduction of nicks on both strands of the plasmid DNA with relatively close proximity in DNA sequence produces linear duplex (Form III) DNA. This situation is illustrated schematically in Figure 2.3, which also shows where the bands will appear on the gel. Figures 2.4–2.6 shows the results of all deglycoBLM A_6 analogues in relaxing supercoiled DNA plasmid in the presence of equimolar Fe^{2+}. All of the deglycoBLM analogues containing modified valerate moieties were shown to exhibit the ability to nick supercoiled DNA. Among these, the potencies of deglycoBLMs **2.27** and **2.32** in DNA relaxation were comparable to those of deglycoBLM, itself (Figures 2.4 and 2.5). DeglycoBLMs **2.29**, **2.30**, **2.31**, **2.33**, **2.34**, **2.35** and **2.36** also displayed quite strong relaxation of supercoiled plasmid DNA, all of them were found to convert completely the supercoiled DNA substrate to nicked and linear forms when employed at 4 μM concentration in the presence of equimolar Fe^{2+}. DeglycoBLM analogues **2.26** and **2.28** exhibited moderate activity in effecting relaxation of supercoiled DNA. It is interesting that some of the analogues (notably **2.30**, **2.31**, **2.32** and **2.35**) displayed quite efficient plasmid DNA relaxation when employed at 1 μM concentration in the presence of equimolar Fe^{2+}. Also, it is notable that

introduction of ortho substituents into the aromatic ring (cf **2.30** vs **2.31** and **2.32** in Figure 2.5) was found to affect greater DNA relaxation.

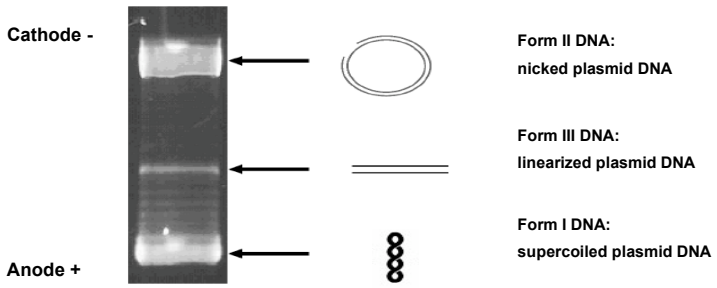

Figure **2.3.** Image of an agarose gel electrophoresis separation of plasmid DNA molecules showing the bands for three forms of plasmid DNA.

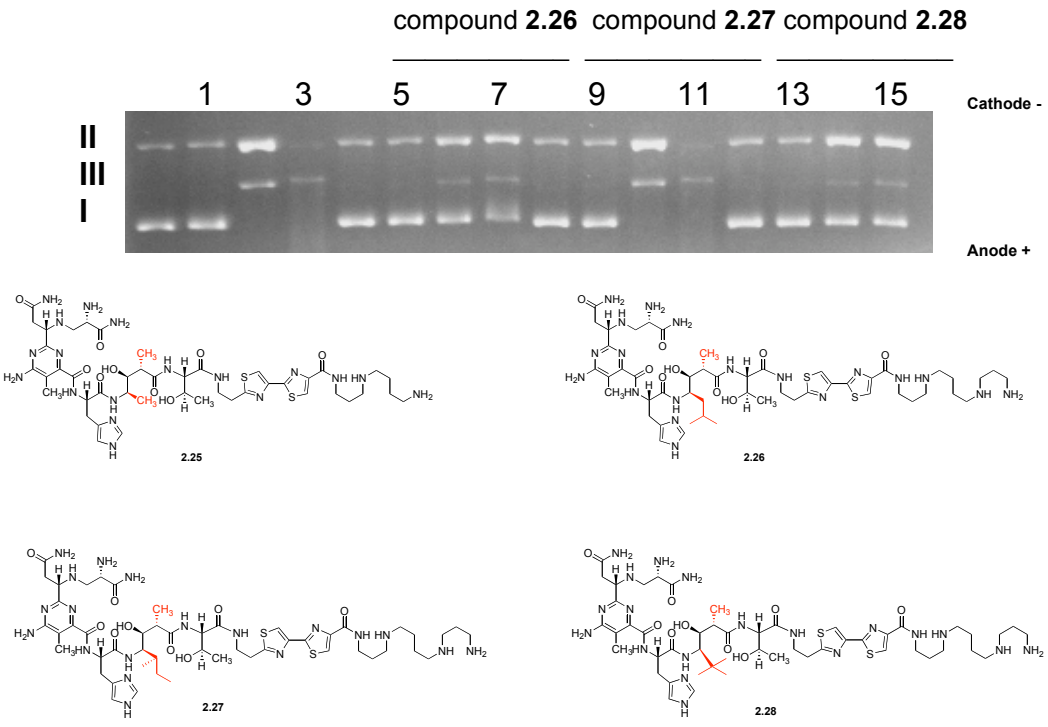

Figure 2.4. Relaxation of supercoiled pBR322 plasmid DNA by Fe(II)•deglycoBLM A_6 analogues **2.26–2.28**. Lane 1, DNA alone; lane 2, 4 μM

deglycoBLM A_5 (**2.25**); lane 3, 2 μM Fe(II)•deglycoBLM A_5 (**2.25**); lane 4, 4 μM Fe(II)•deglycoBLM A_5 (**2.25**); lane 5, 4 μM deglycoBLM **2.26**; lane 6, 1 μM Fe(II)•deglycoBLM **2.26**; lane 7, 2 μM Fe(II)•deglycoBLM **2.26**; lane 8, 4 μM Fe(II)•deglycoBLM **2.26**; lane 9, 4 μM deglycoBLM **2.27**; lane 10, 1 μM Fe(II)•deglycoBLM **2.27**; lane 11, 2 μM Fe(II)•deglycoBLM **2.27**; lane 12, 4 μM Fe(II)•deglycoBLM **2.27**; lane 13, 4 μM deglycoBLM **2.28**; lane 14, 1 μM Fe(II)•deglycoBLM **2.28**; lane 15, 2 μM Fe(II)•deglycoBLM **2.28**; lane 16, 4 μM Fe(II)•deglycoBLM **2.28**. This experiment was performed by Paul Zaleski.

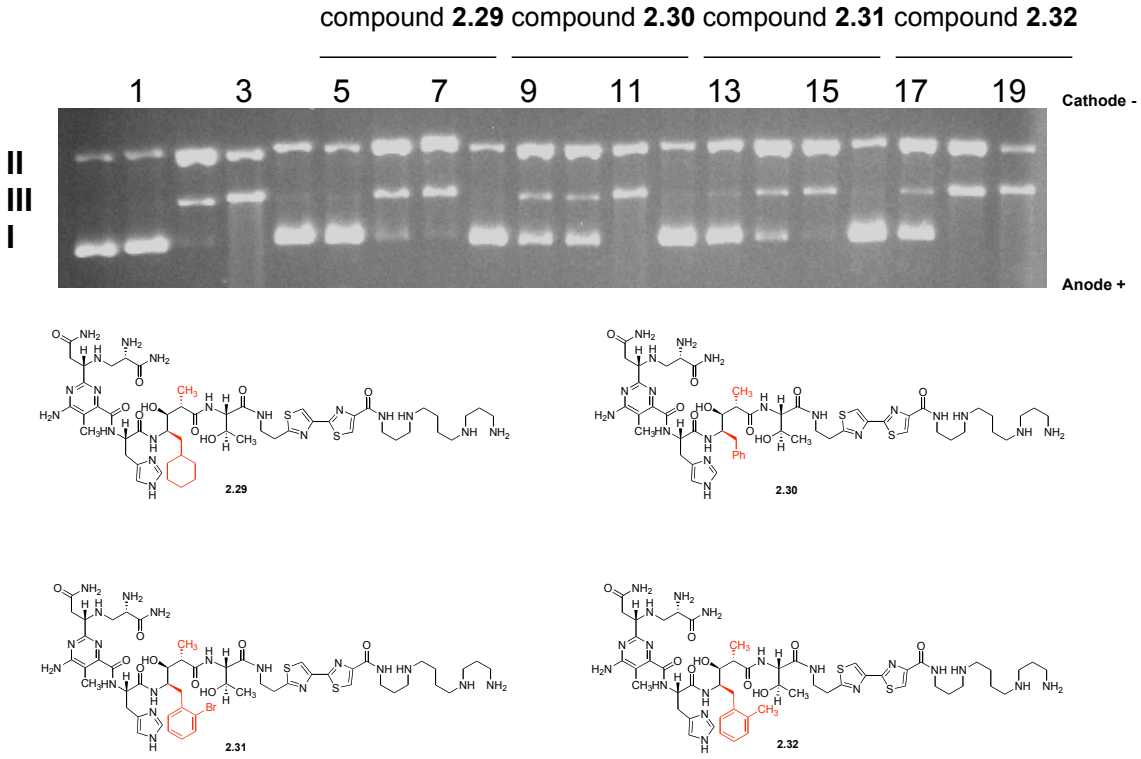

Figure 2.5. Relaxation of supercoiled pBR322 plasmid DNA by Fe(II)•deglycoBLM A_6 analogues **2.29**–**2.32**. Lane 1, DNA alone; lane 2, 4 μM deglycoBLM A_5 (**2.25**); lane 3, 2 μM Fe(II)•deglycoBLM A_5 (**2.25**); lane 4, 4 μM Fe(II)•deglycoBLM A_5 (**2.25**); lane 5, 4 μM deglycoBLM **2.29**; lane 6, 1 μM

Fe(II)•deglycoBLM **2.29**; lane 7, 2 μM Fe(II)•deglycoBLM **2.29**; lane 8, 4 μM Fe(II)•deglycoBLM **2.29**; lane 9, 4 μM deglycoBLM **2.30**; lane 10, 1 μM Fe(II)•deglycoBLM **2.30**; lane 11, 2 μM Fe(II)•deglycoBLM **2.30**; lane 12, 4 μM Fe(II)•deglycoBLM **2.30**; lane 13, 4 μM deglycoBLM **2.31**; lane 14, 1 μM Fe(II)•deglycoBLM **2.31**; lane 15, 2 μM Fe(II)•deglycoBLM **2.31**; lane 16, 4 μM Fe(II)•deglycoBLM **2.31**; lane 17, 4 μM deglycoBLM **2.32**; lane 18, 1 μM Fe(II)•deglycoBLM **2.32**; lane 19, 2 μM Fe(II)•deglycoBLM **2.32**; lane 20, 4 μM Fe(II)•deglycoBLM **2.32**. This experiment was performed by Paul Zaleski.

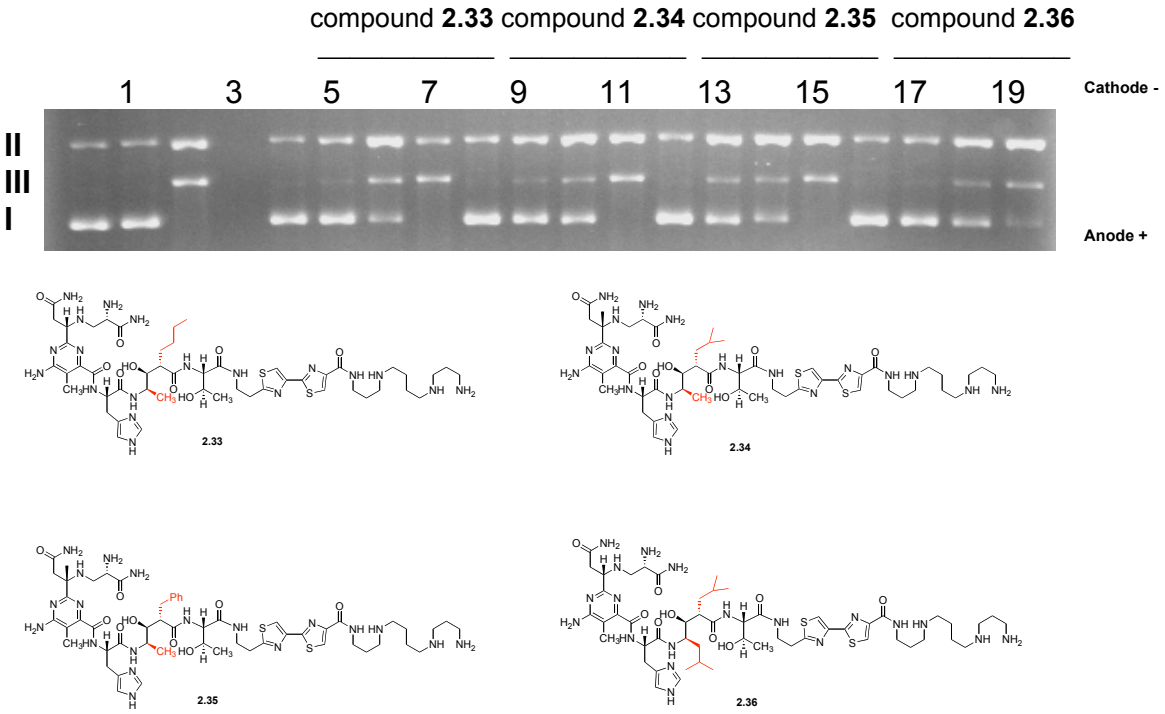

Figure 2.6. Relaxation of supercoiled pBR322 plasmid DNA by Fe(II)•deglycoBLM A_6 analogues **2.33**–**2.36**. Lane 1, DNA alone; lane 2, 4 μM deglycoBLM A_5 (**2.25**); lane 3, 2 μM Fe(II)•deglycoBLM A_5 (**2.25**); lane 4, 4 μM Fe(II)•deglycoBLM A_5 (**2.25**); lane 5, 4 μM deglycoBLM **2.33**; lane 6, 1 μM Fe(II)•deglycoBLM **2.33**; lane 7, 2 μM Fe(II)•deglycoBLM **2.33**; lane 8, 4 μM Fe(II)•deglycoBLM **2.33**; lane 9, 4 μM deglycoBLM **2.34**; lane 10, 1 μM

Fe(II)•deglycoBLM **2.34**; lane 11, 2 μM Fe(II)•deglycoBLM **2.34**; lane 12, 4 μM Fe(II)•deglycoBLM **2.34**; lane 13, 4 μM deglycoBLM **2.35**; lane 14, 1 μM Fe(II)•deglycoBLM **2.35**; lane 15, 2 μM Fe(II)•deglycoBLM **2.35**; lane 16, 4 μM Fe(II)•deglycoBLM **2.35**; lane 17, 4 μM deglycoBLM **2.26**; lane 18, 1 μM Fe(II)•deglycoBLM **2.36**; lane 19, 2 μM Fe(II)•deglycoBLM **2.36**; lane 20, 4 μM Fe(II)•deglycoBLM **2.36**. This experiment was performed by Paul Zaleski.

2.2.5. Sequence-selective DNA cleavage

We also tested the ability of each deglycoBLM analogues to affect the sequence-selective cleavage of a linear duplex DNA. This assay was performed on a 5′-^{32}P-end labeled 158-base pair DNA restriction fragment (Figure 2.7). As shown in Figure 2.8, Fe(II)•deglycoBLM A_5 itself showed several sites of cleavage. The strongest cleavage sites at the 5′-end of the labeled strand were two 5′-GC-3′ sites (5′-GC_{11}-3′ and 5′-GC_{35}-3′) and three 5′-GT-3′ sites (5′-GT_{14}-3′, 5′-GT_{17}-3′ and 5′-GT_{27}-3′). Treatment of deglycoBLM analogues **2.26**–**2.28** to some extent effected cleavage at the same sites. Analogue **2.27**, which displayed the highest potency in the relaxation of supercoiled plasmid DNA, also exhibited the strongest cleavage of the linear duplex DNA. In addition, Fe(II)•deglycoBLM analogue **2.27** was shown to effect cleavage at two new sites, which were not apparent with Fe(II)•deglycoBLM A_5 or with any of the other analogues in the present study (cf Figure 2.8, lanes 11–13). Specifically, deglycoBLM **2.27** induced unique cleavage at G_{12} and A_{15} of the duplex DNA. Compared to deglycoBLM **2.27**, Fe(II)•DeglycoBLM analogues **2.29**–**2.36** produced some but

weaker cleavage of the linear duplex DNA. Also, none of these analogues effected cleavage at G_{12} or A_{15}.

The deglycooBLM analogues were also tested for their cleavage of a 5′-^{32}P-end labeled hairpin DNA, which had been identified on the basis of its strong binding to BLM A_5 [101,172,173]. As shown in Figure 2.11, deglycoBLM analogue **2.27** produced similar but weaker cleavage on the hairpin DNA compared to deglycoBLM A_5, while cleavage by analogues **2.26** and **2.28** was even weaker than analogue **2.27**. The remaining analogues also cleaved this hairpin DNA rather weakly (data not shown).

```
  1
5'-AGCTTTAATG CGGTAGTTTA TCACAGTTAA ATTGCTAACG CAGTCAGGCA
 51
 CCGTGTATGA AATCTAACAA TGCGCTCATC GTCATCCTCG GCACCGTCAC
101
 CCTGGATGCT GTAGGCATAG GCTTGGTTAT GCCGGTACTG CCGGGCCTCT
151
 TGCGGGAT-3'
```

Figure 2.7. Sequence of the 158-base pair DNA duplex used as a substrate for cleavage by deglycoBLM analogues.

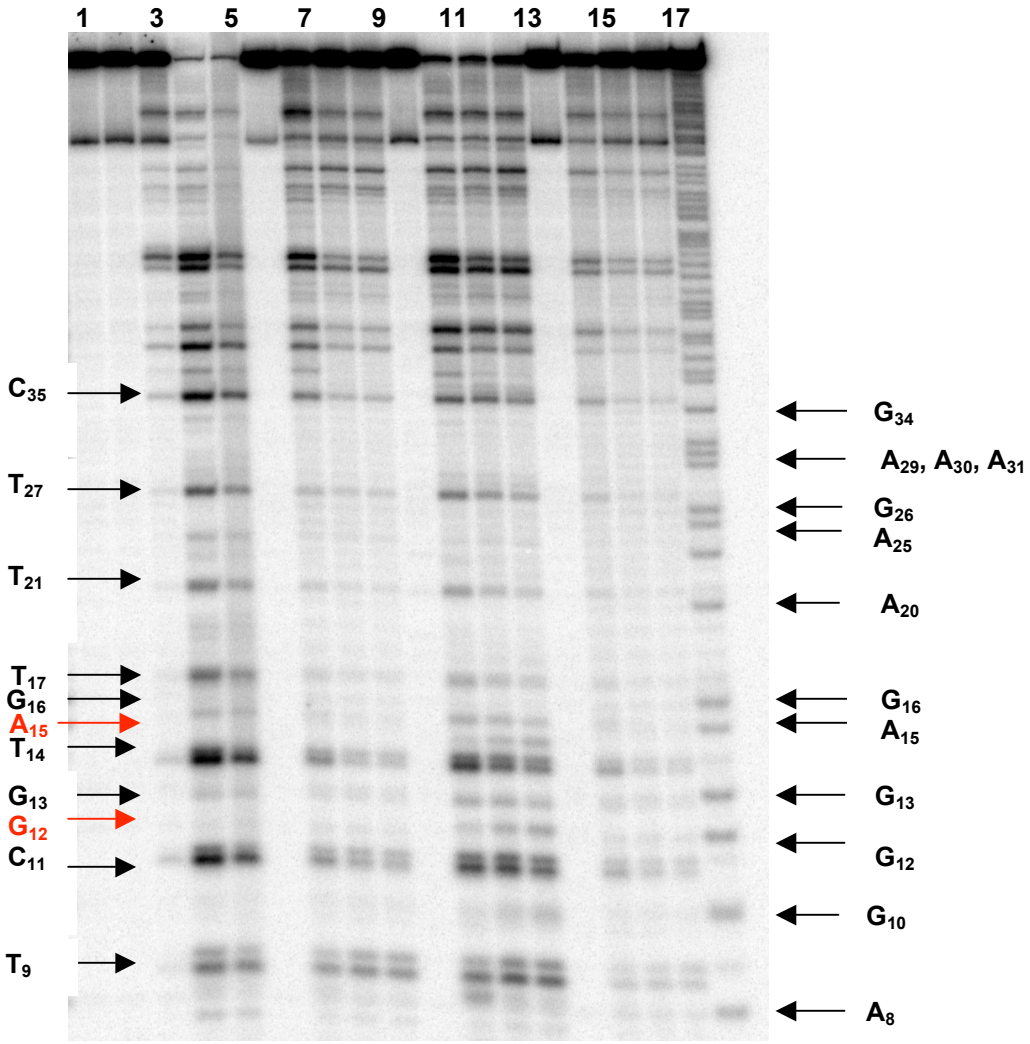

Figure 2.8. Cleavage of a [5′-^{32}P]-end labeled 158-base pair DNA duplex by deglycoBLM A_5 and deglycoBLM analogues **2.26**–**2.28**. Lane 1, DNA alone; lane 2, 10 μM deglycoBLM A_5 (**2.25**); lane 3, 1 μM Fe(II)•deglycoBLM A_5 (**2.25**); lane 4, 5 μM Fe(II)•deglycoBLM A_5 (**2.25**); lane 5, 10 μM Fe(II)•deglycoBLM A_5 (**2.25**); lane 6, 10 μM deglycoBLM **2.26**; lane 7, 1 μM Fe(II)•deglycoBLM **2.26**; lane 8, 5 μM Fe(II)•deglycoBLM **2.26**; lane 9, 10 μM Fe(II)•deglycoBLM **2.26**; lane 10, 10 μM deglycoBLM **2.27**; lane 11, 1 μM Fe(II)•deglycoBLM **2.27**; lane 12, 5 μM Fe(II)•deglycoBLM **2.27**; lane 13, 10 μM Fe(II)•deglycoBLM **2.27**; lane 14, 10 μM deglycoBLM **2.28**; lane 15, 1 μM Fe(II)•deglycoBLM **2.28**;

lane 16, 5 μM Fe(II)•deglycoBLM **2.28**; lane 17, 10 μM Fe(II)•deglycoBLM **2.28**; lane 18, G + A lane. This experiment was performed by Paul Zaleski.

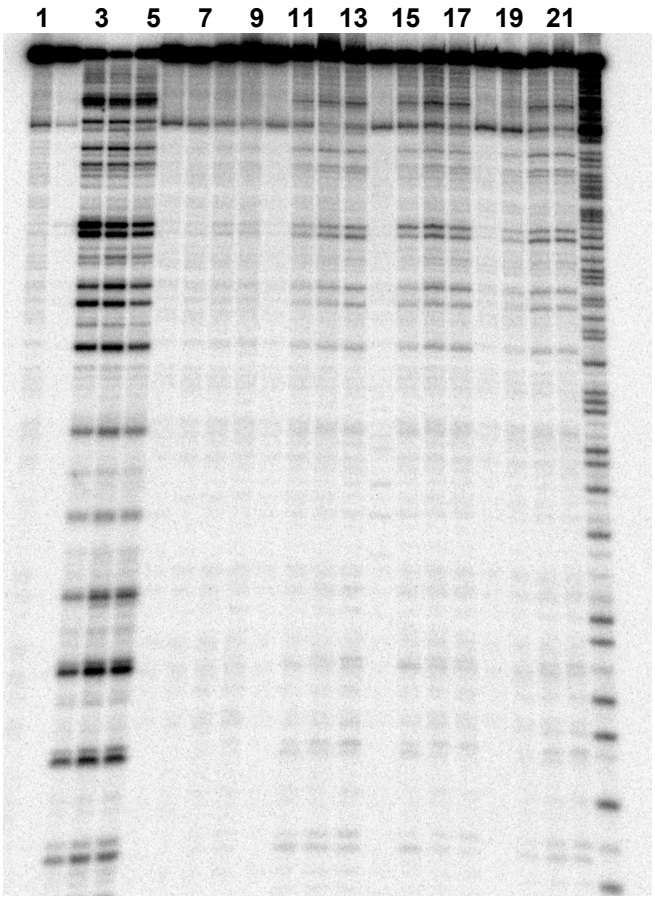

Figure 2.9. Cleavage of a [5′-^{32}P]-end labeled 158-base pair DNA duplex by deglycoBLM A_5 and deglycoBLM analogues **2.29**–**2.32**. Lane 1, DNA alone; lane 2, 10 μM deglycoBLM A_5 (**2.25**); lane 3, 1 μM Fe(II)•deglycoBLM A_5 (**2.25**); lane 4, 5 μM Fe(II)•deglycoBLM A_5 (**2.25**); lane 5, 10 μM Fe(II)•deglycoBLM A_5 (**2.25**); lane 6, 10 μM deglycoBLM **2.29**; lane 7, 1 μM Fe(II)•deglycoBLM **2.29**; lane 8, 5 μM Fe(II)•deglycoBLM **2.29**; lane 9, 10 μM Fe(II)•deglycoBLM **2.29**; lane 10, 10 μM deglycoBLM **2.30**; lane 11, 1 μM Fe(II)•deglycoBLM **2.30**; lane 12, 5 μM Fe(II)•deglycoBLM **2.30**; lane 13, 10 μM Fe(II)•deglycoBLM **2.30**; lane 14, 10 μM deglycoBLM **2.31**; lane 15, 1 μM Fe(II)•deglycoBLM **2.31**; lane 16, 5 μM Fe(II)•deglycoBLM **2.31**; lane 17, 10 μM Fe(II)•deglycoBLM **2.31**; lane 18, 10 μM deglycoBLM **2.32**; lane 19, 1 μM Fe(II)•deglycoBLM **2.32**;

lane 20, 5 μM Fe(II)•deglycoBLM **2.32**; lane 21, 10 μM Fe(II)•deglycoBLM **2.32**; lane 22, G + A lane. This experiment was performed by Paul Zaleski.

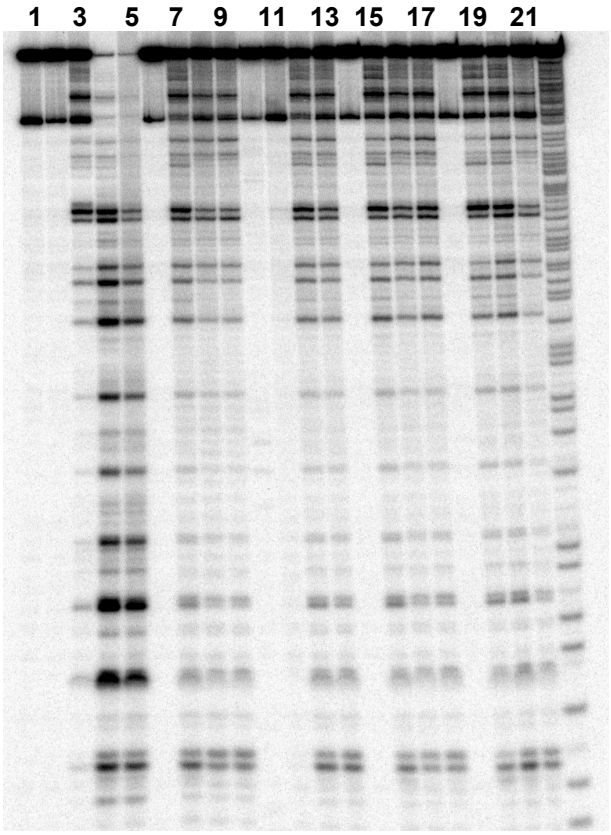

Figure 2.10. Cleavage of a [5′-^{32}P]-end labeled 158-base pair DNA duplex by deglycoBLM A_5 and deglycoBLM analogues **2.33**–**2.36**. Lane 1, DNA alone; lane 2, 10 μM deglycoBLM A_5 (**2.25**); lane 3, 1 μM Fe(II)•deglycoBLM A_5 (**2.25**); lane 4, 5 μM Fe(II)•deglycoBLM A_5 (**2.25**); lane 5, 10 μM Fe(II)•deglycoBLM A_5 (**2.25**); lane 6, 10 μM deglycoBLM **2.33**; lane 7, 1 μM Fe(II)•deglycoBLM **2.33**; lane 8, 5 μM Fe(II)•deglycoBLM **2.33**; lane 9, 10 μM Fe(II)•deglycoBLM **2.33**; lane 10, 10 μM deglycoBLM **2.34**; lane 11, 1 μM Fe(II)•deglycoBLM **2.34**; lane 12, 5 μM Fe(II)•deglycoBLM **2.34**; lane 13, 10 μM Fe(II)•deglycoBLM **2.34**; lane 14, 10 μM deglycoBLM **2.35**; lane 15, 1 μM Fe(II)•deglycoBLM **2.35**; lane 16, 5 μM Fe(II)•deglycoBLM **2.35**; lane 17, 10 μM Fe(II)•deglycoBLM **2.35**; lane 18, 10 μM deglycoBLM **2.36**; lane 19, 1 μM Fe(II)•deglycoBLM **2.36**;

lane 20, 5 μM Fe(II)•deglycoBLM **2.36**; lane 21, 10 μM Fe(II)•deglycoBLM **2.36**; lane 22, G + A lane. This experiment was performed by Paul Zaleski.

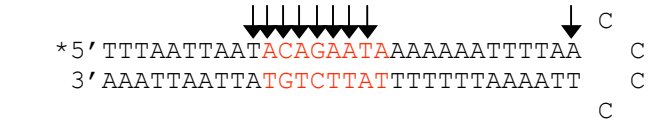

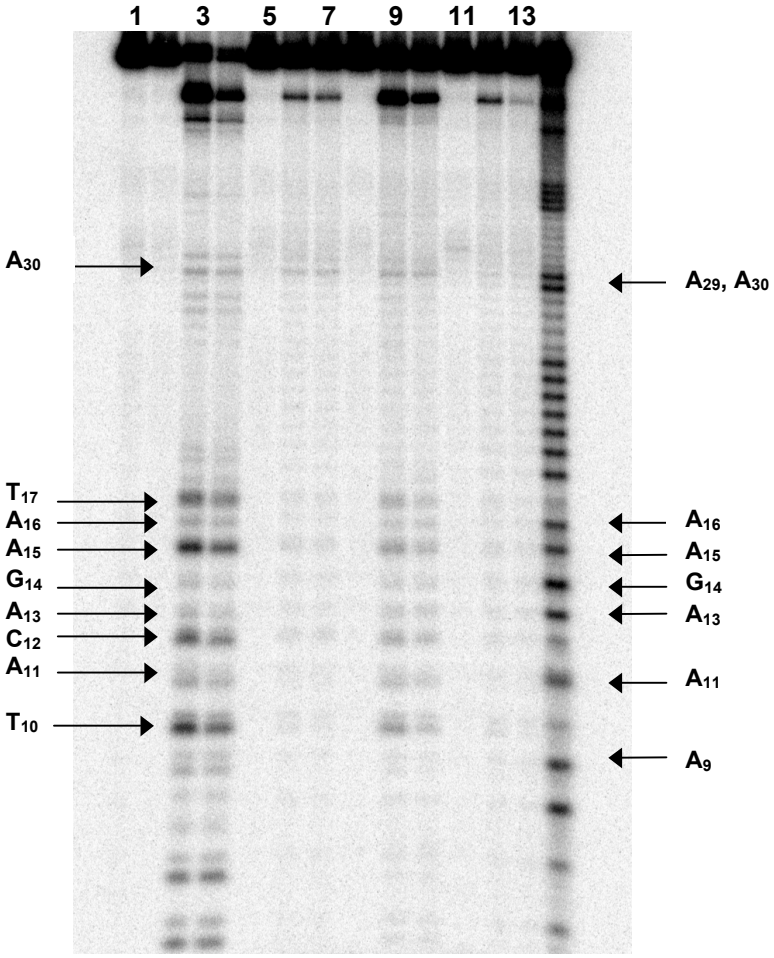

Figure 2.11. Cleavage of a [5′-^{32}P]-end labeled 64-nucleotide hairpin DNA by deglycoBLM A_5 and deglycoBLM analogues **2.26**–**2.28**. Lane 1, DNA alone; lane 2, 20 μM deglycoBLM A_5 (**2.25**); lane 3, 5 μM Fe(II)•deglycoBLM A_5 (**2.25**); lane 4, 20 μM Fe(II)•deglycoBLM A_5 (**2.25**); lane 5, 20 μM deglycoBLM **2.26**; lane 6, 5 μM Fe(II)•deglycoBLM **2.26**; lane 7, 20 μM Fe(II)•deglycoBLM **2.26**; lane 8, 20 μM deglycoBLM **2.27**; lane 9, 5 μM Fe(II)•deglycoBLM **2.27**; lane 10,

20 μM Fe(II)•deglycoBLM **2.27**; lane 11, 20 μM deglycoBLM **2.28**; lane 12, 5 μM Fe(II)•deglycoBLM **2.28**; lane 13, 20 μM Fe(II)•deglycoBLM **2.28**. This experiment performed by Paul Zaleski.

2.3 Discussion

The development of solid-phase methodology has greatly facilitated the preparation of a significant number of (deglyco) BLMs with structure alteration of the "amino acid" constitutes. The elaboration of a combinatorial library of deglycoBLMs having 108 analogues involved both single and multiple substitutions within the deglycoBLM molecule [96]. The biochemical evaluation of the 108-membered deglycoBLM library afforded some deglycoBLM analogues with unique properties, such as improved DNA relaxation potencies or different DNA cleavage patterns. The interesting properties of deglycoBLM analogues resulting from struture alteration of multiple constituents suggest that a larger combinatorial library might provide analogues having improved biochemical properties. Another important finding of this 108-membered library is that when modification of a single amino acid building block rendered the resulting (deglyco) BLM dysfunctional in DNA cleavage, incorporation of other substitutions simultaneously would not restore function [96,101]. This finding argues for the need to assure that every modified amino acid building block employed in the combinatorial library can in principle support BLM analogue function. In this study, 11 methylvalerate analogues (**2.10**–**2.20**) (Figure 2.2) were prepared as

Fmoc derivatives (Scheme 2.10) and incoporated as single modifications in each of 11 deglycoBLM analogues (Scheme 2.12). Each of the newly prepared deglycoBLM analogues was then compared with deglycoBLM A_5 in each of three types of DNA cleavage assays.

Shown in Figures 2.4–2.6 are the results of nicking of supercoiled pBR322 plasmid DNA. This assay permitted the assessment of single-strand (Form II) and double-strand (From III) DNA cleavage activity for each analogue and enabled the identification of those analogues exhibiting the greatest potency. All of the deglycoBLM analogues were found to retain their ability to nick the supercoiled plasmid DNA. As noted in Figures 2.4–2.6, deglycoBLM analogues **2.27** and **2.32** were the most potent in effecting the nicking of supercoiled plasmid DNA with a potency at least as great as deglycoBLM A_5. In comparison, deglycoBLMs **2.26** and **2.28** were the least potent analogues in mediating DNA relaxation, and the remaining seven analogues (**2.29**, **2.30**, **2.31**, **2.33**, **2.34**, **2.35** and **2.36**) displayed intermediate efficiencies. Interestingly, four of the deglycoBLM analogues (**2.30**, **2.31**, **2.32** and **2.35**) were more efficient at nicking the plasmid DNA to afford Form II DNA at a concentration of 1 μM, and analogues **2.30** and **2.35** also produced a significant amount of linear duplex (Form III) DNA when used at 1 μM concentration (Figure 2.5), suggesting a greater propensity to produce double-strand DNA nicks. Interestingly, deglycoBLM analogues **2.26**–**2.28**, which are isomers, differing only in the nature of the butyl substituent at C4-position of the

methylvalerate moiety, exhibited different DNA nicking efficiency. DeglycoBLM **2.27** was one of the two most potent analogues studied while **2.26** and **2.28** were the least potent. The deglycoBLMs having an aromatic substituent at C2- or C4-position of the methylvalerate moiety (**2.30**, **2.31**, **2.32** and **2.35**) all produced a significant amount of Form II DNA. DeglycoBLMs **2.30** and **2.35**, both of which had benzyl substituents within the methylvalerate moiety, produced the greatest amount of Form III DNA. These structural observations can help to guide the choice of additional methylvalerate analogues for preparation and evaluation.

Each of the deglycoBLM analogues was tested for sequence selectivity of DNA cleavage utilizing a 158 base pair 5′-^{32}P end-labeled DNA duplex [174]. As shown in Figure 2.8, Fe(II)•deglycoBLM A_5 produced cleavage at a number of sites, including the expected 5′-GT-3′ and 5′-GC-3′ sites, as well as 5′-AT_9-3′ and 5′-AT_{21}-3′. All 11 deglycoBLMs effected DNA strand scission, producing cleavage bands at the same positions as deglycoBLM A_5. DeglycoBLM **2.27**, which exhibited the greatest efficiency at 158-bp DNA duplex cleavage as well as plasmid DNA relaxaton, produced additional new cleavage bands at 5′-CG_{12}-3′ and 5′-TA_{15}-3′ sequences.

Recently, we have described a strategy for selecting 64-nucleotide hairpin DNAs that are bound strongly by BLM. Hairpin DNAs selected for their ability to bind strongly to BLM were used to determine the relationship between high-affinity DNA binding sites and the cleavage efficiency and selectivity of BLM on

these DNAs. While the characterization of the cleavage of such DNAs by Fe•BLM is ongoing, the first two reports [101,173] make it clear that such strongly bound DNAs are cleaved at sites quite different from those of randomly chosen DNAs, that alkali labile lesions are more prominent, and that BLM analogues (such as deglycoBLM) exhibit cleavage patterns that are significantly different from those displayed by BLM itself [101,173].

Accordingly, one of the strongly bound hairpin DNAs has been employed as a substrate for cleavage by deglycoBLMs **2.26**–**2.36**. As shown in Figure 2.11, deglycoBLM analogue **2.27**, which provide strong cleavage of the 158-base pair DNA duplex, was also the most efficient at mediating cleavage of the 64-nucleotide hairpin DNA substrate. Unlike the linear DNA duplex, which was cleaved by **2.27** at two new sites, the cleavage pattern of the hairpin DNA was the same for **2.27** and for deglycoBLM A_5.

2.4 Experimental

General methods: Chemicals and solvents were of reagent grade and were used without further purification. All reactions involving air or moisture-sensitive reagents or intermediates were performed under an argon atmosphere. Flash chromatography was carried out using Silicycle 200-400 mesh silica gel. Analytical TLC was carried out using 0.25 mm EM silica gel 60 F_{250} plates that were visualized by irradiation (254 nm) or by staining with *p*-anisaldehyde stain. HPLC

separations were performed on a Waters 600 series HPLC multi-solvent delivery system using a Kratos 747 UV detector. The crude products were purified on an Alltech Alltima C_{18} reversed phase semi-preparative (250 x 10 mm, 5 μm) HPLC column using aq 0.1% TFA and CH_3CN mobile phases. A linear gradient was employed (100:0 0.1% aq TFA/CH_3CN → 40:60 0.1% aq TFA/CH_3CN) over a period of 30 min at a flow rate of 4 mL/min. ^1H and ^{13}C NMR spectra were obtained using Inova 400, Inova 500 or VNMRS 800 MHz Varian instruments. Chemical shifts were reported in parts per million (ppm, δ) referenced to the residual ^1H resonance of the solvent ($CDCl_3$, 7.26 ppm). ^{13}C spectra were referenced to the residual ^{13}C resonance of the solvent ($CDCl_3$, 77.0 ppm). Splitting patterns were designated as follows: s, singlet; br, broad; d, doublet; dd, doublet of doublets; t, triplet; q, quartet; m, multiplet. High resolution mass spectra were obtained in the Arizona State University CLAS High Resolution Mass Spectrometry Laboratory.

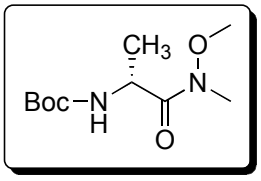

***N*-(*t*-Butoxycarbonyl)-D-alanine *N*-methyoxyl-*N*-methylamine (2.9a) [96].** To a solution of 5.00 g (26.4 mmol) of *N*-D-Boc-alanine in 150 mL of CH_2Cl_2 was added 3.70 mL (26.4 mmol) of NEt_3 and 11.7 g (26.4 mmol) of benzotriazol-1-

yloxytris(dimethylamino)-phosphonium hexafluorophosphate (BOP). The mixture was stirred at room temperature for 5 min, and 2.80 g (29.1 mmol) of *O,N*-dimethylhydroxylamine hydrochloride was added, followed by 4.10 mL (29.1 mmol) of NEt_3. The pH of the reaction was kept at a value higher than 8.0 and the progress of the reaction was monitored by silica gel TLC. The transformation was complete within 2 h. The reaction mixture was then diluted with 300 mL of EtOAc and washed with three 50-mL portions of 1 N HCl and three 50-mL portions of sat aq $NaHCO_3$. The combined organic layer was washed with brine, dried ($MgSO_4$) and concentrated under diminished pressure. The crude product was then purified by chromatography on a silica gel column (15 x 5 cm). Elution with 2:1 hexanes–EtOAc gave **2.9a** as a white solid: yield 5.4 g (88%); silica gel TLC R_f 0.55 (1:1 hexanes–EtOAc); ^{1}H NMR ($CDCl_3$) δ 1.29 (d, 3H, J = 6.8 Hz), 1.42 (s, 9H), 3.19 (s, 3H), 3.75 (s, 3H), 4.66 (d, 1H, J = 6.4 Hz) and 5.25 (d, 1H, J = 7.2 Hz); ^{13}C NMR ($CDCl_3$) δ 18.7, 28.3, 32.1, 46.5, 61.5, 79.5, 155.2 and 173.7; mass spectrum (MALDI-TOF), *m/z* 255.1 $(M+Na)^+$ (theoretical 255.1).

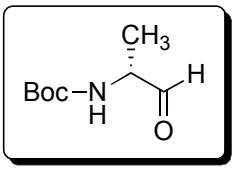

***N*-(*t*-Butoxycarbonyl)-D-alaninal (2.9b) [96].** To a stirred solution of 4.42 g (19.0 mmol) of *N*-(*t*-butoxycarbonyl)-D-alanine *N*-methyoxyl-*N*-methylamine **2.9a** in 120 mL of anhydrous THF was added 903 mg (23.8 mmol) of $LiAlH_4$ at 0 °C. The reaction was slowly warmed to room temperature and its progress was monitored by TLC. Reduction was complete within 2–3 h, and the reaction was quenched by slow addition of 3.70 g (1.40 mmol) of $KHSO_4$ in 20 mL of water at 0 °C. The resulting mixture was extracted with three 50-mL portions of EtOAc, and the organic layer was washed with three 30-mL portions of 1 N HCl and three 30-mL portions of sat aq $NaHCO_3$. The combined organic layer was then washed with brine, dried over Na_2SO_4 and concentrated under diminished pressure to give **2.9b** as a white solid: yield 2.8 g (86%); silica gel TLC R_f 0.60 (1:1 hexanes–EtOAc); ^{1}H NMR ($CDCl_3$) δ 1.31 (d, 3H, J = 7.2), 1.45 (s, 9H), 4.21 (dq, 1H, J = 6), 5.09 (br, 1H) and 9.54 (s, 1H).

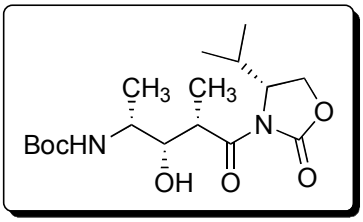

(*1R,2S,3S,4'S*)-[2-Hydroxy-4-(4'-isopropyl-2'-oxo-oxazolidine-3'-yl)-1,3-dimethyl-4-oxobutyl]carbamic acid *tert*-butyl ester (2.9c) [96]. To a stirred solution of 1.10 g (6.49 mmol) of *(S)*-(+)-4-isopropyl-3-propionyl-2-oxazolidinone **2.21** in 1 mL of anhydrous CH_2Cl_2 at 0 °C was added 6.91 mL (6.91 mmol) of a 1.0 M solution of Bu_2BOTf in CH_2Cl_2 followed by 1.20 mL (9.10

mmol) of (iPr)$_2$NEt. After 45 min, the solution was cooled to –78 ^{o}C for 15 min. A solution of 1.10 g (6.51 mmol) of *N*-(*tert*-butoxycarbonyl)-D-alaninal **2.9b** in 4 mL of CH_2Cl_2 was added and the solution was allowed to warm to room temperature overnight. The reaction was quenched by the addition of 10 mL of potassium phosphate buffer, pH 7, and was then extracted with three 50-mL portions of Et_2O. The combined organic layer was washed with brine and concentrated under diminished pressure. The crude oil was dissolved in 21 mL of MeOH and cooled to 0 ^{o}C, then 7mL of 30% H_2O_2 was added slowly. The mixture was stirred at 0 ^{o}C for 4 h, then 20 mL of water was added and the reaction mixture was concentrated under diminished pressure. The residue was extracted with three 30-mL portions of ethyl ether and the combined organic layer was washed with three 30-mL portions of 5% $NaHCO_3$. The resulting organic solution was washed with brine, dried over Na_2SO_4 and concentrated under diminished pressure. The residue was purified by flash chromatography on a silica gel column (25 x 3.2 cm). Elution with 1:4 hexanes/EtOAc gave **2.9c** as a colorless solid: yield 1.90 g (82%); silica gel TLC R_f 0.56 (1:1 hexanes–EtOAc); ^{1}H NMR ($CDCl_3$) δ 0.84 (d, 3H, J = 7.2), 0.88 (d, 3H, J = 7.2), 1.16 (d, 3H, J = 6.4), 1.27 (d, 3H, J = 6.8), 1.41 (s, 9H), 2.31 (m, 1H), 3.05 (br, 1H), 3.72 (br, 2H), 3.95 (br, 1H), 4.16-4.27 (m, 2H), 4.41-4.45 (m, 1H) and 4.60 (br, 1H); mass spectrum (MALDI-TOF), *m/z* 381.2 $(M+Na)^+$ (theoretical 381.2).

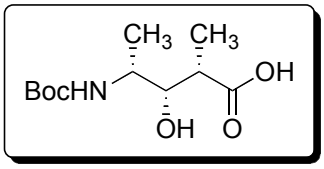

(2*S*,*3S*,*4R*)-4-*tert*-Butoxycarbonylamino-3-hydroxy-2-methylpentanoic acid (2.9d) [96]. To a cooled (0 °C) solution containing 2.96 g (8.27 mmol) of **2.9c** in 64 mL of 3:1 THF–H_2O was added 0.76 mL (49.6 mmol) of 30% H_2O_2 followed by 396 mg (16.5 mmol) of LiOH. After stirring at 0 °C for 3 h, the excess peroxide was quenched at 0 °C by the addition of 33 mL of 1.5 N aq Na_2SO_3 and the pH was adjusted to 9–10 with sat aq $NaHCO_3$. The oxazolidinone was recovered by extraction with three 20-mL portions of CH_2Cl_2. The aqueous layer was then acidified to pH~2 with 1 N HCl, and extracted with three 40-mL portions of EtOAc. The combined organic layer was dried over Na_2SO_4 and concentrated under diminished pressure to give the crude product as a colorless solid: yield 1.94 g (95%); silica gel TLC R_f 0.10 (8:2:0.2:0.1 CH_2Cl_2–hexanes–MeOH–AcOH); $[\alpha]_D^{23}$ +1.61 (*c* 0.50, MeOH); ^{1}H NMR ($CDCl_3$) δ 1.17 (d, 3H, *J* = 6.4 Hz), 1.26 (d, 3H, *J* = 6.8 Hz), 1.41 (s, 9H), 2.64 (m, 1H), 4.09-4.11 (m, 2H), 4.79 (d, 1H, *J* = 6.8 Hz) and 5.98 (br, 1H).

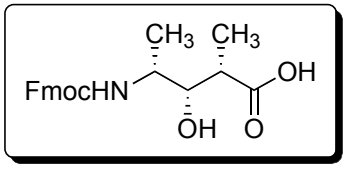

(2*S*,*3S*,*4R*)-4-(*H*-Fluoren-9-ylmethoxycarbonylamino)-3-hydroxy-2-methylpentanoic acid (2.9e) [96]: To a solution of 985 mg (3.98 mmol) of **1d** in

7 mL of Me_2S was added 21 mL of TFA. The reaction mixture was stirred at room temperature for 2 h. The solution was concentrated under a stream of argon and concentrated further under diminished pressure. The resulting oil was dissolved in 21 mL of 5% aq K_2CO_3 solution followed by the addition of 1.50 g (4.38 mmol) of *N*-(9-fluorenyl methoxycarbonyloxy) succinimide (FmocOSu) in 14 mL of dioxane. The reaction was stirred at room temperature overnight, and the solution was extracted successively with three 20-mL portions of ethyl ether and three 20-mL portions of EtOAc. The combined organic layer was dried over Na_2SO_4, filtered and concentrated under diminished pressure. The crude product was purified by flash chromatography on a silica gel column (25 x 3.2 cm). Elution with 93:5:2 CH_2Cl_2–MeOH–AcOH gave **2.9e** as a yellow solid: yield 1.38 g (94%); mp 92-94 ºC; silica gel TLC R_f 0.14 (8:2:0.2:0.1 CH_2Cl_2–hexanes–MeOH–AcOH); $[\alpha]_D^{23}$ +1.6 (*c* 0.50, MeOH); ^{1}H NMR ($CDCl_3$) δ 1.17 (d, 3H, *J* = 5.2), 1.25 (d, 3H, *J* = 6.4), 2.59 (m, 1H), 3.76-3,79 (m, 2H), 4.17-4.18 (m, 1H), 4.39-4.46 (m, 2H), 4.89 (d, 1H, *J* = 7.6), 7.27-7.31 (m, 2H), 7.35-7.39 (m, 2H), 7.55 (d, 2H, *J* = 7.2) and 7.74 (d, 2H, *J* = 7.6); ^{13}C NMR ($CDCl_3$) δ 11.9, 16.2, 41.8, 47.3, 48.9, 66.6, 74.9, 120.0, 124.9, 127.1, 127.8, 141.3, 143.8, 156.1 and 178.0; mass spectrum (MALDI-TOF), *m/z* 392.1 $(M+Na)^+$ (theoretical 392.1).

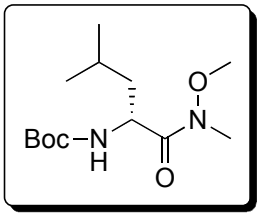

***N*-(*t*-Butoxycarbonyl)-D-leucine *N*-methyoxyl-*N*-methylamine (2.10a) [96].** To a solution of 2.00 g (8.62 mmol) of *N*-D-Boc-leucine in 30 mL of CH_2Cl_2 was added 1.20 mL (8.62 mmol) of NEt_3 and 3.80 g (8.62 mmol) of BOP. The mixture was stirred at room temperature for 5 min, and 0.93 g (9.53 mmol) of *O,N*-dimethylhydroxylamine hydrochloride was added, followed by 1.30 mL (9.53 mmol) of NEt_3. The pH of the reaction was kept at a value higher than 8.0 and the progress was monitored by silica gel TLC. The transformation was complete within 2 h. The reaction mixture was then diluted with 100 mL of EtOAc and washed three 20-mL portions of 1 N HCl and three 20-mL portions of sat aq $NaHCO_3$. The combined organic layer was washed with brine, dried ($MgSO_4$) and the solvent was concentrated under diminished pressure. The crude product was then purified by chromatography on a silica gel column (15 x 5 cm). Elution with 2:1 hexanes–EtOAc gave **2.10a** as a colorless oil: yield 1.90 g (80%); silica gel TLC R_f 0.50 (1:1 hexanes–EtOAc); ^{1}H NMR ($CDCl_3$) δ 0.91 (d, 6H, J = 6.4 Hz), 1.39 (s, 9H), 1.36-1.44 (m, 2H), 1.64-1.71 (m, 1H), 3.19 (s, 3H), 3.75 (s, 3H), 4.68 (d, 1H, J = 3.6 Hz) and 5.03 (d, 1H, J = 9.2 Hz); mass spectrum (MALDI-TOF), *m/z* 297.2 $(M+Na)^+$ (theoretical 297.2).

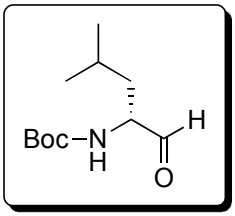

***N*-(*t*-Butoxycarbonyl)-D-leucinal (2.10b) [96].** To a stirred solution of 1.17 g (4.31 mmol) of *N*-(*t*-butoxycarbonyl)-D-leucine *N*-methyoxyl-*N*-methylamine **2.10a** in 50 mL of anhydrous THF was added 203 mg (5.31 mmol) of $LiAlH_4$ at 0 ^oC. The reaction was slowly warmed to room temperature and its progress was monitored by TLC. Reduction was usually completed with 2–3 h, and then was quenched by slow addition of 0.8 g (1.44 mmol) of $KHSO_4$ in 10 mL of water at 0 ^oC. The resulting mixture was extracted with three portions of 30 mL of EtOAc, and the organic layer was washed three times with 20 mL of 1N HCl and three times with 20 mL of sat aq $NaHCO_3$. The combined organic layer was then washed with brine, dried over Na_2SO_4 and concentrated under diminished pressure to give **2.10b** as a colorless oil: yield 805 mg (88%); silica gel TLC R_f 0.56 (1:1 hexanes–EtOAc); ^1H NMR ($CDCl_3$) δ 0.92-0.94 (m, 6H), 1.45 (s, 9H), 1.38-1.91 (m, 3H), 4.23 (m, 1H), 4.94 (s, 1H) and 9.55 (s, 1H).

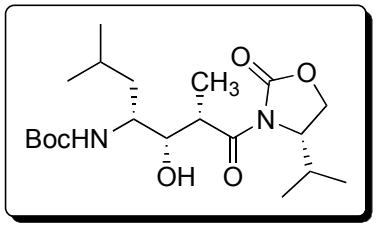

(*1R,2S,3S,4'S*)-[2-Hydroxy-1-isobutyl-4-(4'-isopropyl-2'-oxo-oxazolidine-3'-yl)-3-methyl-4-oxo-butyl]carbamic acid *tert*-butyl ester (2.10c) [96]. To a stirred solution of 650 mg (3.45 mmol) of *(S)*-(+)-4-isopropyl-3-propionyl-2-oxazolidinone **2.21** in 1 mL of anhydrous CH_2Cl_2 at 0 °C was added 4.00 mL (4.00 mmol) of a 1.0 M solution of Bu_2BOTf in CH_2Cl_2 followed by 0.90 mL (5.33 mmol) of $(i\text{Pr})_2\text{NEt}$. After 45 min, the solution was cooled to –78 °C for 15 min. A solution of 816 mg (3.81 mmol) of *N*-(*tert*-butoxycarbonyl)-D-leucinal **2.10b** in 4 mL of CH_2Cl_2 was added and the solution was allowed to warm to room temperature overnight. The reaction was quenched by the addition of 10 mL of pH 7 potassium phosphate buffer, and was then extracted with three portions of 30 mL of Et_2O. The combined organic layer was washed with brine and concentrated under diminished pressure. The crude oil was dissolved in 15 mL of MeOH and cooled to 0 °C, then 5 mL of 30% H_2O_2 was added slowly. The mixture was stirred at 0 °C for 4 h when 10 mL of water was added and the reaction mixture was concentrated under diminished pressure. The residue was extracted with three 20-mL portions of ethyl ether and the combined organic layer was washed with three 30-mL portions of 5% $NaHCO_3$. The resulting organic solution was washed with brine, dried over Na_2SO_4 and concentrated under diminished pressure. The residue was purified by flash chromatography on a silica gel column. Elution with 1:4 hexanes–EtOAc gave **2.10c** as a colorless solid: yield 1.10 g (80%); mp 133-134 °C; silica gel TLC R_f 0.51 (1:1 hexanes–EtOAc); ^{1}H

NMR ($CDCl_3$) δ 0.83-0.90 (m, 12H), 1.29 (d, 3H, J = 7.2), 1.40 (s, 9H), 1.70 (m, 2H), 2.30 (m, 1H), 3.12 (d, 1H, J = 3.6), 3.62-3.70 (m, 2H), 3.94-4.00 (m, 1H), 4.16-4.26 (m, 3H) and 4.35-4.44 (m, 2H); ^{13}C NMR ($CDCl_3$) δ 11.7, 14.6, 17.9, 21.5, 23.8, 24.7, 28.3, 28.3, 39.4, 40.8, 50.6, 58.2, 63.2, 74.7, 79.4, 153.3, 155.7 and 177.6; mass spectrum (MALDI-TOF), *m/z* 423.2 $(M+Na)^+$(theoretical 423.2).

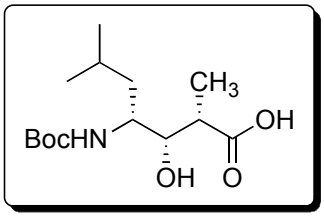

(2*S*,3*S*,4*R*)-4-*tert*-Butoxycarbonylamino-3-hydroxy-2,6-dimethylheptanoic acid (2.10d) [96]. To a cooled (0 °C) solution containing 826 mg (2.06 mmol) of **2.10c** in 36 mL of 3:1 THF–H_2O was added 1.90 mL (13.4 mmol) of 30% H_2O_2 followed by 99.0 mg (4.10 mmol) of LiOH. After stirring at 0 °C for 3 h, the excess peroxide was quenched at 0 °C by the addition of 8.2 mL of 1.5N aq Na_2SO_3 and the pH was adjusted to 9–10 with sat aq $NaHCO_3$, and the oxazolidinone was removed by extraction with three 10-mL portions of CH_2Cl_2. The aqueous layer was then acidified to pH~2 with 1N HCl, and extracted with three 10-mL portions of EtOAc. The combined organic layer was dried over Na_2SO_4 and concentrated under diminished pressure to give the crude product as a colorless solid: yield 512 mg (87%); silica gel TLC R_f 0.15 (8:2:0.2:0.1 CH_2Cl_2–

hexanes–MeOH–AcOH); $[\alpha]_D^{23}$ +31.8 (*c* 1.0, MeOH); ^{1}H NMR ($CDCl_3$) δ 0.88-0.92 (m, 6H), 1.25 (d, 3H, *J* = 6.8), 1.39 (m, 1H), 1.44 (s, 9H), 1.55 (m, 1H), 1.63 (m, 1H), 2.61-2.65 (m, 1H), 3.67-3.78 (m, 2H), 5.55 (d, 1H, *J* = 9.2) and 5.79 (d, 1H, *J* = 9.6); ^{13}C NMR ($CDCl_3$) δ 11.9, 21.4, 23.8, 24.7, 28.3, 39.8, 42.0, 52.5, 74.8, 77.3, 156.1 and 180.4; mass spectrum (MALDI-TOF), *m/z* 312.2 $(M+Na)^+$ (theoretical 312.2).

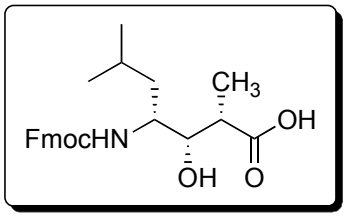

(2*S*,3*S*,4*R*)-4-(*H*-Fluoren-9-ylmethoxycarbonylamino)-3-hydroxy-2,6-dimethylheptanoic acid (2.10e) [96]: To a solution of 624 mg (1.52 mmol) of **2.10d** in 7 mL of Me_2S was added 12 mL of TFA. The reaction mixture was stirred at room temperature for 2 h. The solution was concentrated under a stream of argon and concentrated further under diminished pressure. The resulting oil was dissolved in 12 mL of 5% K_2CO_3 solution followed by the addition of 0.80 g (2.37 mmol) of FmocOSu in 20 mL of dioxane. After the reaction was stirred at room temperature overnight, the solution was extracted with three 20-mL portions of ethyl ether and three 20-mL portions of EtOAc. The combined organic layer was dried over Na_2SO_4, filtered and concentrated under diminished pressure. The crude product was then purified by flash chromatography on a silica gel column. Elution

with 93:5:2 CH_2Cl_2–MeOH–AcOH gave **2.10e** as a yellow solid: yield 825 mg (93%); silica gel TLC R_f 0.20 (8:2:0.2:0.1 CH_2Cl_2–hexanes–MeOH–AcOH);); $[\alpha]_D^{24}$ +18.0 (*c* 0.4, MeOH); ^{1}H NMR ($CDCl_3$) δ 0.90-0.93 (m, 6H), 1.28 (d, 3H, *J* = 6.5), 1.29-1.30 (m, 1H), 1.55-1.62 (m, 2H), 2.60-2.64 (m, 1H), 3.71-3.77 (m, 2H), 4.21 (dd, 1H, *J* = 6.0, *J* = 6.5), 4.48-4.51 (m, 2H), 7.32-7.34 (m, 2H), 7.40-7.43 (m, 2H), 7.60 (d, 2H, *J* = 7.5) and 7.78 (d, 2H, *J* = 7.5); ^{13}C NMR ($CDCl_3$) δ 11.5, 20.8, 21.4, 23.9, 24.6, 39.8, 47.4, 51.6, 66.3, 75.0, 120.0, 124.9, 127.0, 127.7, 141.4, 143.8, 156.4 and 177.2; mass spectrum (MALDI-TOF), *m/z* 434.2 $(M+Na)^+$ (theoretical 434.2).

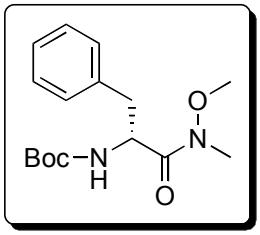

***N*-(*t*-Butoxycarbonyl)-D-phenylalanine *N*-methyoxyl-*N*-methylamine (2.14a) [96].** To a solution of 2.00 g (7.50 mmol) of *N*-D-Boc-phenylalanine in 30 mL of CH_2Cl_2 was added 1.10 mL (7.50 mmol) of NEt_3 and 3.30 g (7.50 mmol) of BOP. The mixture was stirred at room temperature for 5 min, and 0.81 g (8.32 mmol) of *O,N*-dimethylhydroxylamine hydrochloride was added followed by 1.20 mL (8.35 mmol) of NEt_3. The pH of the reaction was kept at a value higher than 8.0 and the reaction progress was monitored by TLC. The transformation was completed within 2 h. The reaction mixture was then diluted with 100 mL of

EtOAc and washed three times with 20 mL of 1N HCl and three times with 20 mL of sat aq $NaHCO_3$. The combined organic layer was washed with brine, dried ($MgSO_4$) and the solvent was removed under diminished pressure. The crude product was then purified by chromatography on a silica gel column. Elution with 2:1 hexanes–EtOAc gave **2.14a** as a colorless oil: yield 2.30 g (98%); silica gel TLC R_f 0.46 (1:1 hexanes–EtOAc); ^{1}H NMR ($CDCl_3$) δ 1.37 (s, 9H), 2.85 (dd, 1H, J = 6.8 Hz, 7.2 Hz), 3.01 (dd, 1H, J = 13.2 Hz, 6.2 Hz), 3.14 (s, 3H), 3.63 (s, 3H), 4.91 (m, 1H), 5.17 (d, 1H, J = 7.6 Hz) and 7.14-7.27 (m, 5H).

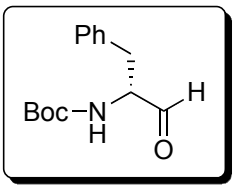

***N*-(*t*-Butoxycarbonyl)-D-phenylalaninal (2.14b) [96].** To a stirred solution of 1.17 g (4.32 mmol) of **2.14a** in 50 mL of anhydrous ethyl ether was added 80.7 mg (2.12 mmol) of $LiAlH_4$ at 0 °C. The reaction was slowly warmed to room temperature and its progress was monitored by TLC. Reduction was usually completed with 2–3 h, and then was quenched by slow addition of 368 mg (2.71 mmol) of $KHSO_4$ in 10 mL of water at 0 °C. The resulting mixture was extracted with three portions of 20 mL of EtOAc, and the organic layer was washed three times with 20 mL of 1N HCl and three times with 20 mL of sat aq $NaHCO_3$. The combined organic layer was then washed with brine, dried over Na_2SO_4 and

concentrated under diminished pressure to give **2.14b** as a white solid: yield 361 mg (80%); silica gel TLC R_f 0.60 (1:1 hexanes–EtOAc); ^{1}H NMR ($CDCl_3$) δ 1.45 (s, 9H), 3.10 (d, 2H, J = 6.4), 4.41 (m, 1H), 5.03 (br, 1H), 7.15-7.32 (m, 5H) and 9.62 (s, 1H).

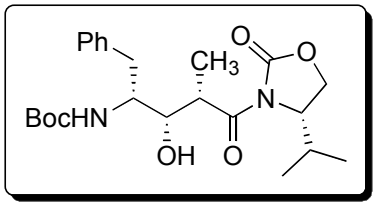

(*1R,2S,3S,4'S*)-[1-Benzyl-2-hydroxy-4-(4'-isopropyl-2'-oxo-oxazolidine-3'-yl)-3-methyl-4-oxo-butyl]carbamic acid *tert*-butyl ester (2.14c) [96]. To a stirred solution of 1.19 g (4.76 mmol) of *(S)*-(+)-4-isopropyl-3-propionyl-2-oxazolidinone **2.21** in 2 mL of anhydrous CH_2Cl_2 at 0 °C was added 5 mL (5.00 mmol) of a 1.0 M solution of Bu_2BOTf in CH_2Cl_2 followed by 1.16 mL (6.67 mmol) of (iPr)$_2$NEt. After 45 min, the solution was cooled to –78 °C for 15 min. A solution of 816 mg (4.33 mmol) of *N*-(*tert*-butoxycarbonyl)-D-phenylalaninal **2.14b** in 4 mL of CH_2Cl_2 was added and the solution was allowed to warm to room temperature overnight. The reaction was quenched by the addition of 10 mL of pH 7 potassium phosphate buffer, and was then extracted with three portions of 30 mL of Et_2O. The combined organic layer was washed with brine and concentrated under diminished pressure. The crude oil was dissolved in 30 mL of MeOH and cooled to 0 °C, then 10 mL of 30% H_2O_2 was added slowly. The

mixture was stirred at 0 °C for 4 h when 10 mL of water was added and the reaction mixture was concentrated under diminished pressure. The residue was extracted with three 20-mL portions of ethyl ether and the combined organic layer was washed with three 30-mL portions of 5% $NaHCO_3$. The resulting organic solution was washed with brine, dried over Na_2SO_4 and concentrated under diminished pressure. The residue was purified by flash chromatography on a silica gel column. Elution with 1:4 hexanes–EtOAc gave **2.14c** as a colorless solid: yield 1.66 g (88%); silica gel TLC R_f 0.51 (1:1 hexanes–EtOAc); $[\alpha]_D^{23}$ +59.4 (*c* 1.4, MeOH); ^{1}H NMR ($CDCl_3$) δ 0.87-0.95 (m, 6H), 1.32 (d, 3H, *J* = 7.2 Hz), 1.40 (s, 9H), 2.29 (m, 1H), 2.93 (m, 1H), 3.02 (m, 1H), 3.40 (br, 1H), 3.75-3.78 (m, 1H), 3.91-3.93 (m, 2H), 4.13-4.21 (m, 2H), 4.34-4.38 (m, 1H), 4.44 (d, 1H, *J* = 9.6) and 7.15-7.27 (m, 5H); ^{13}C NMR ($CDCl_3$) δ 11.4, 14.7, 17.9, 27.9, 36.6, 39.1, 52.3, 58.1, 63.3, 72.4, 79.5, 126.3, 128.3, 129.9, 137.7, 153.2, 155.4 and 177.8; mass spectrum (MALDI-TOF), *m/z* 457.2 $(M+Na)^+$ (theoretical 457.2).

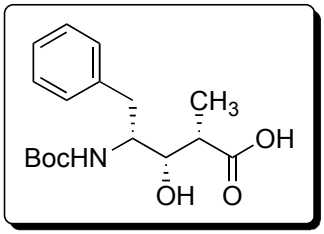

(2*S*,*3S*,*4R*)-4-*tert*-Butoxycarbonylamino-3-hydroxy-2-methyl-5-phenylpentanoic acid (2.14d) [96]. To a cooled (0 °C) solution containing 1.58 g (3.64 mmol) of **2.11c** in 36 mL of 3:1 THF–H_2O was added 3.60 mL (22.8 mmol)

of 30% H_2O_2 followed by 179.6 mg (7.63 mmol) of LiOH. After stirring at 0 °C for 3 h, the excess peroxide was quenched at 0 °C by the addition of 15.2 mL of 1.5N aq Na_2SO_3 and the pH was adjusted to 9–10 with sat aq $NaHCO_3$, and the oxazolidinone was removed by extraction with three 10-mL portions of CH_2Cl_2. The aqueous layer was then acidified to pH~2 with 1N HCl, and extracted with three 10-mL portions of EtOAc. The combined organic layer was dried over Na_2SO_4 and concentrated under diminished pressure to give the crude product as a colorless solid: yield 996 mg (85%); silica gel TLC R_f 0.13 (8:2:0.2:0.1 CH_2Cl_2–hexanes–MeOH–AcOH); $[\alpha]_D^{23}$ +33 (*c* 0.47, MeOH); ^{1}H NMR (MeOH-d_4) δ 1.13 (d, 3H, *J* = 7.2 Hz), 1.21 (s, 9H), 2.48 (m, 1H), 2.60 (m, 1H), 3.12 (dd, 1H, *J* = 3.1 Hz, *J* = 13.5 Hz), 3.66 (m, 1H), 3.83 (br, 1H) and 7.15 (m, 5H); mass spectrum (MALDI-TOF), *m/z* 346.2 $(M+Na)^+$ (theoretical 346.2).

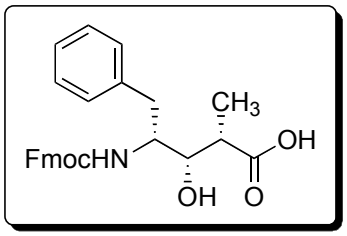

(2*S*,3*S*,4*R*)-4-(*H*-Fluoren-9-ylmethoxycarbonylamino)-3-hydroxy-2-methyl-5-phenylpentanoic acid (2.14e) [96]: To a solution of 996 mg (3.08 mmol) of **2.9d** in 9 mL of Me_2S was added 15 mL of TFA. The reaction mixture was stirred at room temperature for 2 h. The solution was concentrated under a stream of argon and concentrated further under diminished pressure. The resulting oil was

dissolved in 15 mL of 5% K_2CO_3 solution followed by the addition of 1.14 g (3.39 mmol) of FmocOSu in 20 mL of dioxane. After the reaction was stirred at room temperature overnight, the solution was extracted with three 20-mL portions of ethyl ether and three 20-mL portions of EtOAc. The combined organic layer was dried over Na_2SO_4, filtered and concentrated under diminished pressure. The crude product was then purified by flash chromatography on a silica gel column. Elution with 93:5:2 CH_2Cl_2– MeOH–AcOH gave **2.14e** as a yellow solid: yield 1.16 g (85%); mp 149-151 ^oC; silica gel TLC R_f 0.16 (8:2:0.2:0.1 CH_2Cl_2–hexanes–MeOH–AcOH); $[\alpha]_D^{23}$ +34.6 (*c* 0.5, MeOH); ^1H NMR ($CDCl_3$) δ 1.28 (d, 3H, *J* = 7.2 Hz), 2.64-2.66 (m, 1H), 2.78-2.83 (m, 1H), 3.04 (dd, 1H, *J* = 7.2, 13.6 Hz), 3.84-3.94 (m, 1H), 4.07-4.11 (m, 1H), 4.26-4.30 (m, 1H), 4.40-4.44 (m, 1H), 4.72 (d, 1H, *J* = 8.8 Hz), 6.06 (d, 1H, *J* = 10.0), 7.12-7.30 (m, 7H), 7.36-7.40 (m, 1H), 7.44-7.47 (m, 2H) and 7.74 (d, 2H, *J* = 7.6 Hz); ^{13}C NMR ($CDCl_3$) δ 10.7, 36.2, 41.1, 47.3, 53.3, 66.5, 72.4, 120.0, 124.9, 120.6, 127.0, 127.7, 128.5, 129.7, 137.1, 141.3, 143.7, 156.1 and 181.6; mass spectrum (MALDI-TOF), *m/z* 446.2 $(M+Na)^+$ (theoretical 446.2).

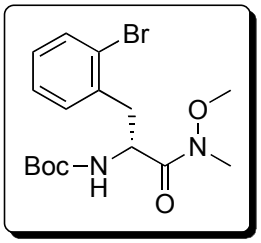

***N*-(*t*-Butoxycarbonyl)-D-2-bromophenylalanine *N*-methyl-*N*-methoxyamide (2.15a).** To a solution of 1.00 g (2.90 mmol) of *N*-Boc-D-2-bromophenylalanine in 20 mL of CH_2Cl_2 was added 405 μL (2.90 mmol) of NEt_3 and 1.30 g (2.90 mmol) of benzotriazol-1-yloxytris(dimethylamino)phosphonium hexafluorophosphate (BOP). The reaction mixture was stirred at room temperature for 5 min, and 312 mg (3.21 mmol) of *N*-methyl-*N*-methoxylamine hydrochloride was added, followed by 446 μL (3.21 mmol) of NEt_3. The pH of the reaction was kept at a value higher than 8.0 and the progress of the reaction was monitored by silica gel TLC. The reaction was complete within 2 h. The reaction mixture was then diluted with 100 mL of EtOAc and washed with three 20-mL portions of 1N HCl and three 20-mL portions of sat aq $NaHCO_3$. The combined organic layer was washed with brine, dried ($MgSO_4$) and the solvent was concentrated under diminished pressure. The crude product was purified by chromatography on a silica gel column (25 x 3.2 cm). Elution with 2:1 hexanes–EtOAc gave **2.15a** as a white solid: yield 931 mg (83%); silica gel TLC R_f 0.46 (1:1 hexanes–EtOAc); ^1H NMR ($CDCl_3$) δ 1.33 (s, 9H), 3.00-3.03 (m, 1H), 3.13 (s, 1H), 3.16-3.17 (m, 1H), 3.69 (s, 3H), 5.07-5.08 (m, 1H), 5.20-5.22 (m, 1H), 7.05-7.08 (m, 1H), 7.17-7.22

(m, 2H) and 7.51 (d, 2H, J = 8.0 Hz); ^{13}C NMR ($CDCl_3$) δ 19.2, 28.3, 32.1, 39.0, 49.9, 61.7, 79.5, 127.1, 128.4, 131.7, 132.7, 136.2, 154.9 and 172.0; mass spectrum (MALDI-TOF), *m/z* 410.8 and 409.2 $(M+Na)^+$ (theoretical 411.1 and 409.1); mass spectrum (APCI), *m/z* 389.0861 and 387.0916 $(M+H)^+$ ($C_{16}H_{24}N_2O_4Br$ requires 389.0899 and 387.0919).

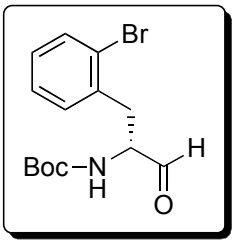

***N*-(*t*-Butoxycarbonyl)-D -2-bromophenyalaninal (2.15b).** To a stirred solution of 902 mg (2.32 mmol) of **2.11b** in 50 mL of anhydrous THF was added 111 mg (2.91 mmol) of $LiAlH_4$ at 0 ^oC. The reaction was warmed slowly to room temperature and its progress was monitored by silica gel TLC. Reduction was complete within 2–3 h, and the reaction was quenched by slow addition of 444 mg (3.33 mmol) of $KHSO_4$ in 10 mL of water at 0 ^oC. The resulting mixture was extracted with three 20-mL portions of EtOAc, and the organic layer was washed with three 20-mL portions of 1N HCl and three 20-mL portions of sat aq $NaHCO_3$. The combined organic layer was then washed with brine, dried over Na_2SO_4 and concentrated under diminished pressure to give **2.15b** as a white solid: yield 629 mg (82%); silica gel TLC R_f 0.51 (1:1 hexanes–EtOAc); ^{1}H NMR

($CDCl_3$) δ 1.41 (s, 9H), 2.75-2.94 (m, 2H), 4.13 (m, 1H), 5.12 (br, 1H), 7.02-7.35 (m, 1H), 7.51-7.61 (m, 3H) and 9.69 (s, 1H). The product was used promptly for the next preparation of **2.15c**.

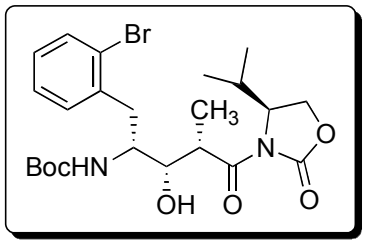

(1*R*,2*S*,3*S*,4′*S*)-[1-(2′-Bromobenzyl)-2-hydroxy-4-(4′-isopropyl-2′-oxo-oxazolidin-3′-yl)-3-methyl-4-oxobutyl]carbamic acid *tert*-butyl ester (2.15c). To a stirred solution of 220 mg (1.2 mmol) of *(S)*-(+)-4-isopropyl-3-propionyl-2-oxazolidinone (**2.21**) in 1 mL of anhydrous CH_2Cl_2 at 0 °C was added 1.39 mL (1.39 mmol) of a 1.0 M solution of Bu_2BOTf in CH_2Cl_2 followed by 319 μL (1.8 mmol) of $(i\text{Pr})_2\text{NEt}$. After 45 min, the solution was cooled to –78 °C for 15 min. A solution of 430 mg (1.31 mmol) of **2.15b** in 1 mL of CH_2Cl_2 was added and the solution was allowed to warm to room temperature overnight. The reaction was quenched by the addition of 10 mL of potassium phosphate buffer, pH 7.0, and was then extracted with three 30-mL portions of Et_2O. The combined organic layer was washed with brine and concentrated under diminished pressure. The crude oil was dissolved in 15 mL of MeOH and cooled to 0 °C, then 5 mL of 30% H_2O_2 was added slowly. The mixture was stirred at 0 °C for 4 h, then 10 mL of

water was added and the reaction mixture was concentrated under diminished pressure. The residue was extracted with three 20-mL portions of ethyl ether and the combined organic layer was washed with three 30-mL portions of 5% $NaHCO_3$. The resulting organic solution was washed with brine, dried over Na_2SO_4 and concentrated under diminished pressure. The residue was purified by flash chromatography on a silica gel column (25 x 3.2 cm). Elution with 1:4 hexanes–EtOAc gave **2.15c** as a colorless solid: yield 507 mg (84%); silica gel TLC R_f 0.45 (1:1 hexanes–EtOAc); $[\alpha]^{24}_D$ +84.9 (*c* 1.5, MeOH); ^{1}H NMR ($CDCl_3$) δ 0.87 (dd, 6H, *J* = 7.6 and 7.2 Hz), 1.11 (s, 3H), 1.28 (s, 9H), 2.28-2.35 (m, 1H), 2.81-2.87 (m, 1H), 3.28-3.39 (m, 2H), 3.91-4.04 (m, 3H), 4.18-4.26 (m, 2H), 4.42-4.44 (m, 1H), 4.58 (d, 1H, *J* = 9.2 Hz), 7.01-7.05 (m, 1H), 7.17-7.25 (m, 2H) and 7.48 (d, 1H, *J* = 8.0 Hz); ^{13}C NMR ($CDCl_3$) δ 12.2, 14.7, 17.9, 19.1, 28.2, 36.8, 39.8, 53.0, 58.2, 63.4, 74.1, 79.4, 125.1, 127.3, 131.7, 132.7, 138.0, 153.3, 155.5 and 177.2; mass spectrum (MALDI-TOF), *m/z* 537.4 and 535.1 $(M+Na)^+$(theoretical 537.1 and 535.1); mass spectrum (APCI), *m/z* 513.1604 and 515.1586 $(M+H)^+$ ($C_{23}H_{34}N_2O_6Br$ requires 513.1600 and 515.1580).

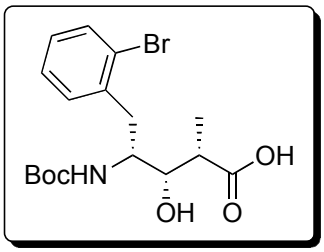

(2*S*,3*S*,4*R*)-4-*tert*-Butoxycarbonylamino-5-(2′-bromophenyl)-3-hydroxy-2-methylpentanoic acid (2.15d). To a cooled (0 °C) solution containing 599 mg (1.17 mmol) of **2.15c** in 24 mL of 3:1 THF/H_2O was added 1.1 mL (7.01 mmol) of 30% H_2O_2 followed by 56 mg (2.32 mmol) of LiOH. After stirring at 0 °C for 3 h, the excess peroxide was quenched at 0 °C by the addition of 4.7 mL of 1.5 N aq Na_2SO_3 and the pH was adjusted to 9–10 with sat aq $NaHCO_3$. The oxazolidinone was recovered by extraction with three 10-mL portions of CH_2Cl_2. The aqueous layer was then acidified to pH ~2 with 1 N HCl, and extracted with three 10-mL portions of EtOAc. The combined organic layer was dried over Na_2SO_4 and concentrated under diminished pressure to give the crude product as a colorless solid: yield 440 mg (94%); silica gel TLC R_f 0.20 (8:2:0.2:0.1 CH_2Cl_2–hexanes–MeOH–AcOH); $[\alpha]^{23}_D$ +55.1 (*c* 0.8, MeOH); ^{1}H NMR ($CDCl_3$) δ 1.15 (d, 3H, *J* = 7.2 Hz), 1.30 (s, 9H), 2.56-2.61 (m, 1H), 2.75 2.85 (m, 1H), 2.91-2.96 (m, 1H), 3.95-4.05 (m, 2H), 7.07-7.10 (m, 1H), 7.24-7.30 (m, 2H) and 7.54 (d, 1H, *J* = 8.0 Hz); mass spectrum (MALDI-TOF), *m/z* 426.1 and 424.0 $(M+Na)^+$ (theoretical 426.1 and 424.1); mass spectrum (APCI), *m/z* 402.0907 and 404.0896 $(M+H)^+$ ($C_{17}H_{25}NO_5Br$ requires 402.0916 and 404.0896).

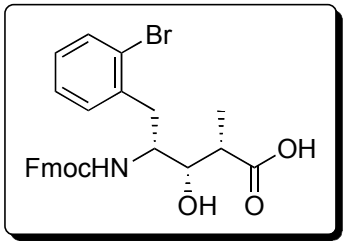

(2*S*,3*S*,4*R*)-5-(2′-Bromophenyl-4-(*9H*-fluoren-9-ylmethoxycarbonylamino)-3-hydroxy-2-methylpentanoic acid (2.15e). To a solution of 409 mg (1.02 mmol) of **2.15d** in 5 mL of Me_2S was added 8 mL of TFA. The reaction mixture was stirred at room temperature for 2 h. The solution was concentrated under a stream of argon and concentrated further under diminished pressure. The resulting oil was dissolved in 8 mL of 5% aq K_2CO_3 solution followed by the addition of 338 mg (1.12 mmol) of FmocOSu in 10 mL of dioxane. The reaction was stirred at room temperature overnight, and the solution was then extracted successively with three 20-mL portions of ethyl ether and three 20-mL portions of EtOAc. The combined organic layer was dried over Na_2SO_4, filtered and concentrated under diminished pressure. The crude product was purified by flash chromatography on a silica gel column (25 x 3.2 cm). Elution with 93:5:2 CH_2Cl_2–MeOH–AcOH gave **2.15e** as a yellow solid: yield 448 mg (84%); mp 104-105 ^{o}C; silica gel TLC R_f 0.18 (8:2:0.2:0.1 CH_2Cl_2–hexanes–MeOH–AcOH); $[\alpha]^{23}_{D}$ +13.0 (*c* 0.54, MeOH); ^{1}H NMR ($CDCl_3$) δ 1.25 (d, 3H, *J* = 7.0 Hz), 2.51-2.59 (m, 1H), 2.62-2.69 (m, 1H), 2.82-2.87 (m, 1H), 3.22 (d, 1H, *J* = 14.0 Hz), 3.40-3.94 (m, 3H), 4.07-4.11 (m, 1H), 4.20-4.24 (m, 1H), 4.87 (d, 1H, *J* = 7.5 Hz), 6.91-6.99

(m, 1H), 7.06 -7.14 (m, 2H), 7.18-7.22 (m, 2H), 7.30 (d, 2H, J = 3.5 Hz), 7.35-7.41 (m, 3H) and 7.65 (d, 2H, J = 7.5 Hz); ^{13}C NMR ($CDCl_3$) δ 10.5, 35.1, 40.6, 46.1, 52.9, 65.8, 73.2, 118.9, 124.0, 126.0, 126.5, 126.7, 127.3, 130.5, 131.8, 136.5, 140.3, 142.6, 142.9, 155.2 and 179.6; mass spectrum (MALDI-TOF), *m/z* 548.4 and 546.7 $(M+Na)^+$ (theoretical 548.1 and 546.1); mass spectrum (APCI), *m/z* 524.1078 and 526.1075 $(M+H)^+$ ($C_{27}H_{27}NO_5Br$ requires 524.1072 and 526.1052).

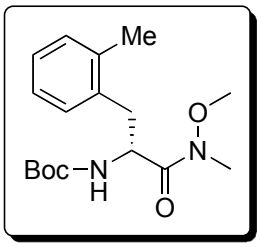

***N*-(*t*-Butoxycarbonyl)-D-2-methylphenylalanine *N*-methyl-*N*-methoxyamide (2.16a).** To a solution of 1.00 g (3.61 mmol) of *N*-Boc-D-2-methylphenylalanine in 30 mL of CH_2Cl_2 was added 499 μL (3.61 mmol) of NEt_3 and 1.60 g (3.61 mmol) of BOP reagent. The reaction mixture was stirred at room temperature for 5 min, and 384 mg (3.93 mmol) of *N*-methyl-*N*-methoxylamine hydrochloride was added, followed by 549 μL (3.93 mmol) of NEt_3. The pH of the reaction was kept at a value higher than 8.0 and the progress of the reaction was monitored by silica gel TLC. The transformation was complete within 2 h. The reaction mixture was then diluted with 100 mL of EtOAc and washed

successively with three 20-mL portions of 1 N HCl and three 20-mL portions of sat aq $NaHCO_3$. The combined organic layer was washed with brine, dried ($MgSO_4$) and the solvent was concentrated under diminished pressure. The crude product was purified by chromatography on a silica gel column (25 x 3.2 cm). Elution with 2:1 hexanes–EtOAc gave **2.16a** as a white solid: yield 1.1 g (97%); silica gel TLC R_f 0.46 (1:1 hexanes–EtOAc); ^{1}H NMR ($CDCl_3$) δ 1.36 (s, 9H), 2.37 (s, 3H), 2.84-2.88 (m, 1H), 3.06 (dd, 1H, J = 7.5 and 6.5 Hz), 3.14 (s, 3H), 3.60 (s, 3H), 4.99-5.00 (m, 1H), 5.27 (d, 1H, J = 8.0 Hz) and 7.10-7.12 (m, 4H); ^{13}C NMR ($CDCl_3$) δ 19.3, 28.3, 32.0, 36.6, 50.1, 61.4, 79.4, 125.7, 126.8, 130.2, 134.8, 136.2, 136.8, 155.1 and 172.6; mass spectrum (MALDI-TOF), *m/z* 345.3 $(M+Na)^+$ (theoretical 345.2); mass spectrum (APCI), *m/z* 323.1981 $(M+H)^+$ ($C_{17}H_{27}N_2O_4$ requires 323.1971).

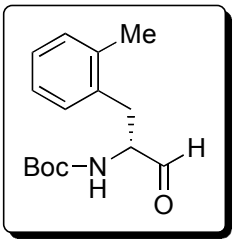

***N*-(*t*-Butoxycarbonyl)-D-2-methylphenylalaninal (2.16b).** To a stirred solution of 947 mg (2.94 mmol) of **2.16a** in 50 mL of anhydrous THF was added 139 mg (3.71 mmol) of $LiAlH_4$ at 0 °C. The reaction was warmed slowly to room temperature and its progress was monitored by silica gel TLC. The reduction was

complete within 2–3 h, and the reaction was quenched by the slow addition of 560 mg (4.13 mmol) of $KHSO_4$ in 10 mL of water at 0 °C. The resulting mixture was extracted with three 20-mL portions of EtOAc, and the organic layer was washed with three 20-mL portions of 1N HCl and three 20-mL portions of sat aq $NaHCO_3$. The combined organic layer was then washed with brine, dried over Na_2SO_4 and concentrated under diminished pressure to give **2.16b** as a white solid: yield 687 mg (89%); silica gel TLC R_f 0.60 (1:1 hexanes–EtOAc); ^{1}H NMR ($CDCl_3$) δ 1.41 (s, 9H), 2.36 (s, 3H), 2.75 (m, 1H), 3.10 (m, 1H), 4.15 (m, 1H), 5.11 (m, 1H), 7.04-7.12 (m, 4H) and 9.60 (s, 1H). The product was used promptly for the preparation of **2.16c**.

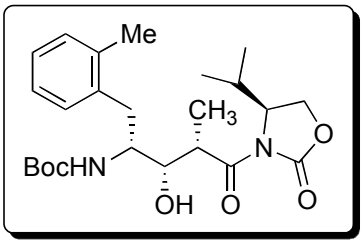

(1*R*,2*S*,3*S*,4′*S*)-[2-Hydroxy-1-(2′-methylbenzyl)-4-(4′-isopropyl-2′-oxo-oxazolidin-3′-yl)-3-methyl-4-oxobutyl]carbamic acid *tert*-butyl ester (2.16c). To a stirred solution of 249 mg (1.34 mmol) of *(S)*-(+)-4-isopropyl-3-propionyl-2-oxazolidinone (**2.21**) in 1 mL of anhydrous CH_2Cl_2 at 0 °C was added 1.57 mL (1.57 mmol) of a 1.0 M solution of Bu_2BOTf in CH_2Cl_2 followed by 361 μL (2.07 mmol) of $(iPr)_2NEt$. After 45 min, the solution was cooled to –78 °C for 15 min.

A solution of 390 mg (1.48 mmol) of **2.16b** in 2 mL of CH_2Cl_2 was added and the solution was allowed to warm to room temperature overnight. The reaction was quenched by the addition of 10 mL of potassium phosphate buffer, pH 7.0, and was then extracted with three 30-mL portions of Et_2O. The combined organic layer was washed with brine and concentrated under diminished pressure. The crude oil was dissolved in 15 mL of MeOH and cooled to 0 ^oC, then 5 mL of 30% H_2O_2 was added slowly. The mixture was stirred at 0 ^oC for 4 h, then 10 mL of water was added and the reaction mixture was concentrated under diminished pressure. The residue was extracted with three 20-mL portions of ethyl ether and the combined organic layer was washed with three 30-mL portions of 5% $NaHCO_3$. The resulting organic solution was washed with brine, dried over Na_2SO_4 and concentrated under diminished pressure. The residue was purified by flash chromatography on a silica gel column (25 x 3.2 cm). Elution with 1:4 hexanes–EtOAc gave **2.16c** as a colorless solid: yield 482 mg (80%); silica gel TLC R_f 0.48 (1:1 hexanes–EtOAc); $[\alpha]^{24}_D$ +83.7 (*c* 1.0, MeOH); ^{1}H NMR ($CDCl_3$) δ 0.86 (dd, 6H, *J* = 8.8 and 7.2 Hz), 1.13 (s, 3H), 1.31 (s, 9H), 2.31 (s, 3H), 2.32-2.33 (m, 1H), 2.65-2.71 (m, 1H), 3.17-3.22 (m, 2H), 3.31 (d, 1H, *J* = 13.2 Hz), 3.77-3.98 (m, 2H), 4.16-4.23 (m, 2H), 4.38-4.41 (m, 1H), 4.46 (d, 1H, *J* = 9.2 Hz) and 7.06-7.11 (m, 4H); ^{13}C NMR ($CDCl_3$) δ 11.8, 14.7, 17.9, 19.5, 28.3, 34.1, 39.5, 52.4, 58.1, 63.3, 73.4, 79.4, 125.7, 126.3, 130.3, 130.4, 136.4, 136.7, 153.3, 155.3 and 177.5; ; mass spectrum (MALDI-TOF), *m/z* 471.5 $(M+Na)^+$

(theoretical 471.2); mass spectrum (APCI), *m/z* 449.2655 $(M+H)^+$ ($C_{24}H_{37}N_2O_6$ requires 449.2652).

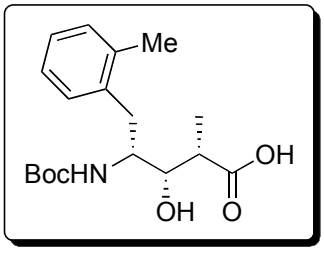

(2*S*,3*S*,4*R*)-4-*tert*-Butoxycarbonylamino-3-hydroxy-2-methyl-5-(2′-methylphenylpentanoic acid (2.16d). To a cooled (0 °C) solution containing 599 mg (1.34 mmol) of **2.16c** in 24 mL of 3:1 THF/H_2O was added 1.20 mL (8.02 mmol) of 30% H_2O_2 followed by 63.9 mg (2.70 mmol) of LiOH. After stirring at 0 °C for 3 h, the excess peroxide was quenched at 0 °C by the addition of 5.3 mL of 1.5 N aq Na_2SO_3 and the pH was adjusted to 9–10 with sat aq $NaHCO_3$. The oxazolidinone was recovered by extraction with three 10-mL portions of CH_2Cl_2. The aqueous layer was then acidified to pH ~2 with 1 N HCl, and extracted with three 10-mL portions of EtOAc. The combined organic layer was dried over Na_2SO_4 and concentrated under diminished pressure to give the crude product as a colorless solid: yield 409 mg (90%); silica gel TLC R_f 0.22 (8:2:0.2:0.1 CH_2Cl_2–hexanes–MeOH–AcOH); $[\alpha]^{23}_D$ +26.4 (*c* 0.45, MeOH); ^{1}H NMR ($CDCl_3$) δ 1.11 (d, 3H, *J* = 7.2 Hz), 1.29 (s, 9H), 2.32 (3H, s), 2.72-2.75 (m, 2H), 3.60 (dd, 2H, *J*

= 7.6 and 7.2 Hz); 3.72-3.96 (m, 2H) and 7.03-7.18 (m, 4H); mass spectrum (APCI), *m/z* 338.1961 $(M+H)^+$ ($C_{18}H_{28}NO_5$ requires 338.1967).

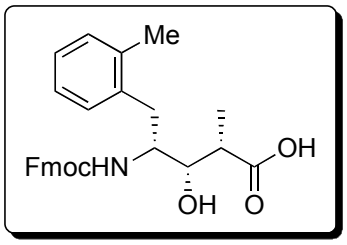

(2*S*,3*S*,4*R*)-4-(*9H*-Fluoren-9-ylmethoxycarbonylamino)-3-hydroxy-2-methyl-5-(2′-methylphenylpentanoic acid (2.16e). To a solution of 386 mg (1.14 mmol) of **2.16d** in 5 mL of Me_2S was added 8 mL of TFA. The reaction mixture was stirred at room temperature for 2 h. The solution was concentrated under a stream of argon and concentrated further under diminished pressure. The resulting oil was dissolved in 8 mL of 5% aq K_2CO_3 solution followed by the addition of 424 mg (1.26 mmol) of FmocOSu in 10 mL of dioxane. The reaction was stirred at room temperature overnight, and the solution was then extracted successively with three 20-mL portions of ethyl ether and three 20-mL portions of EtOAc. The combined organic layer was dried over Na_2SO_4, filtered and concentrated under diminished pressure. The crude product was purified by flash chromatography on a silica gel column (25 x 3.2 cm). Elution with 93:5:2 CH_2Cl_2–MeOH–AcOH gave **2.16e** as a yellow solid: yield 499 mg (95%); mp 118-120 ^oC; silica gel TLC R_f 0.17 (8:2:0.2:0.1 CH_2Cl_2–hexanes–MeOH–AcOH); $[\alpha]^{23}_D$ +104 (*c* 0.2, MeOH); ^1H

NMR ($CDCl_3$) δ 1.23 (d, 3H, J = 9.0 Hz), 2.21 (s, 3H), 2.34-2.41 (m, 1H), 2.60-2.64 (m, 1H), 3.09-3.12 (m, 1H), 3.71-3.84 (m, 1H), 3.89-3.99 (m, 2H), 4.09-4.19 (m, 1H), 4.63 (d, 1H, J = 11.5 Hz), 6.98-7.02 (m, 4H), 7.18-7.21 (m, 3H), 7.30 (t, 2H, J = 9.0 Hz), 7.38 (t, 1H, J = 10.5 Hz) and 7.66 (m, 2H, J = 8.5 Hz); ^{13}C NMR ($CDCl_3$) δ 11.3, 19.5, 33.5, 41.5, 47.2, 53.3, 66.6, 73.8, 119.9, 125.0, 125.9, 126.7, 127.0, 127.7, 130.3, 130.5, 135.9, 136.7, 141.3, 143.6, 156.2 and 181.1; mass spectrum (MALDI-TOF), *m/z* 482.7 $(M+Na)^+$ (theoretical 482.2); mass spectrum (APCI), *m/z* 460.2114 $(M+H)^+$ ($C_{28}H_{30}NO_5$ requires 460.2124).

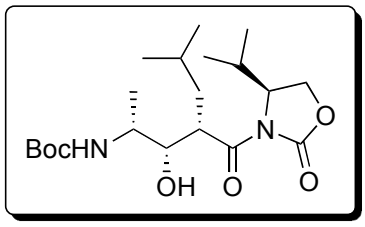

(1*R*,2*S*,3*S*,4′*S*)-[2-Hydroxy-3-isobutyl-4-(4′-isopropyl-2′-oxo-oxazolidin-3′-yl)-1-methyl-4-oxobutyl]carbamic acid *tert*-butyl ester (2.18c). To a stirred solution of 2.00 g (8.92 mmol) of **2.24** in 2 mL of anhydrous CH_2Cl_2 at 0 °C was added 10.4 mL (10.4 mmol) of a 1.0 M solution of Bu_2BOTf in CH_2Cl_2 followed by 2.40 mL (13.7 mmol) of $(i\text{Pr})_2\text{NEt}$. After 45 min, the solution was cooled to –78 °C for 15 min. A solution of 1.70 g (9.81 mmol) of **2.9b** in 5 mL of CH_2Cl_2 was added and the solution was allowed to warm to room temperature overnight. The reaction was quenched by the addition of 10 mL of potassium phosphate buffer, pH 7.0, and was then extracted with three 30-mL portions of Et_2O. The combined

organic layer was washed with brine and concentrated under diminished pressure. The crude oil was dissolved in 24 mL of MeOH and cooled to 0 ^{o}C, then 8 mL of 30% H_2O_2 was added slowly. The mixture was stirred at 0 ^{o}C for 4 h, then 10 mL of water was added and the reaction mixture was concentrated under diminished pressure. The residue was extracted with three 20-mL portions of ethyl ether and the combined organic layer was washed with three 30-mL portions of 5% aq $NaHCO_3$. The resulting solution was washed with brine, dried over Na_2SO_4 and concentrated under diminished pressure. The residue was purified by flash chromatography on a silica gel column (25 x 3.2 cm). Elution with 1:4 hexanes–EtOAc gave **2.18c** as a colorless solid: yield 2.4 g (67%); silica gel TLC R_f 0.45(1:1 hexanes–EtOAc); $[\alpha]^{23}_D$ +42.5 (*c* 1.0, MeOH); ^{1}H NMR ($CDCl_3$) δ 0.83-0.90 (m, 12H), 1.16 (d, 3H, *J* = 6.5 Hz), 1.40 (s, 9H), 1.42-1.48 (m, 2H), 1.84-1.89 (m, 1H), 2.34 (d, 1H, *J* = 3.0 Hz), 2.77 (br, 1H), 3.59-3.61 (m, 1H), 3.69-3.70 (m, 1H), 4.18-4.20 (m, 1H), 4.23-4.30 (m, 2H), 4.49-4.51 (m, 1H) and 4.86 (d, 1H, *J* = 9.0 Hz); ^{13}C NMR ($CDCl_3$) δ 14.4, 18.0, 21.6, 23.8, 26.4, 28.3, 35.4, 43.2, 48.4, 58.7, 63.1, 75.8, 79.5, 154.0, 155.9 and 175.8; mass spectrum (MALDI-TOF), *m/z* 423.5 $(M+Na)^+$ (theoretical 423.2); mass spectrum (APCI), *m/z* 401.2666 $(M+H)^+$ ($C_{20}H_{37}N_2O_6$ requires 401.2652).

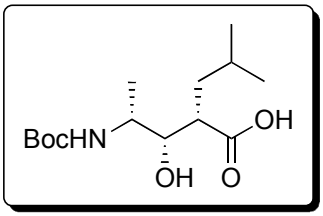

(2*S*,3*S*,4*R*)-4-*tert*-Butoxycarbonylamino-3-hydroxy-2-isobutylpentanoic acid (2.18d). To a cooled (0 °C) solution containing 1.95 g (4.88 mmol) of **2.18c** in 64 mL of 3:1 THF H_2O was added 4.60 mL (29.3 mmol) of 30% H_2O_2 followed by 234 mg (9.80 mmol) of LiOH. After stirring at 0 °C for 3 h, the excess peroxide was quenched at 0 °C by the addition of 19.5 mL of 1.5 N aq Na_2SO_3 and the pH was adjusted to 9–10 with sat aq $NaHCO_3$. The oxazolidinone was recovered by extraction with three 10-mL portions of CH_2Cl_2. The aqueous layer was then acidified to pH ~2 with 1 N HCl, and extracted with three 10-mL portions of EtOAc. The combined organic layer was dried over Na_2SO_4 and concentrated under diminished pressure to give the crude product as a colorless solid: yield 1.21 g (84%); silica gel TLC R_f 0.25 (8:2:0.2:0.1 CH_2Cl_2–hexanes–MeOH–AcOH); $[\alpha]^{23}_D$ +9.8 (*c* 0.3, MeOH); ^{1}H NMR ($CDCl_3$) δ 0.86-0.91 (m, 6H), 1.16 (d, 3H, *J* = 6.4 Hz), 1.41 (s, 9H), 1.60 (m, 2H), 2.55-2.59 (m, 2H), 3.60-3.70 (m, 2H), 4.91 (br, 1H) and 6.14 (br, 1H); mass spectrum (MALDI-TOF), *m/z* 312.2 $(M+Na)^+$ (theoretical 312.2); mass spectrum (APCI), *m/z* 290.1960 $(M+H)^+$ ($C_{14}H_{28}NO_5$ requires 290.1967).

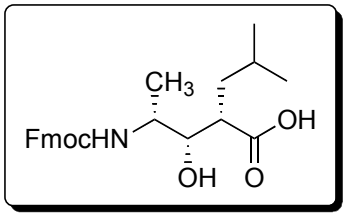

(2*S*,3*S*,4*R*)-4-(*9H*-Fluoren-9-ylmethoxycarbonylamino)-3-hydroxy-2-isobutylpentanoic acid (2.18e). To a solution of 985 mg (3.98 mmol) of **2.18d** in 12 mL of Me_2S was added 20 mL of TFA. The reaction mixture was stirred at room temperature for 2 h. The solution was concentrated under a stream of argon and concentrated further under diminished pressure. The resulting oil was dissolved in 20 mL of 5% aq K_2CO_3 solution followed by the addition of 1.50 g (4.51 mmol) of FmocOSu in 14 mL of dioxane. The reaction was stirred at room temperature overnight, and the solution was then extracted successively with three 20-mL portions of ethyl ether and three 20-mL portions of EtOAc. The combined organic layer was dried over Na_2SO_4, filtered and concentrated under diminished pressure. The crude product was then purified by flash chromatography on a silica gel column (25 x 3.2 cm). Elution with 93:5:2 CH_2Cl_2–MeOH–AcOH gave **2.18e** as a yellow solid: yield 1.44 g (85%); mp 70-72 ^oC; silica gel TLC R_f 0.23 (8:2:0.2:0.1 CH_2Cl_2–hexanes–MeOH–AcOH); $[\alpha]^{23}_D$ +9.8 (*c* 0.3, MeOH); ^1H NMR ($CDCl_3$) δ 0.78-0.82 (m, 6H), 1.09 (d, 3H, *J* = 7.0 Hz), 1.39-1.43 (m, 1H), 1.51-1.61 (m, 2H), 2.48-2.51 (m, 2H), 3.62-3.70 (m, 2H), 4.09 (t, 1H, *J* = 6.5 Hz), 5.07 (d, 1H, *J* = 8.5 Hz), 7.20-7.22 (m, 2H), 7.29-7.31 (m, 2H), 7.48 (d, 2H, *J* = 8.5 Hz) and 7.66 (d, 2H, *J* = 7.5 Hz); ^{13}C NMR ($CDCl_3$) δ 14.1, 20.3, 22.6, 25.2,

36.2, 45.8, 46.2, 48.3, 65.8, 74.2, 119.0, 124.0, 126.1, 126.7, 140.3, 142.8, 155.1 and 178.0; mass spectrum (MALDI-TOF), *m/z* 434.5 $(M+Na)^+$ (theoretical 434.2); mass spectrum (APCI), *m/z* 412.2126 $(M+H)^+$ ($C_{24}H_{30}NO_5$ requires 412.2124).

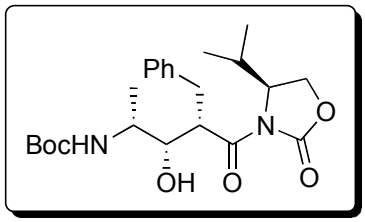

(1*R*,2*S*,3*S*,4′*S*)-[3-Benzyl-2-hydroxy-4-(4′-isopropyl-2′-oxo-oxazolidin-3′-yl)-1-methyl-4-oxobutyl]carbamic acid *tert*-butyl ester (2.19c). To a stirred solution of 1.50 g (5.74 mmol) of **2.23** in 2 mL of anhydrous CH_2Cl_2 at 0 °C was added 6.71 mL (6.71 mmol) of a 1.0 M solution of Bu_2BOTf in CH_2Cl_2 followed by 1.54 mL (8.83 mmol) of $(i\text{Pr})_2\text{NEt}$. After 45 min, the solution was cooled to –78 °C for 15 min. A solution of 1.10 g (6.33 mmol) of **2.9b** in 5 mL of CH_2Cl_2 was added and the solution was allowed to warm to room temperature overnight. The reaction was quenched by the addition of 10 mL of potassium phosphate buffer, pH 7.0, and was then extracted with three 30-mL portions of Et_2O. The combined organic layer was washed with brine and concentrated under diminished pressure. The crude oil was dissolved in 21 mL of MeOH and cooled to 0 °C, then 7 mL of 30% H_2O_2 was added slowly. The mixture was stirred at 0 °C for 4 h, then 10 mL of water was added and the reaction mixture was concentrated under diminished

pressure. The residue was extracted with three 20-mL portions of ethyl ether and the combined organic layer was washed with three 30-mL portions of 5% aq $NaHCO_3$. The resulting solution was washed with brine, dried over Na_2SO_4 and concentrated under diminished pressure. The residue was purified by flash chromatography on a silica gel column (25 x 3.2 cm). Elution with 1:4 hexanes–EtOAc gave **2.19c** as a colorless solid: yield 1.84 g (74%); silica gel TLC R_f 0.43 (1:1 hexanes–EtOAc); $[\alpha]^{24}_D$ +13.0 (*c* 0.46, MeOH); ^{1}H NMR ($CDCl_3$) δ 0.20 (d, 3H, *J* = 7.0 Hz), 0.74 (d, 3H, *J* = 7.0 Hz), 1.25 (d, 3H, *J* = 6.5 Hz), 1.50 (s, 9H), 1.90-1.98 (m, 1H), 3.03-3.08 (m, 1H), 3.25-3.28 (m, 1H), 3.72 (br, 1H), 3.87 (m, 1H), 4.03-4.06 (m, 1H), 4.16 (t, 1H, *J* = 9.0 Hz), 4.38-4.39 (m, 1H), 4.65-4.69 (m, 2H), 4.82 (d, 1H, *J* = 9.0 Hz) and 7.12-7.29 (m, 5H); ^{13}C NMR ($CDCl_3$) δ 13.7, 17.7, 28.0, 28.3, 33.1, 46.2, 48.2, 58.5, 62.7, 75.6, 79.6, 126.3, 128.3, 129.4, 138.7, 153.6, 155.6 and 175.2; mass spectrum (MALDI-TOF), *m/z* 457.5 $(M+Na)^+$ (theoretical 457.2); mass spectrum (APCI), *m/z* 435.2494 $(M+H)^+$ ($C_{23}H_{35}N_2O_6$ requires 435.2495).

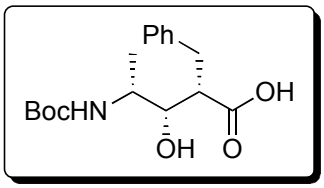

(2*S*,3*S*,4*R*)-2-Benzyl-4-*tert*-butoxycarbonylamino-3-hydroxypentanoic acid (2.19d). To a cooled (0 °C) solution containing 1.60 g (3.56 mmol) of **2.19c** in 40

mL of 3:1 THF/H_2O was added 3.34 mL (21.4 mmol) of 30% H_2O_2 followed by 171 mg (7.11 mmol) of LiOH. After stirring at 0 °C for 3 h, the excess peroxide was quenched at 0 °C by the addition of 14.2 mL of 1.5 N aq Na_2SO_3 and the pH was adjusted to 9–10 with sat aq $NaHCO_3$. The oxazolidinone was recovered by extraction with three 10-mL portions of CH_2Cl_2. The aqueous layer was then acidified to pH ~2 with 1N HCl, and extracted with three 10-mL portions of EtOAc. The combined organic layer was dried over Na_2SO_4 and concentrated under diminished pressure to give the crude product as a colorless solid: yield 283 mg (68%); silica gel TLC R_f 0.23 (8:2:0.2:0.1 CH_2Cl_2–hexanes–MeOH–AcOH); ^{1}H NMR ($CDCl_3$) δ 1.18 (d, 3H, J = 6.5 Hz), 1.46 (s, 9H), 2.81-2.86 (m, 1H), 2.95-2.98 (m, 1H), 3.10 (m, 1H), 3.19-3.22 (m, 1H), 3.85 (m, 2H) and 7.21-7.32 (m, 5H); mass spectrum (MALDI-TOF), *m/z* 346.4 $(M+Na)^+$ (theoretical 346.2); mass spectrum (APCI), *m/z* 324.1732 $(M+H)^+$ ($C_{17}H_{26}NO_5$ requires 324.1733).

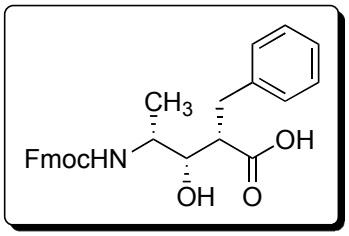

(2*S*,3*S*,4*R*)-2-Benzyl-4-(*9H*-fluoren-9-ylmethoxycarbonylamino)-3-hydroxypentanoic acid (2.19e). To a solution of 783 mg (2.42 mmol) of **2.19d** in 9 mL of Me_2S was added 15 mL of TFA. The reaction mixture was stirred at room temperature for 2 h. The solution was concentrated under a stream of argon and

concentrated further under diminished pressure. The resulting oil was dissolved in 15 mL of 5% aq K_2CO_3 solution followed by the addition of 899 mg (2.66 mmol) of FmocOSu in 14 mL of dioxane. The reaction was stirred at room temperature overnight, and the solution was then extracted successively with three 20-mL portions of ethyl ether and three 20-mL portions of EtOAc. The combined organic layer was dried over Na_2SO_4, filtered and concentrated under diminished pressure. The crude product was then purified by flash chromatography on a silica gel column (25 x 3.2 cm). Elution with 93:5:2 CH_2Cl_2–MeOH–AcOH gave **2.19e** as a yellow solid: yield 1.03 g (94%); mp 73-75 ^oC; silica gel TLC R_f 0.20 (8:2:0.2:0.1 CH_2Cl_2–hexanes–MeOH–AcOH); $[\alpha]^{23}_D$ -20.8 (*c* 1.0, MeOH); ^1H NMR ($CDCl_3$) δ 1.09 (d, 3H, *J* = 5.5 Hz), 2.70-2.72 (m, 1H), 2.83 (t, 1H, *J* = 11.5 Hz), 3.03-3.06 (m, 1H), 3.60-3.75 (m, 2H), 4.08 (t, 1H, *J* = 6.5 Hz), 4.28-4.32 (m, 2H), 5.02 (d, 1H, *J* = 7.5 Hz), 7.07-7.14 (m, 4H), 7.16-7.19 (m, 2H), 7.26-7.31 (m, 2H), 7.45 (d, 2H, *J* = 7.0 Hz) and 7.66 (d, 2H, *J* = 7.5 Hz); ^{13}C NMR ($CDCl_3$) δ 14.1, 33.4, 46.2, 48.4, 49.9, 65.8, 73.9, 119.1, 123.9, 124.2, 125.5, 126.1, 126.4, 127.5, 137.6, 140.3, 142.7, 155.3 and 176.8; mass spectrum (MALDI-TOF), *m/z* 468.6 $(M+Na)^+$ (theoretical 468.2); mass spectrum (APCI), *m/z* 446.1972 $(M+H)^+$ ($C_{27}H_{28}NO_5$ requires 446.1967).

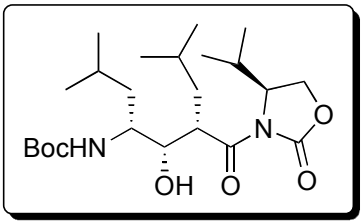

(1*R*,2*S*,3*S*,4′*S*)-[1,3-Di-isobutyl-2-hydroxy-4-(4′-isopropyl-2′-oxo-oxazolidin-3′-yl)-4-oxobutyl]carbamic acid *tert*-butyl ester (2.20c). To a stirred solution of 1.47 g (6.50 mmol) of **2.24** in 2 mL of anhydrous CH_2Cl_2 at 0 °C was added 7.53 mL (7.53 mmol) of a 1.0 M solution of Bu_2BOTf in CH_2Cl_2 followed by 1.74 mL (9.95 mmol) of $(i\text{Pr})_2\text{NEt}$. After 45 min, the solution was cooled to –78 °C for 15 min. A solution of 1.53 mg (7.11 mmol) of **2.10b** in 5 mL of CH_2Cl_2 was added and the solution was allowed to warm to room temperature overnight. The reaction was quenched by the addition of 10 mL of potassium phosphate buffer, pH 7.0, and was then extracted with three 30-mL portions of Et_2O. The combined organic layer was washed with brine and concentrated under diminished pressure. The crude oil was dissolved in 24 mL of MeOH and cooled to 0 °C, then 8 mL of 30% H_2O_2 was added slowly. The mixture was stirred at 0 °C for 4 h, then 10 mL of water was added and the reaction mixture was concentrated under diminished pressure. The residue was extracted with three 20-mL portions of ethyl ether and the combined organic layer was washed with three 30-mL portions of 5% $NaHCO_3$. The resulting organic solution was washed with brine, dried over Na_2SO_4 and concentrated under diminished pressure. The residue was purified by flash chromatography on a silica gel column (25 x 3.2 cm). Elution with 1:4

hexane/EtOAc gave **2.20c** as a colorless solid: yield 2.0 g (71%); silica gel TLC R_f 0.56 (1:1 hexanes–EtOAc); $[\alpha]^{24}_D$ +31.8 (*c* 1.5, MeOH); ^{1}H NMR ($CDCl_3$) δ 0.86-0.89 (m, 18H), 1.39-1.42 (m, 15H), 2.32-2.36 (m, 1H), 3.52-3.55 (m, 1H), 3.66-3.69 (m, 1H), 4.16-4.30 (m, 1H), 4.47-4.50 (m, 1H) and 4.52-4.55 (d, 1H, *J* = 10.0 Hz); ^{13}C NMR ($CDCl_3$) δ 14.3, 18.0, 21.5, 21.6, 23.9, 24.7, 26.4, 28.2, 28.3, 35.0, 41.4, 42.9, 46.1, 50.8, 58.6, 62.9, 75.7, 79.1, 153.8, 155.6 and 176.1; mass spectrum (MALDI-TOF), *m/z* 465.3 $(M+Na)^+$ (theoretical 465.3); mass spectrum (APCI), *m/z* 443.3117 $(M+H)^+$ ($C_{23}H_{43}N_2O_6$ requires 443.3121).

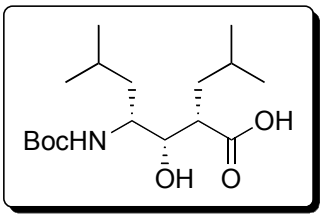

(2*S*,3*S*,4*R*)-4-*tert*-Butoxycarbonylamino-2′,4-di-isobutyl-3-hydroxybutyric acid (2.20d). To a cooled (0 °C) solution containing 1.16 g (2.63 mmol) of **2.20c** in 36 mL of 3:1 THF/H_2O was added 2.50 mL (15.8 mmol) of 30% H_2O_2 followed by 126 mg (5.26 mmol) of LiOH. After stirring at 0 °C for 3 h, the excess peroxide was quenched at 0 °C by the addition of 10.5 mL of 1.5 N aq Na_2SO_3 and the pH was adjusted to 9–10 with sat aq $NaHCO_3$. The oxazolidinone was recovered by extraction with three 10-mL portions of CH_2Cl_2. The aqueous layer was then acidified to pH ~2 with 1 N HCl, and extracted with three 10-mL portions of EtOAc. The combined organic layer was dried over Na_2SO_4 and concentrated

under diminished pressure to give the crude product as a colorless solid: yield 570 mg (66%); silica gel TLC R_f 0.18 (8:2:0.2:0.1 CH_2Cl_2–hexanes–MeOH–AcOH); $[\alpha]^{23}_D$ +19.8 (*c* 1.3, MeOH); ^{1}H NMR ($CDCl_3$) δ 0.92-0.99 (m, 12H), 1.45-1.67 (m, 15H), 2.60-2.70 (m, 1H) and 3.61-3.73 (m, 2H); ^{13}C NMR ($CDCl_3$) δ 18.0, 21.3, 22.4, 22.9, 23.8, 26.2, 28.3, 32.6, 46.4, 51.6, 58.4, 68.7, 76.0, 158.0 and 179.6; mass spectrum (MALDI-TOF), *m/z* 354.4 $(M+Na)^+$ (theoretical 354.2); mass spectrum (APCI), *m/z* 332.2445 $(M+H)^+$ ($C_{17}H_{34}NO_5$ requires 332.2437).

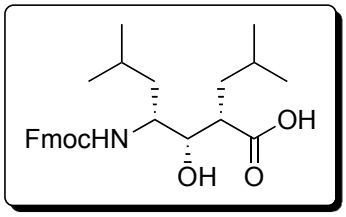

(2*S*,3*S*,4*R*)-2,4-di-isobutyl-4-(*9H*-fluoren-9-ylmethoxycarbonylamino)-3-hydroxy-butyric acid (2.20e). To a solution of 561 mg (1.69 mmol) of **2.20d** in 6 mL of Me_2S was added 10 mL of TFA. The reaction mixture was stirred at room temperature for 2 h. The solution was concentrated under a stream of argon and concentrated further under diminished pressure. The resulting oil was dissolved in 10 mL of 5% aq K_2CO_3 solution followed by the addition of 628 mg (1.86 mmol) of FmocOSu in 14 mL of dioxane. The reaction was stirred at room temperature overnight, and the solution was extracted successively with three 20-mL portions of ethyl ether and three 20-mL portions of EtOAc. The combined organic layer was dried over Na_2SO_4, filtered and concentrated under diminished pressure. The

crude product was then purified by flash chromatography on a silica gel column (25 x 3.2 cm). Elution with 93:5:2 CH_2Cl_2–MeOH–AcOH gave **2.20e** as a yellow solid: yield 691 mg (90%); mp 78-80 °C; silica gel TLC R_f 0.25 (8:2:0.2:0.1 CH_2Cl_2–hexanes–MeOH–AcOH); $[\alpha]^{23}_D$ +25.8 (*c* 1.2, MeOH); ^{1}H NMR ($CDCl_3$) δ 0.77-0.83 (m, 12H), 1.24-1.62 (m, 6H), 2.50-2.55 (m, 1H), 3.53-3.64 (m, 2H), 4.08-4.13 (m, 1H), 4.29-4.38 (m, 1H), 4.85 (d, 1H, *J* = 9.0 Hz), 7.20-7.23 (m, 2H), 7.29-7.32 (m, 2H), 7.48 (d, 2H, *J* = 7.5 Hz) and 7.67 (d, 2H, *J* = 7.5 H); ^{13}C NMR ($CDCl_3$) δ 21.2, 21.3, 23.7, 23.9, 24.6, 26.2, 36.9, 38.6, 46.8, 47.3, 52.1, 66.7, 75.8, 120.0, 125.0, 127.1, 127.7, 141.3, 143.8, 156.5 and 179.5; mass spectrum (MALDI-TOF), *m/z* 476.6 $(M+Na)^+$ (theoretical 476.2); mass spectrum (APCI), *m/z* 454.2589 $(M+H)^+$ ($C_{27}H_{36}NO_5$ requires 454.2593).

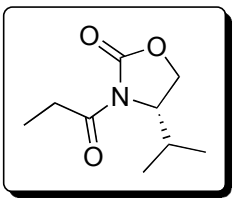

***(S)*-(+)-4-Isopropyl-3-propionyl-2-oxazolidinone (2.21) [96].** A stirred solution of 4.0 g (31.0 mmol) of oxazolidone in 100 mL of anhydrous THF was cooled to –78 °C. The 21.3 mL (34.1 mmol) of 1.6 M *n*-BuLi in hexane was added slowly and the mixture was stirred for 10 min. The 3.03 mL (34.1 mmol) of propionly chloride was then added slowly and the mixture was stirred for another 30 min. Then mixture was then warmed to room temperature over 30 min. Excess

propionyl chloride was quenched by the addition of 10 mL of sat aq NH_4Cl and the THF was removed under diminished pressure. The resulting slurry was then extracted with three 40-mL portions of CH_2Cl_2, and the combined organic layer was washed with 25 mL of 1N NaOH solution and then 25 mL of brine, dried over Na_2SO_4 and concentrated under diminished pressure to give the crude product as yellow oil. The residue was purified by flash chromatography on a silica gel column. Elution with 3:1 hexanes–EtOAc gave **2.21** as a colorless oil: yield 5.60 g (95%); silica gel TLC R_f 0.75 (1:1 hexanes–EtOAc); ^{1}H NMR ($CDCl_3$) δ 0.85 (d, 3H, J = 6.8 Hz), 0.89 (d, 3H, J = 7.2 Hz), 1.14 (t, 3H, J = 7.4 Hz), 2.36 (m, 1H), 2.95 (m, 2H), 4.17-4.27 (m, 2H) and 4.39-4.43 (m, 1H); mass spectrum (MALDI-TOF), *m/z* 186.1 $(M+H)^+$ (theoretical 186.1).

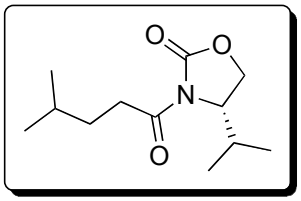

***(S)*-(+)-4-Isopropyl-3-(4'-methylvaleryl)-2-oxazolidinone (2.22) [162].** A stirred solution of 3.00 g (23.2 mmol) of oxazolidone in 100 mL of anhydrous THF was cooled to –78 ºC. The 5.50 mL (39.6 mmol) of 2.5 M *n*-BuLi in hexane was added slowly and the mixture was stirred for 30 min. To a separate flask containing 3.53 mL (27.9 mmol) 4-methylvaleric acid in 100 mL of THF was added 5.51 mL (39.6 mmol) of NEt_3 and 3.73 mL (30.3 mmol) of pivaloyl chloride at 0 ºC. After stirring for 30 min, the lithio-(4*S*)-4-isopropyl-2-

oxazolidinone was added. The mixture was warmed to room temperature over 2 h. The solution was extracted with EtOAc and the organic layer was washed with sat aq $NaHCO_3$, brine, and dried over Na_2SO_4 and concentrated under diminished pressure. The residue was purified by flash chromatography on a silica gel column. Elution with 3:1 hexanes–EtOAc gave **2.22** as a colorless oil: yield 5.10 g (93%); silica gel TLC R_f 0.28 (4:1 hexanes–EtOAc); [a] $_D^{23}$ +75.6 (*c* 0.92, $CHCl_3$); ^{1}H NMR ($CDCl_3$) δ 0.86 (d, 3H, *J* = 6.8 Hz), 0.89-0.92 (m, 9H), 1.50-1.62 (m, 3H), 2.35 (m, 1H), 2.81-2.89 (m, 1H), 2.94-3.02 (m, 1H), 4.17-4.27 (m, 2H) and 4.40-4.44 (m, 1H); ^{13}C NMR ($CDCl_3$) δ 14.6, 18.0, 22.3, 22.3, 27.7, 28.3, 33.3, 33.6, 58.4, and 63.3; mass spectrum (MALDI-TOF), *m/z* 228.2 $(M+H)^+$ (theoretical 228.2).

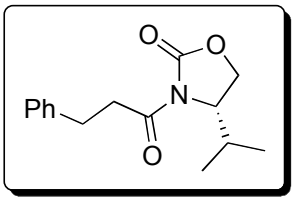

***(S)*-(+)-4-Isopropyl-3-phenylpropionyl-2-oxazolidinone (2.24) [164].** A stirred solution of 1.12 g (8.65 mmol) of oxazolidone in 25 mL of anhydrous THF was cooled to –78 ºC. The 6.0 mL (9.95 mmol) of 1.6 M *n*-BuLi in hexane was added slowly and the mixture was stirred for 10 min. The 1.41 mL (9.51 mmol) of 3-phenylpropionyl chloride was then added slowly and the mixture was stirred for another 30 min. Then mixture was then warmed to room temperature over 30 min.

Excess 3-phenylpropionyl chloride was quenched by the addition of 6 mL of sat aq NH_4Cl and the THF was removed under diminished pressure. The resulting slurry was then extracted with three 20-mL portions of CH_2Cl_2, and the combined organic layer was washed with 20 mL of 1N NaOH solution and then 20 mL of brine, dried over Na_2SO_4 and concentrated under diminished pressure to give the crude product as yellowish solid. The residue was purified by flash chromatography on a silica gel column. Elution with 3:1 hexanes–EtOAc gave **2.24** as a white solid: yield 2.3 g (88%); silica gel TLC R_f 0.70 (1:1 hexanes–EtOAc); $[a]_D^{20}$ +74.7 (*c* 0.73, EtOH); ^{1}H NMR ($CDCl_3$) δ 0.82 (d, 3H, *J* = 7.2 Hz), 0.88 (d, 3H, *J* = 6.8 Hz), 2.33 (m, 1H), 2.95-3.00 (m, 2H), 3.16-3.35 (m, 2H), 4.16-4.24 (m, 2H), 4.38-4.42 (m, 1H) and 7.16-7.29 (m, 5H); mass spectrum (MALDI-TOF), *m/z* 262.1 $(M+H)^+$ (theoretical 262.1).

General procedure for the attachment of bithiazole to the solid support. To a suspension containing 1.0 g (0.48 mmol/g) of NovaSyn TentaGel amino functionalized resin was added a solution containing 0.89 g (2.20 mmol) of Boc-protected spermine and 460 μL (2.64 mmol) of Hünig's base in 4 mL of DMF. After 24 h, the resin was filtered, and washed for 30 sec each with three 5-mL portions of DMF, three 5-mL portions of CH_2Cl_2, and then three 5-mL portions of DMF. A solution containing 0.63 g (1.32 mmol) of Fmoc-bithiazole, 0.51 g (1.32 mmol) of HBTU, and 460 μL (2.64 mmol) of Hünig's base in 2 mL of DMF

was added. After 30 min, the resin was filtered, and washed for 30 sec each with three 5-mL portions of DMF, three 5-mL portions of CH_2Cl_2, and three 5-mL portions of methanol. The resulting resin was dried under diminished pressure over KOH pellets. Quantitative Fmoc cleavage analysis indicated a loading of 0.12 mmol/g (25% over 3 steps).

General procedure for the attachment of threonine to the resin-bound dipeptide. To a suspension containing 200 mg of bithiazole-functionalized resin was added, sequentially for 5 min each, three 4-mL solutions containing 20% piperidine in DMF. The resulting resin was washed for 30 sec each with three 5-mL portions of DMF, three 5-mL portions of CH_2Cl_2, and then three 5-mL portions of DMF. A solution containing 27.0 mg (0.079 mmol) of commercially available Fmoc-threonine, 29.7 mg (0.079 mmol) of HBTU, 12.1 mg (0.079 mmol) of HOBt, and 28 μL (0.16 mmol) of Hünig's base in 2 mL of DMF was added. After 30 min, the resin was filtered and washed for 30 sec each with three 5-mL portions of DMF, three 5-mL portions of CH_2Cl_2, and three 5-mL portions of methanol. The resulting resin was dried under diminished pressure over KOH pellets. Quantitative Fmoc cleavage analysis indicated a loading of 0.10 mmol/g (83%).

General procedure for the attachment of methylvalerate (analogues) to the resin-bound tripeptide. To a suspension containing 200 mg of the derivatized resin was added sequentially for 5 min each, three 4-mL solutions containing 20% piperidine in DMF. The resulting resin was washed for 30 sec each with three 5-mL portions of DMF, three 5-mL portions of CH_2Cl_2, and then three 5-mL portions of DMF. A solution containing 35 mg (77 μmol) of an Fmoc-methylvalerate (analogue), 29 mg (77 μmol) of HBTU, 12 mg (77 μmol) of HOBt, and 27 μL (0.16 mmol) of Hünig's base in 2 mL of DMF was added. After 30 min, the resin was filtered and washed for 30 sec each with three 5-mL portions of DMF, three 5-mL portions of CH_2Cl_2, and three 5-mL portions of methanol. The resulting resin was dried under diminished pressure over KOH pellets. Quantitative Fmoc cleavage analysis indicated a loading of 0.09 mmol/g (90%).

General procedure for the attachment of histidine to the resin-bound tetrapeptide. To a suspension containing 100 mg of the derivatized resin was added sequentially for 5 min each, three 4-mL solutions containing 20% piperidine in DMF. The resulting resin was washed for 30 sec each with three 5-mL portions of DMF, three 5-mL portions of CH_2Cl_2, and then three 5-mL portions of DMF. A solution containing 30 mg (49 μmol) of commercially available Fmoc-histidine, 19 mg (49 μmol) of HATU, 7.0 mg (49 μmol) of HOAt, and 17 μL (97 μmol) of Hünig's base in 2 mL of DMF was added. After 30 min, the resin was filtered and

washed for 30 sec each with three 5-mL portions of DMF, three 5-mL portions of CH_2Cl_2, and three 5-mL portions of methanol. The resulting resin was dried under diminished pressure over KOH pellets. Quantitative Fmoc cleavage analysis indicated a loading of 0.07 mmol/g (78%).

General procedure for the synthesis of deglycobleomycin analogues. To a suspension containing 40 mg of the derivatized resin was added sequentially for 10 min each, three 1-mL solutions containing 20% piperidine in DMF. The resulting resin was washed for 30 sec each with three 5-mL portions of DMF, three 5-mL portions of CH_2Cl_2, and three 5-mL portions of DMF. The resin was then added to a 10-mL round bottom flask containing 1 mL of DMF and cooled to 0 ^oC for 10 min. A mixture containing 5.0 mg (12 μmol) of Boc-pyrimidoblamic acid and 16 mg (36 μmol) of BOP reagent was added to the resin with an additional 1 mL of DMF. The reaction mixture was cooled for an additional 10 min, followed by the addition of 13 μL (72 μmol) of Hünig's base. After 16 h, the resin was filtered and washed for 30 sec each with three 5-mL portions of DMF, three 5-mL portions of CH_2Cl_2, and three 5-mL portions of methanol. The resulting resin was dried under diminished pressure over KOH pellets.

General procedure for the cleavage of deglycoBLM analogues from the resin. To a suspension containing 35–50 mg of resin-bound fully protected

deglycobleomycin A_6 analogue was added a solution containing 200 μL of triisopropylsilane and 200 μL of dimethyl sulfide. After 5 min, 3.6 mL of trifluoroacetic acid (TFA) was added to the suspension. After 4 h, the resin was filtered and washed for 30 sec each with three 5-mL portions of DMF, three 5-mL portions of CH_2Cl_2, and three 5-mL portions of DMF. The resulting resin was treated with 0.5 mL of 2% hydrazine in DMF. The resin was filtered and then treated with three 0.5-mL portions of 2% hydrazine in DMF solution for an additional 10 min. The eluate was collected and concentrated under diminished pressure. The resulting oil was dissolved in 0.1% aq TFA, frozen and lyophilized.

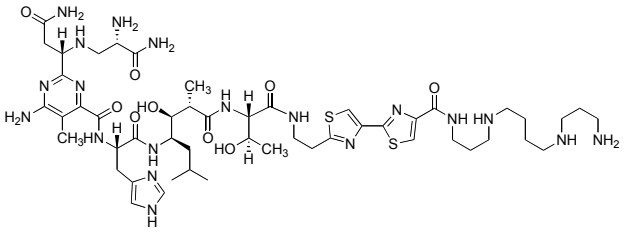

Deglycobleomycin analogue 2.26. HPLC retention time (using the conditions described under General Methods): 15.1 min; colorless solid; yield 1.8 mg (55%); ^{1}H NMR (D_2O) δ 0.53 (s, 1H), 0.65 (s, 1H), 0.90 (d, 3H, J = 6.4 Hz), 1.02 (d, 3H, J = 6.4 Hz), 1.16 (m, 2H), 1.63-1.64 (m, 4H), 1.88-1.95 (m, 7H), 2.45-2.48 (m, 1H), 2.57-2.64 (m, 2H), 2.94-3.01 (m, 12H), 3.09-3.11 (m, 2H), 3.14-3.19 (m, 4H), 3.38-3.41 (m, 2H), 3.44-3.47 (m, 2H), 3.53 (t, 1H, J = 5.6 Hz), 3.56-3.60 (m, 2H), 3.68-3.70 (m, 2H), 3.88-3.90 (m, 2H), 3.97-3.98 (m, 1H), 4.02 (t, 1H, J = 5.6 Hz), 4.12 (d, 1H, J = 4.2), 7.24 (s, 1H), 7.96 (s, 1H), 8.09 (s, 1H) and 8.58 (s,

1H); mass spectrum (MALDI-TOF), *m/z* 1178.4 $(M+Na)^+$ (theoretical 1178.6); mass spectrum (ESI), *m/z* 1156. 5977 $(M + H)^+$ ($C_{50}H_{82}N_{19}O_9S_2$ requires 1156.5984).

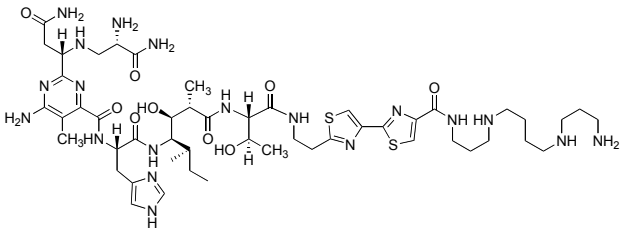

Deglycobleomycin analogue 2.27. HPLC retention time: 14.5 min; colorless solid; yield 1.5 mg (47%); ^{1}H NMR (D_2O) δ 0.15 (d, 3H, *J* = 7.2 Hz), 0.30 (d, 3H, *J* = 7.2 Hz), 0.57 (d, 3H, *J* = 7.2 Hz), 0.59 (d, 3H, *J* = 6.4 Hz), 0.85-0.87 (m, 2H), 1.08-1.19 (m, 3H), 1.28-1.29 (m, 4H), 1.53-1.61 (m, 7H), 2.22-2.29 (m, 3H), 2.59-2.66 (m, 9H), 2.71-2.73 (m, 1H), 2.78-2.84 (m, 3H), 3.05 (t, 2H, *J* = 5.6 Hz), 3.14-3.33 (m, 3H), 3.31-3.33 (m, 1H), 3.50 (dd, 1H, *J* = 5.6 and 3.2 Hz), 3.62-3.68 (m, 3H), 3.75 (d, 1H, *J* = 4.0 Hz), 4.34 (t, 1H, *J* = 7.2 Hz), 6.95 (s, 1H), 7.60 (s, 1H), 7.67 (s, 1H) and 8.25 (s, 1H); mass spectrum (MALDI-TOF), *m/z* 1156.6 $(M+H)^+$ (theoretical 1156.6); mass spectrum (ESI), *m/z* 1156.5991 $(M + H)^+$ ($C_{50}H_{82}N_{19}O_9S_2$ requires 1156.5984).

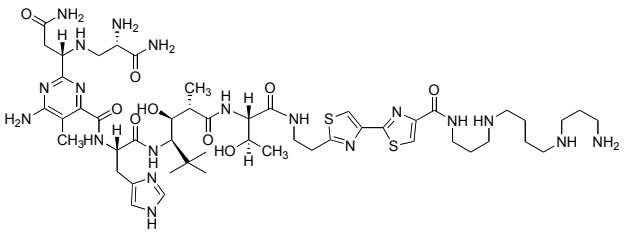

Deglycobleomycin analogue 2.28. HPLC retention time (using the conditions described under General Methods): 14.3 min; colorless solid; yield 0.98 mg (40%); ^{1}H NMR (D_2O) δ 0.78-1.00 (m, 15H), 1.60 (m, 4H), 1.85-1.91 (m, 7H), 2.08 (m, 1H), 2.53-2.54 (m, 1H), 2.90-2.98 (m, 14H), 3.03-3.05 (m, 2H), 3.11-3.18 (m, 3H), 3.34-3.38 (m, 2H), 3.46-3.53 (m, 3H), 3.83-3.85 (m, 2H), 4.18 (d, 1H, J = 7.2 Hz), 4.29 (t, 1H, J = 7.2 Hz), 7.23 (s, 1H), 7.96 (s, 1H), 8.08 (s, 1H) and 8.50 (s, 1H); mass spectrum (MALDI-TOF), *m/z* 1156.4 $(M+H)^+$ (theoretical 1156.6); mass spectrum (ESI), *m/z* 1156.5991 $(M + H)^+$ ($C_{50}H_{82}N_{19}O_9S_2$ requires 1156.5984).

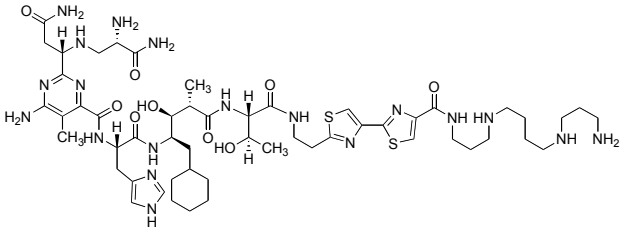

Deglycobleomycin analogue 2.29. HPLC retention time: 15.7 min; colorless solid; yield 1.9 mg (59%); ^{1}H NMR (D_2O) δ 1.00 (d, 3H, J = 6.4 Hz), 1.11 (d, 3H, J = 7.2 Hz), 1.19-1.26 (m, 2H), 1.35 (d, 3H, J = 11.2 Hz), 1.71-1.55 (m, 5H), 1.71-1.73 (m, 4H), 1.96-2.03 (m, 9H), 2.53-2.55 (m, 1H), 2.62-2.65 (m, 2H),

2.92-2.97 (m, 2H), 3.02-3.09 (m, 12H), 3.05 (dd, 1H, *J* = 8.0 and 7.2), 3.24-3.29 (m, 4H), 3.46-3.48 (m, 1H), 3.52-3.55 (m, 1H), 3.56-3.61 (m, 1H), 3.61-3.68 (m, 1H), 3.69-3.83 (m, 2H), 3.84-3.98 (m, 1H), 4.23 (d, 1H, *J* = 5.6 Hz), 4.29 (t, 1H, *J* = 7.2), 7.33 (s, 1H), 8.05 (s, 1H), 8.17 (s, 1H) and 8.66 (s, 1H); mass spectrum (MALDI-TOF), *m/z* 1218.5 $(M+Na)^+$ (theoretical 1218.6); mass spectrum (ESI), *m/z* 1196.6289 $(M + H)^+$ ($C_{53}H_{86}N_{19}O_9S_2$ requires 1196.6297).

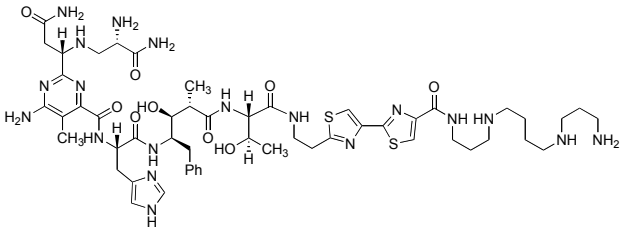

Deglycobleomycin analogue 2.30. HPLC retention time: 14.7 min; colorless solid; yield 1.4 mg (47%); ^{1}H NMR (D_2O) δ 0.97 (d, 3H, *J* = 6.4 Hz), 1.07 (d, 3H, *J* = 7.2 Hz), 1.63-1.64 (m, 4H), 1.84-1.95 (m, 7H), 2.35 (t, 1H, *J* = 12.0 Hz), 2.56-2.60 (m, 3H), 2.73-2.76 (m, 2H), 2.94-3.01 (m, 14H), 3.15 (t, 2H, *J* = 5.6 Hz), 3.32-3.38 (m, 4H), 3.53 (t, 1H, *J* = 6.4 Hz), 3.66 (t, 1H, *J* = 5.6 Hz), 3.96-4.03 (m, 4H), 4.19 (d, 1H, *J* = 5.6 Hz), 4.55 (t, 1H, *J* = 6.4 Hz), 6.73 (s, 1H), 6.98 (d, 1H, *J* = 8.0 Hz), 7.02 (t, 1H, *J* = 7.2 Hz), 7.08 (d, 1H, *J* = 8.0 Hz), 7.91 (s, 1H), 8.06 (s, 1H) and 8.38 (s, 1H); mass spectrum (MALDI-TOF), *m/z* 1212.4 $(M+Na)^+$ (theoretical 1212.6); mass spectrum (ESI), *m/z* 1190.5833 $(M + H)^+$ ($C_{53}H_{80}N_{19}O_9S_2$ requires 1190.5828).

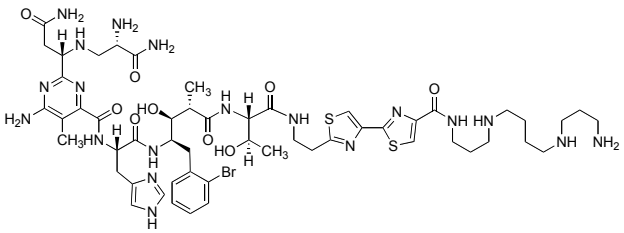

Deglycobleomycin analogue 2.31. HPLC retention time: 19.0 min; colorless solid; yield 1.2 mg (27%); ^{1}H NMR (D_2O) δ 0.99 (d, 3H, J = 7.2 Hz), 1.09 (d, 3H, J = 7.2 Hz), 1.63-1.64 (m, 4H), 1.83-1.95 (m, 7H), 2.40 (t, 1H, J = 12.0 Hz), 2.53-2.61 (m, 3H), 2.66-2.69 (m, 1H), 2.94-3.01 (m, 14H), 3.15-3.20 (m, 2H), 3.31-3.36 (m, 2H), 3.50-3.53 (m, 1H), 3.63-3.67 (m, 2H), 3.84-3.85 (m, 1H), 3.93-3.94 (m, 1H), 4.01-4.04 (m, 1H), 4.22 (d, 1H, J = 4.8 Hz), 4.23-4.25 (m, 1H), 4.55 (t, 1H, J = 6.4 Hz), 6.82 (s, 1H), 6.87 (t, 1H, J = 8.0 Hz), 6.96 (d, 1H, J = 7.2 Hz), 7.01 (t, 1H, J = 7.2 Hz), 7.05 (d, 1H, J = 8.0 Hz), 7.87 (s, 1H), 8.01 (s, 1H) and 8.43 (s, 1H); mass spectrum (MALDI-TOF), *m/z* 1290.7 and 1292.0 $(M+Na)^+$ (theoretical 1290.5 and 1292.5); mass spectrum (ESI), *m/z* 1268.4986 and 1270.4956 $(M + H)^+$ ($C_{53}H_{79}N_{19}O_9S_2Br$ requires 1268.4933 and 1270.4913).

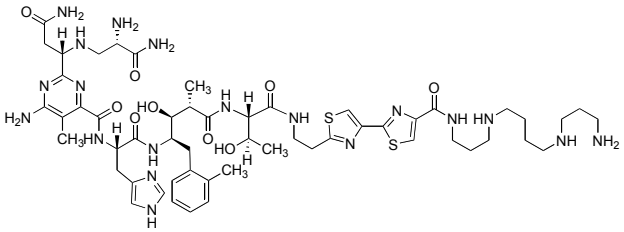

Deglycobleomycin analogue 2.32. HPLC retention time: 15.5 min; colorless solid; yield 1.5 mg (47%); ^{1}H NMR (D_2O) δ 0.98 (d, 3H, J = 6.4 Hz), 1.08 (d,

3H, J = 7.2 Hz), 1.63-1.64 (m, 4H), 1.85-1.95 (m, 7H), 2.00 (s, 3H), 2.33 (t, 1H, J = 12.0 Hz), 2.58-2.66 (m, 4H), 2.74 (dd, 1H, J = 9.6 and 5.6 Hz), 2.80 (dd, 1H, J = 11.2 and 3.2 Hz), 2.94-2.97 (m, 12H), 3.00 (t, 2H, J = 8.0 Hz), 3.31-3.37 (m, 2H), 3.51-3.59 (m, 2H), 3.67 (t, 1H, J = 7.2 Hz), 3.99 (t, 1H, J = 5.6 Hz), 4.04-4.07 (m, 2H), 4.08-4.11 (m, 1H), 4.20 (d, 1H, J = 4.8 Hz), 4.55 (t, 1H, J = 7.2 Hz), 6.72 (s, 1H), 6.84-6.87 (m, 2H), 6.90 (d, 2H, J = 7.2 Hz), 7.90 (s, 1H), 8.03 (s, 1H) and 8.39 (s, 1H); mass spectrum (MALDI-TOF), *m/z* 1226.6 $(M+Na)^+$ (theoretical 1226.6); mass spectrum (ESI), *m/z* 1204.5968 $(M + H)^+$ ($C_{54}H_{82}N_{19}O_9S_2$ requires 1204.5984).

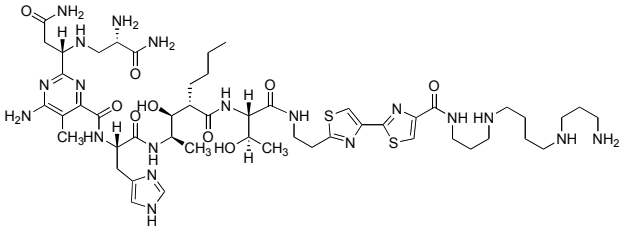

Deglycobleomycin analogue 2.33. HPLC retention time: 16.7 min; colorless solid; yield 1.8 mg (56%); ^{1}H NMR (D_2O) δ 0.61 (t, 3H, J = 7.2 Hz), 0.89 (d, 3H, J = 7.2 Hz), 0.96 (d, 3H, J = 5.6 Hz), 1.03-1.06 (m, 2H), 1.38-1.40 (m, 2H), 1.53-1.54 (m, 2H), 1.64 (m, 2H), 1.86-1.95 (m, 8H), 2.35-2.36 (m, 1H), 2.60-2.64 (m, 3H), 2.94-3.01 (m, 14H), 3.09-3.18 (m, 4H), 3.37-3.41 (m, 3H), 3.52-3.56 (m, 4H), 4.02 (t, 1H, J = 5.6 Hz), 4.11 (d, 1H, J = 4.0 Hz), 7.21 (s, 1H), 7.92 (s, 1H), 8.08 (s, 1H) and 8.53 (s, 1H); mass spectrum (MALDI-TOF), *m/z* 1178.0

$(M+Na)^+$ (theoretical 1178.6); mass spectrum (ESI), *m/z* 1156. 5979 $(M + H)^+$ ($C_{50}H_{82}N_{19}O_9S_2$ requires 1156.5984).

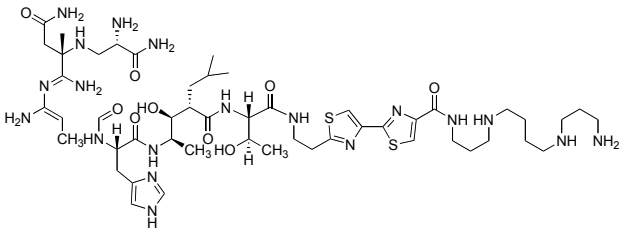

Deglycobleomycin analogue 2.34. HPLC retention time: 17.6 min; colorless solid; yield 1.4 mg (43%); ^{1}H NMR (D_2O) δ 0.65 (d, 3H, *J* = 6.4 Hz), 0.69 (d, 3H, *J* = 6.4 Hz), 0.90 (d, 3H, *J* = 7.2 Hz), 0.95 (d, 3H, *J* = 6.4 Hz), 1.21-1.29 (m, 3H), 1.42-1.48 (m, 2H), 1.64 (m, 4H), 1.87-1.95 (m, 7H), 2.41-2.44 (m, 1H), 2.57-2.67 (m, 2H), 2.91-3.03 (m, 12H), 3.06-3.18 (m, 4H), 3.38-3.49 (m, 2H), 3.41-3.56 (m, 3H), 3.67-3.69 (m, 2H), 3.93 (t, 1H, *J* = 5.6 Hz), 4.11 (d, 1H, *J* = 4.8 Hz), 7.21 (s, 1H), 7.93 (s, 1H), 8.08 (s, 1H) and 8.53 (s, 1H); mass spectrum (MALDI-TOF), *m/z* 1178.4 $(M+Na)^+$ (theoretical 1178.6); mass spectrum (ESI), *m/z* 1156. 5995 $(M + H)^+$ ($C_{50}H_{82}N_{19}O_9S_2$ requires 1156.5984).

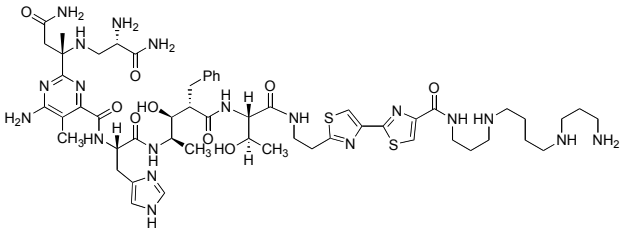

Deglycobleomycin analogue 2.35. HPLC retention time: 17.2 min; colorless solid; yield 1.0 mg (30%); ^{1}H NMR (D_2O) δ 0.53 (d, 3H, J = 6.4 Hz), 0.93 (d, 3H, J = 6.4 Hz), 1.63-1.64 (m, 4H), 1.86-1.94 (m, 7H), 2.52-2.59 (m, 2H), 2.61 (t, 1H, J = 4.8 Hz), 2.69-2.72 (m, 1H), 2.82-2.86 (m, 1H), 2.93-3.01 (m, 14H), 3.09-3.14 (m, 3H), 3.17-3.20 (m, 2H), 3.27-3.49 (m, 4H), 3.66-3.68 (m, 2H), 3.78 (t, 1H, J = 6.4 Hz), 3.89 (d, 1H, J = 4.8 Hz), 6.95 (d, 2H, J = 7.2 Hz), 6.99-7.00 (m, 3H), 7.23 (s, 1H), 7.92 (s, 1H), 8.07 (s, 1H) and 8.54 (s, 1H); mass spectrum (MALDI-TOF), *m/z* 1212.4 $(M+Na)^+$ (theoretical 1212.6); mass spectrum (ESI), *m/z* 1190.5823 $(M + H)^+$ ($C_{53}H_{80}N_{19}O_9S_2$ requires 1190.5828).

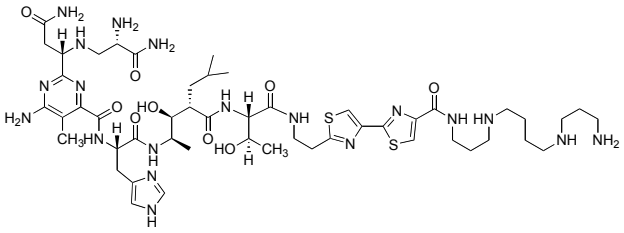

Deglycobleomycin analogue 2.36. HPLC retention time: 16.4 min; colorless solid; yield 1.2 mg (36%); ^{1}H NMR (D_2O) δ 0.53 (d, 3H, J = 7.2 Hz), 0.59 (d, 3H, J = 6.4 Hz), 0.65-0.66 (m, 9H), 0.91-0.92 (m, 5H), 1.15-1.25 (m, 4H), 1.40-1.42 (m, 1H), 1.63-1.64 (m, 2H), 1.88-1.95 (m, 7H), 2.57-2.61 (m, 3H), 2.93-3.01 (m, 12H), 3.07-3.11 (m, 1H), 3.17-3.20 (m, 2H), 3.38-3.40 (m, 2H), 3.44-3.50 (m, 2H), 3.57-3.60 (m, 1H), 3.65-3.67 (m, 1H), 3.89 (t, 1H, J = 6.4 Hz), 3.92-3.93 (m, 1H), 3.99-4.02 (m, 1H), 4.15 (d, 1H, J = 4.8 Hz), 7.23 (s, 1H), 7.97 (s, 1H), 8.09 (s, 1H) and 8.57 (s, 1H); mass spectrum (MALDI-TOF), *m/z* 1220.5 $(M+Na)^+$

(theoretical 1220.6); mass spectrum (ESI), *m/z* 1198.6442 $(M + H)^+$

($C_{53}H_{88}N_{19}O_9S_2$ requires 1198.6454).

CHAPTER 3

SYNTHESIS OF BICYCLIC PYRIDINOL ANTIOXIDANT

3.1 Introduction

One of the research projects ongoing in our laboratory is focused on the discovery of drugs for the treatment of inherited mitochondrial diseases. Mitochondria are membrane-enclosed organelles found in eukaryotic cells [175]. Mitochondria generate most of the ATP produced by the cell, which is used as the source of chemical energy in the human body. In addition to supplying cellular energy, mitochondria are involved in a range of other processes, such as signaling, apoptosis and the control of the cell cycle and cell growth [176]. Mitochondrial dysfunction is implicated in the pathogenesis of a number of human diseases, including respiratory disorders and cardiac dysfunction as well as the aging process [177,178]. Mitochondrial electron transport chain has been recognized as a major intracellular source of reactive oxygen species (ROS) [179]. The leakage of ROS from the respiratory chain complexes may lead to lipid peroxidation, DNA oxidation and damage of other macromolecules [180]. Mitochondria are one of the key targets for the oxidative action of ROS. The natural lipophilic antioxidants, ubiquinone and vitamin E, have attracted enormous attention recently as potential agents to prevent radical damage of mitochondria. In particular, α-tocopherol (α-TOH), a form of vitamin E, is perhaps the best known natural antioxidant [125(a)]. By transferring its phenolic H atom to propagating lipid radicals, it

quenches lipid peroxidation [132]. The development of synthetic radical scavenging antioxidants with activity superior to α-TOH is an ongoing aim of many studies.

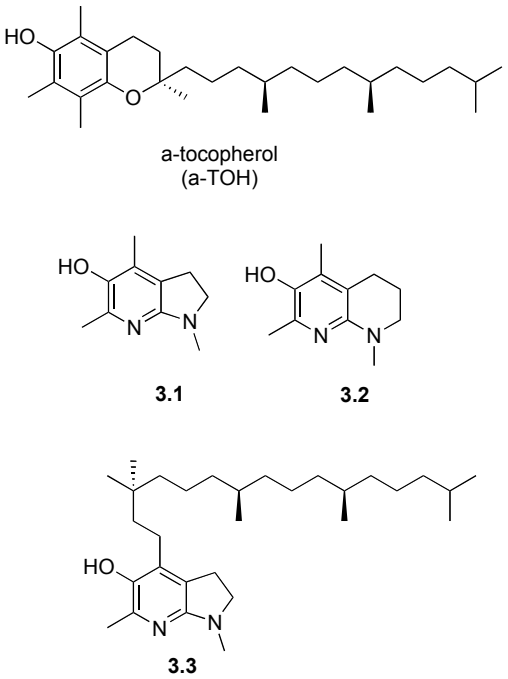

Figure 3.1. Structures of α-tocopherol and tocopherol-like antioxidants **3.1**, **3.2** and **3.3**.

6-Amino-3-pyridinols have been synthesized and demonstrated to be very efficient antioxidants. In particular, the bicyclic pyridinols **3.1** and **3.2** (Figure 3.1) displayed 88- and 28-fold greater inhibition rate constants, respectively, than α-TOH in quenching the oxidation of methyl linoleate in benzene solution [139]. To improve the effectiveness of compound **3.1**, we reasoned that conjugation of the pyridinol antioxidant core to a lipophilic side chain might facilitate delivery of the antioxidant to membranes, including mitochondrial membranes, and thereby confer cytoprotective properties at the level of mitochondrial function. Recently our

laboratory has reported a lipophilic pyridinol analogue of tocopherol **3.3**, in which the phytyl side chain of α-tocopherol was conjugated to the 5-position of the pyridinol core [140(c)]. This analogue was shown to suppress the level of reactive oxygen species in cultured cells, and to quench peroxidation of mitochondrial membranes. However, reported syntheses of analogue **3.3** required 16 steps and proceeded in moderate yields.

In a recent study, we have reported a short and scalable route to synthesize the bicyclic pyridinol antioxidants (compounds **1** and **2**) [181]. The novel feature of this synthesis is the installation of the bicyclic structures by a cyclocondensation reaction of lactam acetal with an enaminone. Based on this methodology, a lipophilic side chain can readily be coupled to the pyridinol core via regioselective metalation of the 2-methyl group. Moreover, the structural function of the phytyl group is thought to be related to its lipophilicity [141(a),182]; however, generation of this side chain requires multiple steps due to its three chiral centers. To avoid its tedious synthesis, we chose to replace the phytyl group with varying alkyl chains, which could potentially mimic the phytyl chain. Clearly, the question was whether biological function of the analogues would be retained with a simpler alkyl "tail" attached to a more accessible position at the antioxidant core. If so, valuable aminopyridinol analogues of α-TOH might become more accessible. A new series of antioxidants have been designed and prepared to diminish the effects of oxidative stress within the

mitochondrial electron transport chain as well as develop a facile synthesis to provide this novel group of antioxidants. The analogues of interest involve modifications that introduce a simpler lipophilic side chain to the 6-position of the pyridinol core (Figure 3.2). Analogues **3.4**–**3.9** were evaluated for their ability to suppress reactive oxygen species in cells under oxidative stress, and to protect cultured Friedreich's ataxia fibroblasts from oxidative stress.

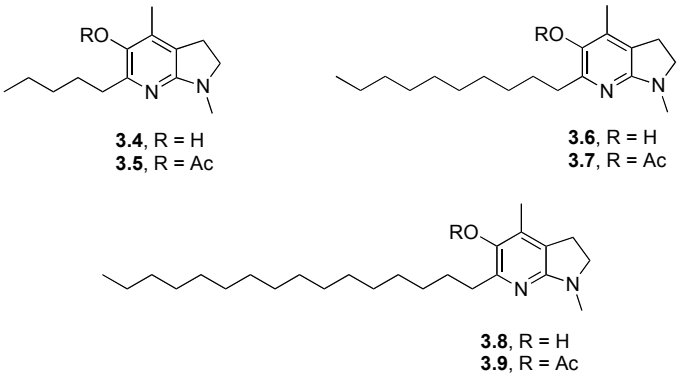

Figure 3.2. Structures of bicyclic pyridinol antioxidants **3.4**–**3.9**.

3.2 Results and discussion

3.2.1 Synthesis of bicyclic pyridinols

A retrosynthetic analysis of pyridinols **3.1** and **3.2** is shown in Figure 3.3. The desired compounds could be prepared from 4,6-dimethylpyrrolo[2,3-*b*]pyridine (**3.12**) or piperidinyl[2,3-*b*]pyridine (**3.19**) by appropriate functional group transformations. The formation of **3.12** and **3.19** was envisioned by a cyclocondensation reaction of enaminone **3.10** with lactam acetals **3.11** and **3.18**, respectively.

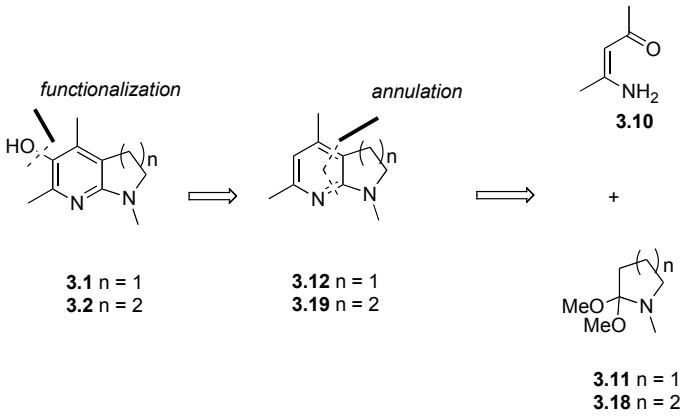

Figure 3.3. Retrosynthetic analysis of pyridinol antioxidants **3.1** and **3.2**.

As outlined in Scheme 3.1, the formation of the dihydropyrrolopyridine (azaindoline) intermediate is the key step of the synthesis of **3.1**. Accordingly, 1,4,6-trimethyl-2,3-dihydro-1*H*-pyrrolo[2,3-*b*]pyridine (**3.12**) was prepared in 62% yield by treatment of enaminone **3.10** with lactam acetal **3.11** in *t*-BuOH–*t*-BuONa at 90 ^{o}C [183]. The bromination of **3.12** was first attempted using NBS as the bromination reagent in concentrated H_2SO_4–TFA [184]. However, the bromination conditions provided di-brominated by-product as well as the desired monobrominated product. Since these two products were difficult to separate, we chose a milder bromination agent 1,3-dibromo-5,5-dimethylhydantoin [185] for the selective bromination of **3.12**. The reaction was carried out at 0 ^{o}C in chloroform and gave **3.13** in 82% yield; no dibrominated by-product was observed. In the final step, the hydroxylation of **3.13** was attempted by using KOH in the presence of a Pd catalyst [186]. Due to the instability of the final product **3.1** toward air oxidation, we also attempted to convert this compound to

its acetate ester **3.17** following the *in situ* formation of **3.1**. This strategy would also permit easy scale-up and storage of the intermediates prior to conversion to the unstable pyridinol. At first, **3.13** was treated with KOH in 1:1 H_2O–1,4-dioxane in the presence of Pd_2dba_3 and ligand **3.14** at 100 °C, followed by the addition of Ac_2O. Unexpectedly, we obtained 7-azaindole **3.15** in 45% yield, rather than 7-azaindoline **3.17**. Presumably, the generated **3.17** could be oxidized quickly to **3.15** under the reaction conditions in spite of efforts to maintain an inert atmosphere. Although **3.15** was obtained unexpectedly, we reasoned that its corresponding pyridinol **3.16** might also prove to be an interesting antioxidant. Accordingly, pyridinol **3.16** was prepared from **3.15** by hydrolysis with

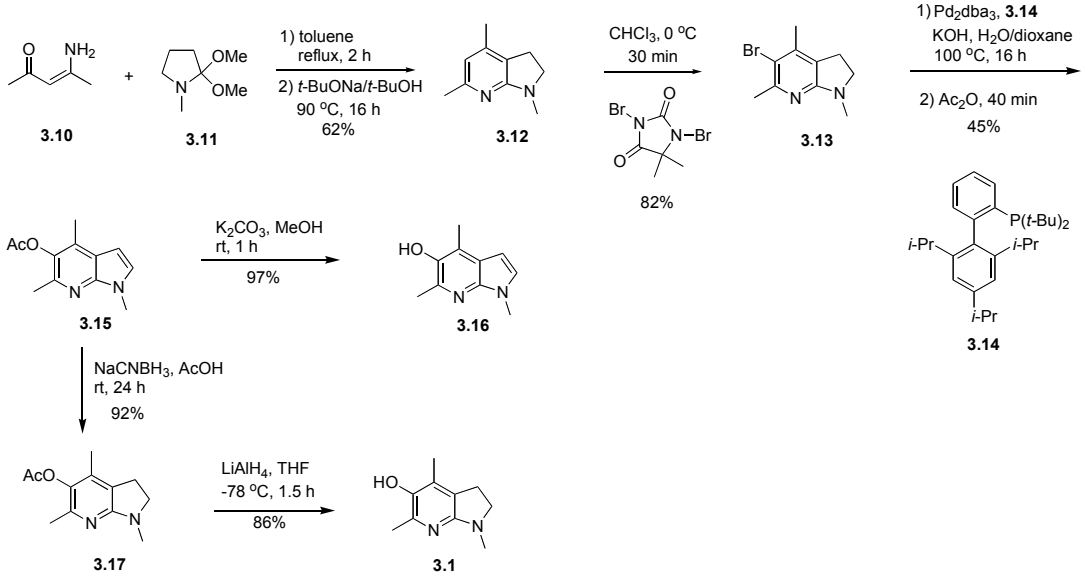

Scheme 3.1. Synthesis of pyridinol **3.1**.

K_2CO_3 in methanol in 97% yield. The desired 7-azaindole was prepared readily from azaindole **3.15** by reduction. The reduction of azaindole was achieved by using $NaCNBH_3$ in acetic acid media, affording compound **3.17** in 92% yield [187]. The acetyl group was removed reductively using $LiAH_4$ in THF to provide **3.1** in 86% yield. The synthesis of **3.1** was thus achieved in 5 steps and 18.1% overall yield, as compared to the previous reported route which required 11 total steps and provided **3.1** in 5.8% yield [193b]. Further, this new route proceeds through a stable *O*-acetate derivative that can be stored conveniently.

As shown in Scheme 3.2, pyridinol **3.2**, having a fused six-membered ring, was synthesized using a similar strategy. The cyclocondensation of **3.10** with **3.18** afforded **3.19** in 59% yield. Bromination of **3.19** gave compound **3.20** in 86% yield. Hydroxylation of **3.20**, followed by acetylation of the nascent OH group, afforded **3.21** in 55% yield. Finally, pyridinol **3.2** was obtained by treatment with $LiAH_4$ in 95% yield. This method provided **3.2** in 26.5% overall yield (4 total steps), while **3.2** was obtained previously in 3.3% overall yield over 6 steps [139(b)].

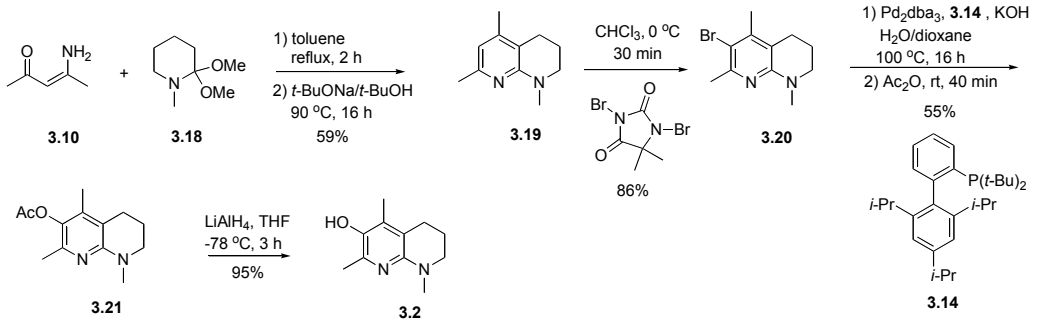

Scheme 3.2. Synthesis of pyridinol **3.2**.

3.2.2 Synthesis of bicyclic pyridinols with lipophilic side chains

Our goal was to develop simplified and easily accessible analogues of α-tocopherol bearing a lipophilic side chain on an appropriate antioxidant core. All the analogues were designed to possess a pyridinol structure with a fused five-membered ring due to its superior radical-scavenging ability over the phenol ring. The phenolic group of α-TOH is responsible for the antioxidant activity, whereas the phytyl side chain favors the insertion of α-TOH into liposomes and suppresses the migration of α-TOH between liposomal membranes. This suggests that the "delivery" of the antioxidants into the lipid bilayer region is dependent on the lipophilicity of the side chain. This hypothesis led us to design analogues with a simpler lipophilic side chain attached to a more accessible position on the pyridine ring. Since the 2-methyl group can be selectively metalated, an alkyl bromide can be directly coupled to this ionized carbon. This coupling strategy is much more straightforward compared to previous methods, which involved the functionalization of the pyridine ring either with an aldehyde group followed by a Witting reaction [140(a)(b)(d)], or with a triflate group followed by a metal-catalyzed cross coupling reaction [140(c)].

A retrosynthetic analysis, shown in Figure 3.4, suggested that the targeted compounds could be prepared from pyridines **3.22**, **3.24** and **3.26** by functional group transformations. Conjugation of alkyl side chains to compound **3.12** was

envisioned by initial metalation of the 2-methyl group, followed by a subsequent nucleophilic substitution reaction on alkyl bromides.

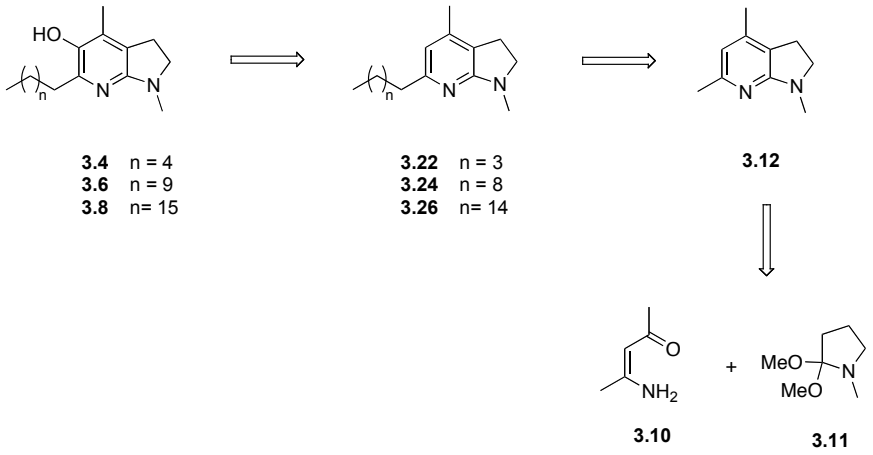

Figure 3.4. Retrosynthetic analysis of pyridinol antioxidants **3.4**, **3.6** and **3.8**.

Based on the synthetic studies we described in preparing the bicyclic pyridinols, compound **3.12** could be constructed by a cyclocondensation reaction of amide acetal **3.10** with enaminone **3.11**. The synthesis of the desired antioxidants **3.4**, **3.6** and **3.8** and the corresponding acetate **3.5**, **3.7** and **3.9** is illustrated in Scheme 3.3. Accordingly, 1,4,6-trimethyl-2,3-dihydro-1*H*-pyrrolo[2,3-*b*]pyridine **3.12** was prepared in 45% yield by the cylocondensation of amide acetal **3.10** and enaminone **3.11**. Aliphatic side chains were introduced by regioselective metalation of the 2-methyl group of azaindoline **3.12** in the presence of *n*-BuLi, followed by treatment of 1-bromobutane to generate **3.22** in 68% yield, 1-bromonane to generate **3.24** in 64% yield and 1-bromopentadecane to generate

3.26 in 52% yield. Azaindoline **3.22**, **3.24** and **3.26** were brominated using 1,3-dibromo-5,5-dimethylhydantoin in chloroform at 0 ^{o}C to afford the brominated azaindoline **3.23**, **3.25** and **3.27** in 92%, 94% and 98% yields, respectively. The bromides **3.23**, **3.25** and **3.27** were hydroxylated using *n*-BuLi and tetramethylethylenediamine followed by treatment of trimethoxy boron and finally with peracetic acid. Due to the instability of pyridinol toward air oxidation, we protected the generated hydroxyl groups as their acetate esters. The reaction was carried out in the presence of NEt_3, DMAP followed by the addition of Ac_2O at 0 ^{o}C and afforded **3.5**, **3.7** and **3.9** in 80%, 76% and 82% yields. This strategy permits the easy scale-up and storage of the acetate ester intermediates prior to conversion to the unstable pyridinol products. Additionally, the acetate esters could potentially act as prodrugs for the corresponding pyridinols. The removal of the acetyl group was achieved by treatment with DIBAL-H in CH_2Cl_2 at –78 ^{o}C. Due to their tendency to be oxidized, the final products **3.4**, **3.6** and **3.8** were converted to their trifluoroacetate salts. Compounds **3.4**, **3.6** and **3.8** were further purified by reversed-phase HPLC prior to bioassay, and were tested as their trifluoroacetate salts.

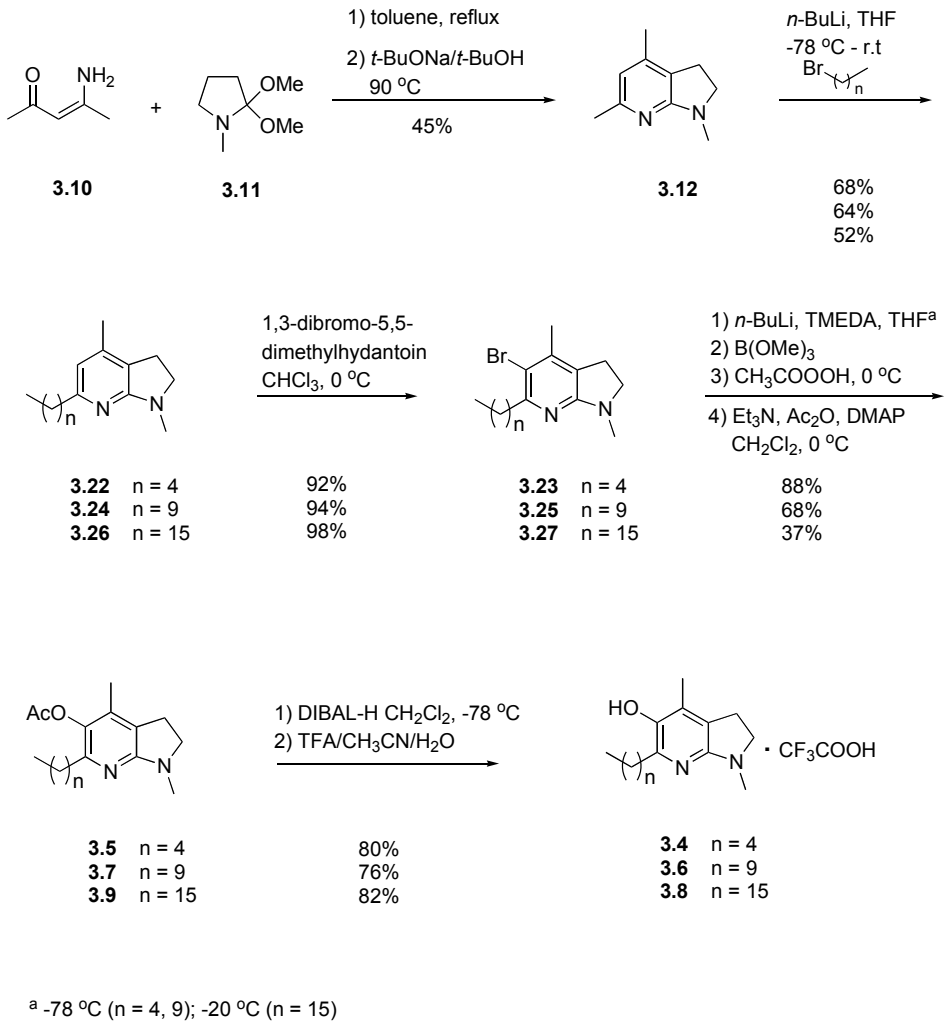

3.10 **3.11** **3.12**

3.22 n = 4 **3.24** n = 9 **3.26** n = 15 — 92% 94% 98%

3.23 n = 4 **3.25** n = 9 **3.27** n = 15 — 88% 68% 37%

3.5 n = 4 **3.7** n = 9 **3.9** n = 15 — 80% 76% 82%

3.4 n = 4 **3.6** n = 9 **3.8** n = 15

[a] -78 °C (n = 4, 9); -20 °C (n = 15)

Scheme 3.3. Synthesis of pyridinol analogues of α-TOH **3.4**–**3.9**.

3.2.3 Biochemical and biological evaluation of the tocopherol analogues

3.2.3.1 Assessment of lipid peroxidation in a membrane model system

All the analogues were tested for their ability to quench lipid peroxidation using a C_{11}-BODIPY$^{581/591}$ liposome system as illustrated in Figure 3.5. The oxidation of the probe results in a change of its emitted fluorescence from red to green [188]. The experiment emplyed small unilamellar phospholipid vesicles

incorporating the fluorescent peroxidation probe C_{11}-BODIPY$^{581/591}$, and the peroxidation was initiated by addition of the radical generator 2,2'-azo-bis-(2-amidinopropane) (AAPH). When treated with AAPH, the fluorescence of the fluorophore diminished with time, reflecting peroxidation of the (lipid) fluorophore. As shown, pyridinol analogues **3.4**, **3.6** and **3.8** (left panel) were much more effective than α-TOH in quenching lipid peroxidation, and acetate analogues **3.5**, **3.7** and **3.9** (right panel) were also found to be slightly more effective than α-TOH acetate. The lipophilic side chain appeared to be very important to enable the quenching of lipid peroxidation in this system. Pyridinol analogue **3.6** with a ten-carbon side chain displayed much higher efficiency compared with the other two pyridinol analogues **3.4** and **3.8**.

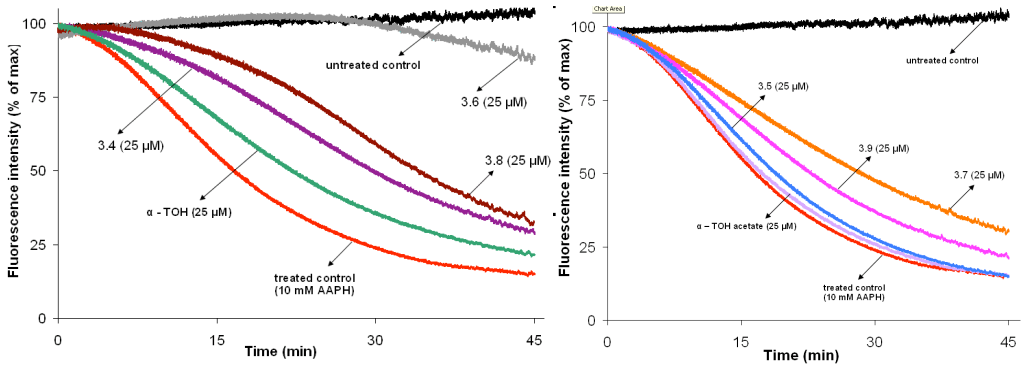

Figure 3.5. Effect of pyridinol analogues of α-TOH **3.4**, **3.6** and **3.8** (left panel), and **3.5**, **3.7** and **3.9** (right panel) on lipid peroxidation induced by peroxyl radicals generated from thermal decomposition of AAPH in phospholipids liposomes containing C_{11}-BODIPY$^{581/591}$ in Tris-HCl buffer at 40 ^{o}C. Relative fluorescence units are normalized to 100% intensity. Identical results were obtained in replicate exmperiments. Mouse liver mitochondria (2 mg of protein/mL) were suspended in 10 mM Tris-HCl, pH 7.6, containing 100 mM KCl at 37 ^{o}C. Aliquots (0.8 mL) were preincubated with the test compounds at 37 ^{o}C for 5 min in presence of 5 mM succinate and 10 μM rotenone (energized mitochondria) or 20 mM malonate (nonenergized mitochondria). Ascorbic acid (300 μM) and 100 μM ferric ammonium sulfate were then added to induce lipid peroxidation. Data are expressed as % of control samples lacking any test compound and expressed as means ± SE (n = 3). This experiment was performed by Dr. Omar Khdour.

3.2.3.2 Assessment of lipid peroxidation in cultured cells

Lipid peroxidation was determined in CEM leukemia cells by monitoring the fluorescence of the peroxidation-sensitive dye C_{11}-BODIPY$^{581/591}$. Diethyl maleate (DEM) depletes cellular glutathione (GSH), which is a physiological oxidant scavenger, reacting as either a one-electron donor to radicals or a two-electron donor to electrophiles [189]. Lowering GSH levels in CEM cells can cause a

significant increase in both cellular and mitochondrial ROS levels [190]. Increased C_{11}-BODIPY$^{581/591}$-green (oxidized) fluorescence, a measure of peroxyl radical production, was determined by a shift in green fluorescence to the right on the *x*-axis of the FACS histogram. Figure 3.6 shows representative C_{11}-BODIPY$^{581/591}$-green FACS histograms overlay and analyzed using the FL1-H channel. Glutathione depletion by DEM treatment caused the C_{11}-BODIPY$^{581/591}$-green fluorescence to shift right on the *x*-axis of the FACS histogram, indicting increased peroxidation as a result of GSH depletion. Pretreatment of the CEM cells with compound **3.6**, **3.7**, **3.8** and **3.9** blocked lipid peroxidation in a concentration manner. The acetate forms of the pyridinol analogues act as prodrugs, presumably due to susceptibility to enzymatic hydrolysis, exhibited an antioxidant effect. Analogues with ten-carbon side chain (compound **3.6** and its acetate form **3.7**) were shown to be more effective than analogues with sixteen-carbon side chain (compound **3.8** and its acetate form **3.9**).

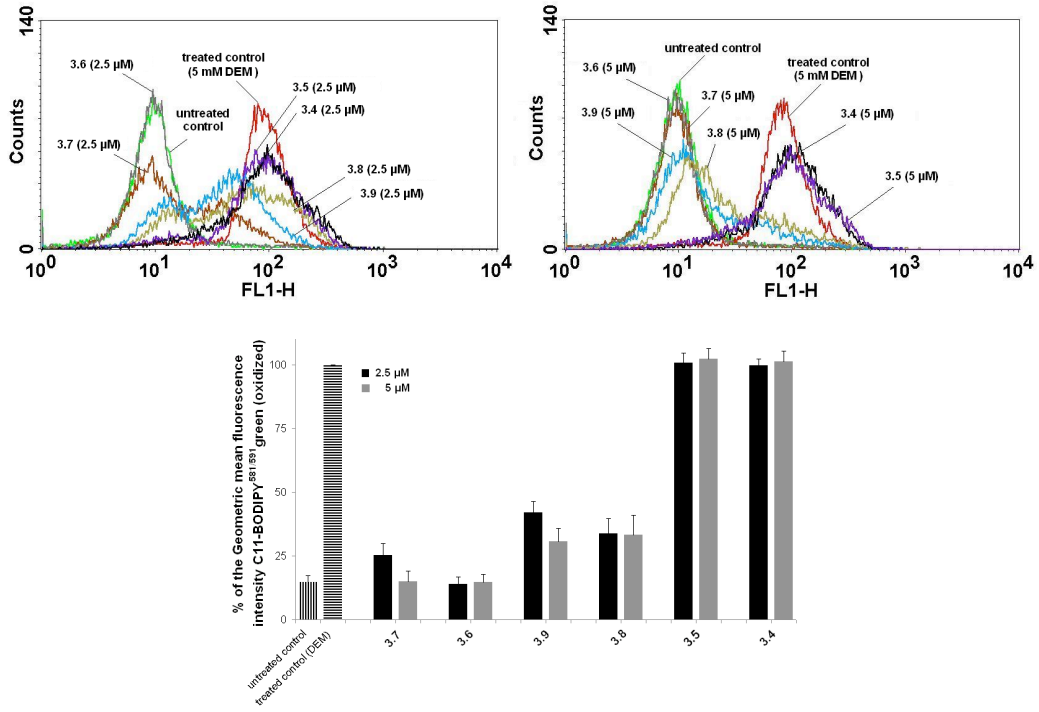

Figure 3.6. Lipid peroxidation in CEM leukemia cells depleted of glutathione. Representative flow cytometric histograms overlay showing lipid peroxidation in glutathione depleted CEM cells. Following pretreatment with the indicated compounds at 2.5 µM concentration (left panel) or 5 µM concentration (right panel) for 16 hours, the cells were treated with 5 mM diethyl maleate (DEM) for 90 minutes in phenol red free media. Then cells were treated with 500 nM C_{11}-BODIPY$^{581/591}$ in the dark at 37 °C for 30 minutes. The cells were washed twice in phosphate buffered saline, and resuspended in Hanks' Balanced Salt Solution buffer before they were subjected to flow cytometry analysis using the FL1-H channel for C_{11}-BODIPY$^{581/591}$ – green (oxidized form). The figure shows a representative example of three independent experiments. In each analysis, 10,000 events were recorded. Bottom panel shows a bar graph of mean C_{11}-BODIPY$^{581/591}$ – green (oxidized form) fluorescence (a.u.) recorded by FACS and represents the percentage of the fluorescence means of the above flow cytogram profiles calculated using CellQuest software. Data are expressed as means ± SE (n = 3). This experiment was performed by Dr. Omar Khdour.

3.2.3.3 Protection against mitochondrial membrane depolarization induced by GSH depletion

To demonstrate that reduction in mitochondrial oxidative stress can protect against mitochondrial dysfunction, we examined the effect of pyridinol analogues of α-TOH on mitochondrial membrane depolarization caused by treatment of CEM leukemia cells with DEM. Mitochondrial membrane depolarization is a critical antecedent event to cell death. Tetramethylrhodamine methyl ester (TMRM), a fluorescent cationic indicator, is taken up into mitochondria in a potential-dependent manner, and the opening of the mitochondrial permeability transition pore and depolarization leads to diminished labeling of the mitochondria by the fluoroprobe. Figure 3.7 demonstrates representative two-dimensional density dot plots of TMRM-stained cells showing the percentage of cells with intact $\Delta\psi_m$ (TMRM fluorescence in top right quadrant) vs the percentage of cells with reduced $\Delta\psi_m$ (TMRM fluorescence in bottom left and right quadrants). Figure 3.7 (bottom panel) shows a bar graph of the percentage (mean ± SE) of CEM cells with intact $\Delta\psi_m$. The results show that DEM treatment reduced the percentage of cells with TMRM fluorescence in the top right quadrant, indicating that DEM treatment caused depolarization of $\Delta\psi_m$. Preincubation of the CEM cells for 16 hr with 1 μM test compounds prior to stressing the cells with DEM resulted in nearly full protection by compounds **3.6** and **3.7**. Increasing the concentration of test compounds to 2.5 μM resulted in increasing protection.

Analogues with ten-carbon side chain were again shown to be more effective compared with anaogues with five-carbon and sixteen-carbon side chains.

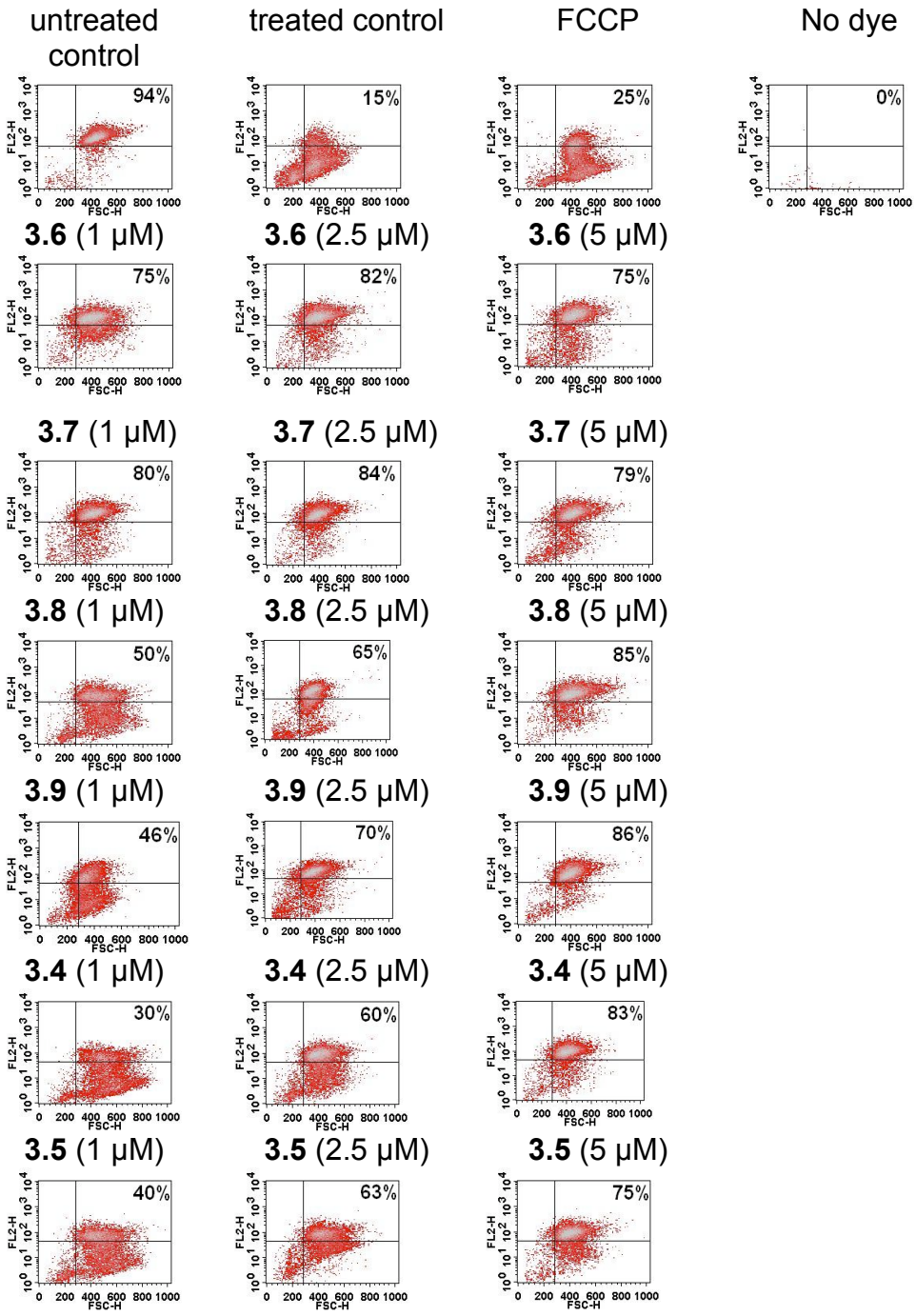

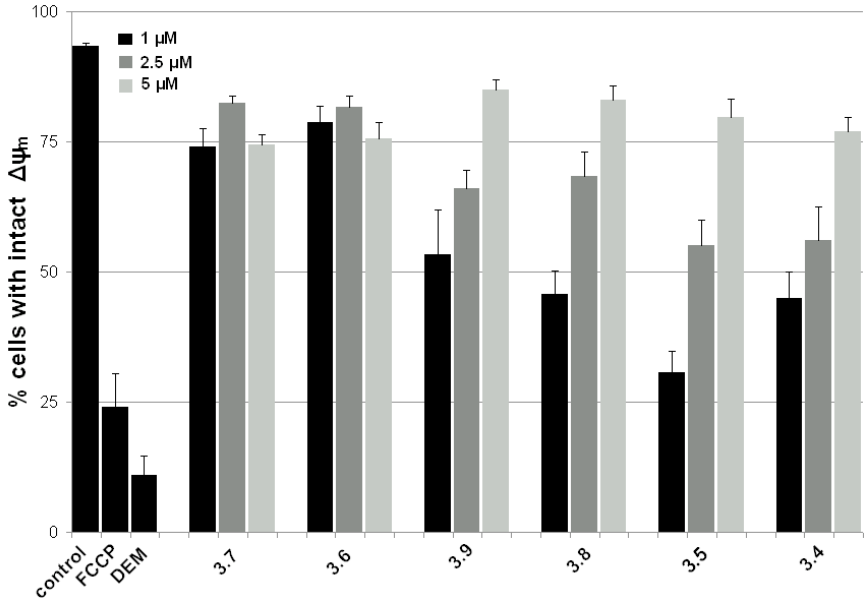

Figure 3.7. Protection against mitochondrial membrane depolarization induced by glutathione depletion. Representative flow cytometric two dimensional color dot plot analyses of mitochondrial membrane potential $\Delta\psi_m$ in CEM cells stained with 250 nM TMRM and analyzed using the FL2-H channel. Following pretreatment with the indicated compounds (1, 2.5 or 5 μM concentrations) for 16 hours, the cells were treated with 5 mM DEM for 120 min. The cells were washed twice in phosphate buffered saline, and suspended in Hanks' Balanced Salt Solution buffer. Cells were loaded with 250 nM TMRM for 15 min, and the red fluorescence was measured by flow cytometry using the FL2-H channel. The percentage of cells with intact $\Delta\psi_m$ is indicated in the top right quadrant of captions. Representative example from at least three independent experiments. In each analysis, 10,000 events were recorded. Bottom panel shows a bar graph of means the percentage of cells with intact $\Delta\psi_m$ recorded by FACS. Data are expressed as means ± SE (n = 3). This experiment was performed by Dr. Omar Khdour.

3.2.4 Proposed catalytic mode of action of α-TOH analogues

In the experiments described in Figue 3.6 and 3.7, diethyl maleate was used to deplete celluar glutathione, a physiological oxidant scavenger typically present at ~1–10 mM concentration in cells [191]. Both experiments demonstrated that much lower concentrations of **3.6** (at low micromolar levels) were capable to replace cellular glutathione to inhibit lipid peroxidation and maintain mitochondrial membrane potential. Presumably, **3.6** may function catalytically to suppress ROS and protect lipid membranes. Figure 3.8 depicts a proposed mechanism of action of **3.6**. This cycle illustrates the simultaneous quenching of lipid radicals and superoxide, in a fashion that should be catalytic [192]. Compound **3.6** can donate a phenolic H to quench lipid peroxidation, leading to the formation of an antioxidant-derived radical. By virtue of the prooxidant character, this generated species should be capable of reacting with superoxide; in this way antioxidant **3.6** could be recycled.

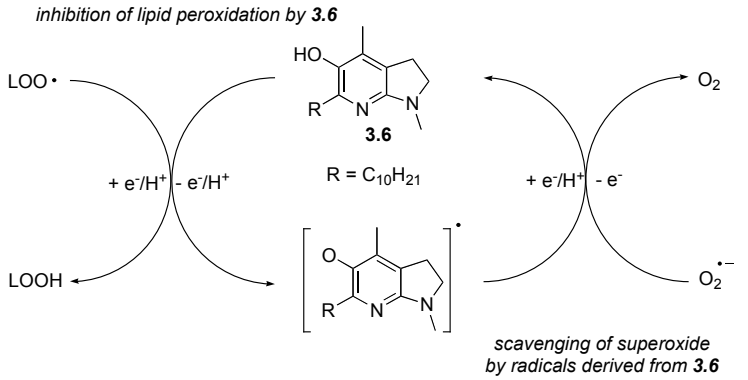

Figure 3.8. Proposed catalytic mode of action of **3.6** as a quencher of lipid peroxyl radicals and superoxide.

3.3 Experimental

General methods: Chemicals and solvents were of reagent grade and were used without further purification. Anhydrous tetrahydrofuran (THF) was distilled from sodium/benzophenone under argon. Dichloromethane (CH_2Cl_2) was distilled from calcium hydride under argon. All reactions involving air or moisture sensitive reagents or intermediates were performed under an argon atmosphere. Flash chromatography was carried out using Silicycle 200-400 mesh silica gel. Analytical TLC was carried out using 0.25 mm EM silica gel 60 F_{250} plates that were visualized by UV irradiation (254 nm) or by staining with *p*-anisaldehyde stain. ^1H and ^{13}C NMR spectra were obtained using 400 or 500 MHz Varian NMR instruments. Chemical shifts were reported in parts per million (ppm, δ) referenced to the residual ^1H resonance of the solvent ($CDCl_3$, 7.26 ppm). ^{13}C spectra were referenced to the residual ^{13}C resonance of the solvent ($CDCl_3$, 77.0 ppm). Splitting patterns were designated as follows: s, singlet; br, broad; d, doublet; dd, doublet of doublets; t, triplet; q, quartet; m, multiplet. High resolution mass spectra were obtained at the Ohio State University Mass Spectrometry Facility or at the ASU CLAS High Resolution Mass Spectrometry Laboratory.

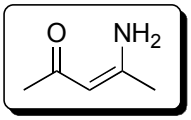

4-Amino-3-penten-1-one (3.10) [193]. To 102.7 mL (1.00 mol) of 2,4-pentanedione was added 1.00 g of silica gel and 81.1 mL (1.20 mg) of 14.8 M aq NH_4OH solutions (14.8 M) at room temperature. After the reaction mixture was stirred at room temperature for 16 h, the silica gel was filtered. The crude products were obtained after extraction with CH_2Cl_2 and the solvent was concentrated under diminished pressure. The crude product was obtained as a yellow solid and used directly for the next step: yield 95.2 g (96%); silica gel TLC R_f 0.15 (7:3 hexanes–ethyl acetate); ^{1}H NMR ($CDCl_3$) δ 1.87 (s, 3H), 1.99 (s, 3H), 4.99 (s, 1H), 5.18 (br s, 1H) and 9.66 (br s, 1H); ^{13}C NMR ($CDCl_3$) δ 22.2, 29.2, 95.7, 161.1 and 196.6; mass spectrum (APCI), *m/z* 100.0766 $(M + H)^+$ ($C_5H_{10}NO$ requires 100.0762).

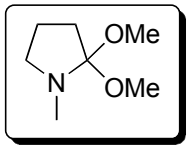

***N*-Methyl-2,2-dimethoxypyrrolidine (3.11) [194].** A solution of 52 mL (0.54 mol) of *N*-methylpyrrolidone and 52 mL (0.55 mol) of dimethyl sulfate was heated at 90 ^{o}C for 1 h. The resulting mixture was added dropwise over 1 h to 500 mL of 1.5 M NaOMe solution at –78 °C. The reaction solution was stirred at room temperature for another 2 h, and then 200 mL of ethyl ether was added. The resulting mixture was filtered and the solvent was concentrated under diminished pressure. The product was collected by fractional distillation (15 mmHg, 58–60

°C) as a light yellow oil: yield 23.4g (30%); ^{1}H NMR ($CDCl_3$) δ 1.71-1.76 (m, 2H), 1.88 (t, 2H, J = 7.2 Hz), 2.32 (s, 3H), 2.83 (t, 2H, J = 6.0 Hz) and 3.20 (s, 6H); mass spectrum (MALDI-TOF), *m/z* 146.1 $(M+H)^+$ (theoretical 146.1).

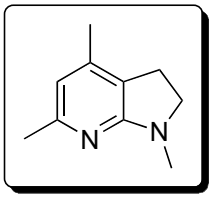

1,4,6-Trimethyl-2,3-dihydro-1*H*-pyrrolo[2,3-*b*]pyridine (3.12) [183]. To a solution of 2.36 g (23.8 mmol) of enaminone **3.10** in 8 mL of toluene was added 5.88 g (40.5 mmol) of lactam acetal **3.11**. The reaction mixture was heated at reflux and stirred for 2 h, cooled to 90 °C, and then treated with 4.65 g (48.4 mmol) of *t*-BuONa and 4 mL of *t*-BuOH. The reaction mixture was stirred at 90 °C for another 16 h. The cooled reaction mixture was quenched by the addition of 20 mL of sat aq NH_4Cl. The mixture was extracted with EtOAc. The combined organic layer was washed with brine, dried ($MgSO_4$) and concentrated under diminished pressure. The residue was purified by flash chromatography on a silica gel column (25.4 × 2.6 cm). Elution with 10:1 hexanes/ethyl acetate gave the product **3.12** as a yellow oil: yield 1.6 g (42%); silica gel TLC R_f 0.15 (4:1 hexanes/ethyl acetate); ^{1}H NMR ($CDCl_3$) δ 2.05 (s, 3H), 2.32 (s, 3H), 2.76 (t, 2H, J = 8.4 Hz), 2.86 (s, 3H), 3.34 (t, 2H, J = 8.4 Hz) and 6.10 (s, 1H); ^{13}C NMR ($CDCl_3$) δ 17.8, 24.0, 24.3,

33.1, 52.4, 113.1, 118.1, 141.2, 154.5 and 163.7; mass spectrum (MALDI-TOF), *m/z* 162.1 (M^+) (theoretical 162.1).

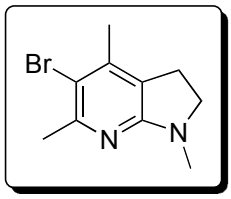

5-Bromo-1,4,6-trimethyl-2,3-dihydro-1*H*-pyrrolo[2,3-*b*]-pyridine (3.13) [139(b)]. To a solution of 490 mg (3.02 mmol) of **3.12** in 5 mL of chloroform was added 432 mg (1.51 mmol) of 1,3-dibromo-5,5-dimethylhydantoin in portions at 0 ^oC. The reaction mixture was stirred at 0 ^oC for 30 min at which point silica gel TLC analysis indicated that all starting material had been consumed. The reaction was quenched by the addition of 5 mL of sat aq $NaHCO_3$. The mixture was extracted with portions of chloroform and the combined organic layer was washed with brine and dried over $MgSO_4$. The concentrated residue was purified by flash chromatography on a silica gel column (20 × 1.7 cm). Elution with 100:1 hexanes–ethyl acetate gave **3.13** as a yellow solid: yield 598 mg (82%); silica gel TLC R_f 0.65 (4:1 hexanes–ethyl acetate); ^1H NMR ($CDCl_3$) δ 2.19 (s, 3H), 2.51 (s, 3H), 2.88 (t, 2H, J = 8.4 Hz), 2.89 (s, 3H) and 3.44 (t, 2H, J = 8.8 Hz); ^{13}C NMR ($CDCl_3$) δ 19.4, 25.2, 25.5, 33.0, 52.5, 111.2, 120.5, 141.2, 152.8 and 161.6; mass spectrum, *m/z* 240.1 and 242.0 (M^+) (theoretical 240.0 and 242.0).

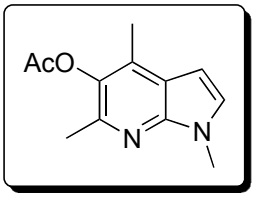

1,4,6-Trimethyl-1*H*-pyrrolo[2,3-*b*]pyridin-5-yl Acetate (3.15). A reaction mixture containing 73 mg (0.30 mmol) of **3.13**, 11 mg (12 μmol) of Pd_2dba_3, 10 mg (24 μmol) of ligand **3.14** and 68 mg (1.2 mmol) of potassium hydroxide in 0.5 mL of dioxane and 0.5 mL of degassed water was heated to 100 ^oC overnight under an argon atmosphere. After the starting material was consumed, 60 μL (0.54 mmol) of acetic anhydride was added to the reaction mixture. The resulting mixture was stirred for another 40 min, then permitted to cool to room temperature. Two mL of sat aq NH_4Cl was added, and the mixture was extracted with EtOAc. The organic layer was washed successively with sat aq $NaHCO_3$ and brine, then dried ($MgSO_4$) and concentrated under diminished pressure. The residue was purified by flash chromatography on a silica gel column (20 × 1.7 cm). Elution with 10:1 hexanes–ethyl acetate gave **3.15** as colorless solid: yield 29.6 mg (45%); silica gel TLC R_f 0.59 (1:1 EtOAc–hexanes); ^1H NMR ($CDCl_3$) δ 2.34 (s, 3H), 2.38 (s, 3H), 2.47 (s, 3H), 3.84 (s, 3H), 6.39 (d, 1H, J = 3.6 Hz) and 7.08 (d, 1H, J = 3.6 Hz); ^{13}C NMR ($CDCl_3$) δ 12.8, 20.0, 20.7, 31.5, 98.0, 119.7, 128.5, 131.2, 139.1, 144.6, 144.9 and 169.5; mass spectrum (ESI), *m/z* 219.1136 $(M + H)^+$ ($C_{12}H_{15}N_2O_2$ requires 219.1128).

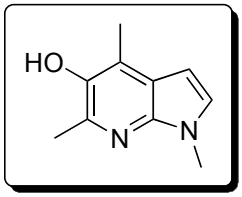

1,4,6-Trimethyl-1*H*-pyrrolo[2,3-*b*]pyridin-5-ol (3.16). To a solution of 6.0 mg (28 μmol) of **3.15** in 0.5 mL of methanol was added 10 mg (94 μmol) of K_2CO_3. The reaction mixture was stirred at room temperature for 1 h then concentrated under diminished pressure. The residue was diluted with 2 mL of water and adjusted to pH ~ 6 by the addition of aqueous acetic acid (10% in water). The mixture was extracted with ethyl ether. The organic layer was washed with brine, dried (Na_2SO_4) and concentrated under diminished pressure to give **3.16** as a pink solid: yield 4.7 mg (97%); silica gel TLC R_f 0.45 (1:1 hexanes–ethyl acetate); ^{1}H NMR ($CDCl_3$) δ 2.42 (s, 3H), 2.57 (s, 3H), 3.81 (s, 3H), 5.16 (br s, 1H), 6.31 (d, 1H, J = 3.6 Hz) and 7.02 (d, 1H, J = 3.6 Hz); ^{13}C NMR ($CDCl_3$) δ 12.3, 19.9, 31.6, 97.2, 120.1, 124.5, 128.0, 140.8, 142.4 and 143.; mass spectrum, *m*/*z* 176.1 (M^+) (theoretical 176.1); mass spectrum (ESI), *m/z* 177.1026 $(M + H)^+$ ($C_{10}H_{13}N_2O$ requires 177.1022).

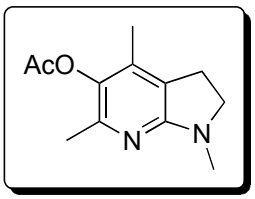

1,4,6-Trimethyl-2,3-dihydro-1*H*-pyrrolo[2,3-*b*]pyridin-5-yl Acetate (3.17). To a solution of 28 mg (0.13 mmol) of **3.15** in 1 mL of acetic acid was added 41 mg (0.65 mmol) of $NaCNBH_3$. The reaction mixture was stirred at room temperature for 24 h then poured into 10 mL of sat aq Na_2CO_3. The mixture was extracted with ethyl acetate. The organic layer was washed with brine, dried ($MgSO_4$) and concentrated under diminished pressure. The residue was purified by flash chromatography on a silica gel column (20 × 1.7 cm). Elution with 10:1 hexanes–ethyl acetate gave **3.17** as a yellowish solid: yield 26.0 mg, (92%); silica gel TLC R_f 0.52 (1:1 hexanes–ethyl acetate); ^{1}H NMR ($CDCl_3$) δ 1.88 (s, 3H), 2.13 (s, 3H), 2.23 (s, 3H), 2.73-2.81 (m, 2H), 2.81 (s, 3H) and 3.36 (t, 2H, J = 8.7 Hz); ^{13}C NMR ($CDCl_3$) δ 12.9, 19.0, 20.6, 24.7, 33.3 52.9, 120.3, 134.8, 136.8, 145.5, 160.9 and 169.5; mass spectrum (ESI), *m/z* 221.1286 $(M + H)^+$ ($C_{12}H_{17}N_2O_2$ requires 221.1290).

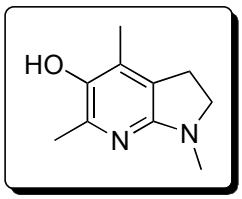

1,4,6-Trimethyl-2,3-dihydro-1*H*-pyrrolo[2,3-*b*]pyridin-5-ol (3.1) [139(b)]. To a solution of 17.0 mg (770 μmol) of **3.17** in 0.5 mL of THF was added 154 μL (1M in THF, 154 μmol) of $LiAlH_4$ at –78 °C. The reaction mixture was stirred at –78 °C for 1.5 h, then the reaction was quenched cautiously with 3 mL of sat aq

NH_4Cl. The resulting mixture was allowed to warm to room temperature slowly and then extracted with ether. The organic layer was washed with brine, dried (Na_2SO_4) and concentrated under diminished pressure to afford **3.1** as an orange solid: yield 11 mg (86%); silica gel TLC R_f 0.37 (1:1 hexanes–ethyl acetate); ^1H NMR ($CDCl_3$) δ 2.09 (br s, 3H), 2.34 (br s, 3H), 2.82 (br s, 2H), 2.85 (br s, 3H) and 3.36 (br s, 2H); mass spectrum, *m/z* 178.1 (M^+) (theoretical 178.1).

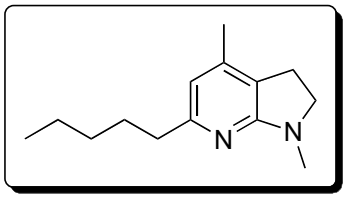

1,4-Dimethyl-6-pentyl-2,3-dihydro-1*H*-pyrrolo[2,3-*b*]pyridine (3.22). To a solution of 225.0 mg (1.39 mmol) of **3.12** in 4 mL of THF was added 1.39 mL (2.22 mmol, 1.6 M in hexanes) of *n*-BuLi followed by 157.0 μL (1.46 mmol) of 1-bromobutane at –78 °C. The reaction mixture was slowly warmed to room temperature and stirred for another 16 h. The reaction mixture was quenched by the addition of 10 mL of sat aq NH_4Cl at 0 °C. The mixture was extracted with EtOAc. The combined organic layer was washed with brine, dried ($MgSO_4$) and concentrated under diminished pressure. The residue was purified by flash chromatography on a silica gel column (25 × 3.2 cm). Elution with 10:1 hexanes–

ethyl acetate gave the product **3.22** as a yellow oil: yield 0.20 g (66%); silica gel TLC R_f 0.15 (8:1:1 hexanes–ethyl acetate–MeOH); ^{1}H NMR ($CDCl_3$) δ 0.88 (t, 3H, J = 7.2 Hz), 1.30-1.36 (m, 4H), 1.66 (quint, 2H, J = 7.6 Hz), 2.08 (s, 3H), 2.55 (t, 2H, J = 8.0 Hz), 2.81 (t, 2H, J = 8.0 Hz), 2.88 (s, 3H), 3.38 (t, 2H, J = 8.0 Hz) and 6.13 (s, 1H); ^{13}C NMR ($CDCl_3$) δ 14.1, 18.0, 22.6, 24.4, 29.6, 31.8, 33.3, 38.0, 52.5, 112.4, 118.2, 141.1, 159.1 and 163.7; mass spectrum (MALDI-TOF), *m/z* 218.2 (M^+) (theoretical 218.3); mass spectrum (APCI), *m/z* 219.1864 (M + H)$^+$ ($C_{14}H_{23}N_2$ requires 219.1861).

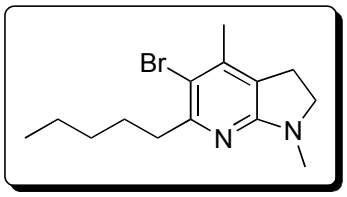

5-Bromo-1,4-dimethyl-6-pentyl-2,3-dihydro-1*H*-pyrrolo[2,3-*b*]-pyridine (3.23). To a solution of 108.2 mg (0.50 mmol) of **3.22** in 3 mL of chloroform was added 70.7 mg (0.25 mmol) of 1,3-dibromo-5,5-dimethylhydantoin in portions at 0 °C. The reaction mixture was stirred at 0 °C for 30 min. The reaction was quenched by the addition of 5 mL of sat aq $NaHCO_3$. The mixture was extracted with chloroform and the combined organic layer was washed with brine and dried over $MgSO_4$. The concentrated residue was purified by flash chromatography on a silica gel column (20 × 1.7 cm). Elution with 100:1 hexanes–ethyl acetate gave **3.23** as a yellow oil: yield 135.5 mg (92%); silica gel TLC R_f 0.65 (8:1:1 hexanes–

ethyl acetate–methanol); ^{1}H NMR ($CDCl_3$) δ 0.89 (t, 3H, J = 7.2 Hz), 1.33-1.38 (m, 4H), 1.66 (quint, 2H, J = 7.6 Hz), 2.16 (s, 3H), 2.77 (t, 2H, J = 8.0 Hz), 2.82-2.87 (m, 5H) and 3.40 (t, 2H, J = 8.0 Hz); ^{13}C NMR ($CDCl_3$) δ 14.1, 19.5, 22.6, 25.2, 28.4, 31.8, 33.0, 38.1, 52.4, 110.9, 120.4, 141.1, 156.8 and 161.8; mass spectrum (MALDI-TOF), *m/z* 297.1 and 299.1 $(M + H)^+$ (theoretical 297.1 and 299.1); mass spectrum (APCI), *m/z* 297.0968 and 199.0937 $(M + H)^+$ ($C_{14}H_{22}N_2Br$ requires 297.0966 and 299.0946).

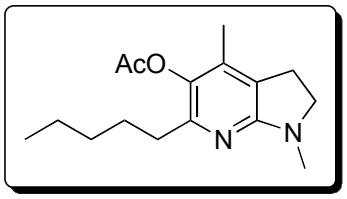

1,4-Dimethyl-6-pentyl-1*H*-pyrrolo[2,3-*b*]pyridin-5-yl Acetate (3.5). To a solution of 33.0 mg (0.11 mmol) of **3.23** in 1 mL of THF was added 16.5 μL (0.11 mmol) of tetramethylethylenediamine (TMEDA) at –78 °C followed by 139.0 μL (0.22 mmol, 1.6 M in hexanes) of *n*-BuLi. After 30 min, 27.2 μL (0.24 mmol) of trimethoxy boron was added and the resulting mixture was stirred for another 1 hr. To the reaction mixture was slowly added 51.4 μL (0.24 mmol, 32 wt%) of peracetic acid and the solution was then warmed to 0 °C over 30 min. The mixture was diluted by 5 mL of H_2O and extracted with three 5-mL portions of EtOAc. The combined organic layer was washed with brine, dried ($MgSO_4$) and the solvent was concentrated under diminished pressure. The resulting oil was

dissolved in 2 mL of CH_2Cl_2 at 0 °C, followed by the addition of 92.8 μL (0.66 mmol) of triethylamine, 1.4 mg (0.01 mmol) of DMAP and 31.4 μL (0.33 mmol) of acetic anhydride. The reaction was stirred at room temperature for 1 hr and quenched by the addition of 2 mL of sat aq NH_4Cl. The solution was then extracted with three 5-mL portions of EtOAc. The combined organic layer was washed with brine, dried ($MgSO_4$) and the solvent was concentrated under diminished pressure. The residue was purified by flash chromatography on a silica gel column (20 × 1.7 cm). Elution with 100:1 hexanes–ethyl acetate gave **3.5** as a yellow oil: yield 26.7 mg (88%); silica gel TLC R_f 0.1 (3:7 EtOAt–hexanes); ^{1}H NMR ($CDCl_3$) δ 0.90 (t, 3H, J = 7.0 Hz), 1.32-1.37 (m, 4H), 1.64 (quint, 2H, J = 7.5 Hz), 1.95 (s, 3H), 2.31 (s, 3H), 2.47 (t, 2H, J = 8.0 Hz), 2.85 (t, 2H, J = 8.0 Hz), 2.89 (s, 3H) and 3.44 (t, 2H, J = 8.0 Hz); ^{13}C NMR ($CDCl_3$) δ 14.0, 20.6, 22.5, 24.7, 28.4, 29.6, 31.8, 32.5, 33.3, 52.4, 120.1, 134.7, 136.5, 149.7, 161.2 and 169.9; mass spectrum (MALDI-TOF), *m/z* 276.2 (M^+) (theoretical 276.2); mass spectrum (APCI), *m/z* 277.1910 $(M + H)^+$ ($C_{16}H_{25}N_2O_2$ requires 277.1916).

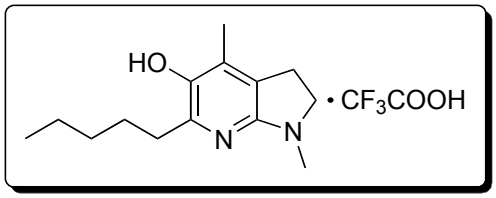

1,4-Dimethyl-6-pentyl-1*H*-pyrrolo[2,3-*b*]pyridin-5-ol and its trifluoroacetic acid salt (3.4). To a solution of 20.0 mg (72.4 μmol) of **3.5** in 1 mL of CH_2Cl_2

was added 217.1 μL (84.0 μmol, 1.0 M in hexanes) of DIBAL-H at –78 °C. The reaction mixture was stirred at the same temperature for 1 h before 2 mL of sat aq sodium potassium tartrate was added slowly. The reaction mixture was slowly warmed to room temperature over 30 min. The solution was extracted with three 5-mL portions of ethyl acetate. The combined organic layer was washed with brine, dried ($MgSO_4$) and concentrated under diminished pressure to give the crude product as a yellow oil: silica gel TLC R_f 0.12 (1:9 MeOH–CH_2Cl_2). The residue was then dissolved in 1 mL of CH_3CN and 1% aq TFA, frozen and lyophilized. The crude product was purified by Prepex C_8 reversed phase semi-preparative (250 mm x 10 mm) HPLC column using a gradient of methanol and water. Linear gradients were employed using 1:4 methanol/water → 4:1 methanol/water over a period of 20 min, and then 4:1 methanol/water → methanol over a period of 40 min, at a flow rate of 3.5 mL/min (monitoring at 260 nm); Fractions containing the desired product eluted at 21.6 min, and were collected, frozen, and lyophilized to give **3.4** as a light yellow solid: yield 13.5 mg (80%); ^{1}H NMR (CD_3CN) δ 0.88 (t, 3H, J = 6.8 Hz), 1.27-1.32 (m, 4H), 1.54 (quint, 2H, J = 7.6 Hz), 2.13 (s, 3H), 2.69 (t, 2H, J = 8.0 Hz), 2.99 (t, 2H, J = 8.4 Hz), 3.06 (s, 3H) and 3.72 (t, 2H, J = 8.4 Hz); ^{13}C NMR ($CDCl_3$) δ 13.0, 13.3, 22.1, 24.4, 27.2, 28.3, 31.1, 32.4, 53.1, 117.3, 126.1, 132.1, 140.4, 141.6 and 152.0; mass spectrum (MALDI-TOF), *m/z* 234.2 (M^+) (theoretical 234.2); mass spectrum (APCI), *m/z* 235.1806 $(M + H)^+$ ($C_{14}H_{23}N_2O$ requires 235.1810).

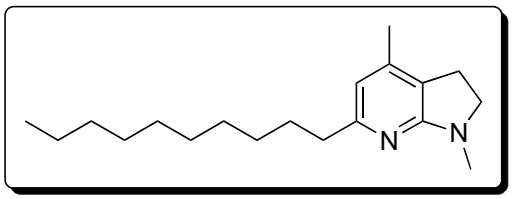

1,4-Dimethyl-6-decyl-2,3-dihydro-1*H*-pyrrolo[2,3-*b*]pyridine (3.24). To a solution of 181 mg (1.12 mmol) of **3.12** in 3 mL of THF was added 1.19 mL (1.90 mmol, 1.6 M in hexanes) of *n*-BuLi followed by 255 μL (1.34 mmol) of 1-bromononane at –78 °C. The reaction mixture was slowly warmed to room temperature and stirred for another 16 h. The reaction mixture was quenched by the addition of 10 mL of sat aq NH_4Cl at 0 °C. The mixture was extracted with EtOAc. The combined organic layer was washed with brine, dried ($MgSO_4$) and concentrated under diminished pressure. The residue was purified by flash chromatography on a silica gel column (25.4 × 3.2 cm). Elution with 10:1 hexanes–ethyl acetate gave the product **3.24** as a yellow oil: yield 210 mg (66%); silica gel TLC R_f 0.18 (8:1:1 hexanes–ethyl acetate–MeOH); ^{1}H NMR ($CDCl_3$) δ 0.86 (t, 3H, J = 6.8 Hz), 1.24-1.30 (m, 16H), 1.65 (quint, 2H, J = 7.6 Hz), 2.08 (s, 3H), 2.54 (t, 2H, J = 8.0 Hz), 2.81 (t, 2H, J = 8.0 Hz), 2.90 (s, 3H), 3.38 (t, 2H, J = 8.0 Hz) and 6.13 (s, 1H); ^{13}C NMR ($CDCl_3$) δ 14.24, 18.11, 22.82, 24.52, 29.48, 29.68, 29.73, 29.75, 29.77, 30.10, 32.05, 33.40, 38.19, 52.60, 112.60, 118.38, 141.25, 159.26 and 163.86; mass spectrum, *m/z* 288.3 (M^+) (theoretical 288.3); mass spectrum (APCI), *m/z* 289.2653 $(M + H)^+$ ($C_{19}H_{33}N_2$ requires 289.2644).

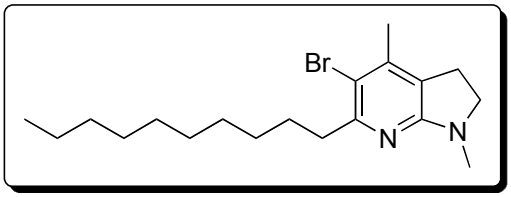

5-Bromo-1,4-dimethyl-6-decyl-2,3-dihydro-1*H*-pyrrolo[2,3-*b*]-pyridine (3.25). To a solution of 286 mg (0.99 mmol) of **3.24** in 4 mL of chloroform was added 143 mg (0.50 mmol) of 1,3-dibromo-5,5-dimethylhydantoin in portions at 0 ^{o}C. The reaction mixture was stirred at 0 ^{o}C for 30 min. The reaction was quenched by the addition of 5 mL of sat aq $NaHCO_3$. The mixture was extracted with chloroform and the combined organic layer was washed with brine and dried over $MgSO_4$. The concentrated residue was purified by flash chromatography on a silica gel column (20 × 1.7 cm). Elution with 100:1 hexanes–ethyl acetate gave **3.25** as a yellow oil: yield 342 mg (94%); silica gel TLC R_f 0.7 (8:1:1 hexanes–ethyl acetate–methanol); ^{1}H NMR ($CDCl_3$) δ 0.87 (t, 3H, J = 6.8 Hz), 1.25-1.39 (m, 16H), 1.66 (quint, 2H, J = 7.2 Hz), 2.17 (s, 3H), 2.77 (t, 2H, J = 8.0 Hz), 2.83-2.87 (m, 5H) and 3.40 (t, 2H, J = 8.0 Hz); ^{13}C NMR ($CDCl_3$) δ 14.11, 19.50, 22.68, 25.22, 28.69, 29.36, 29.54, 29.59, 29.64, 29.64, 31.92, 33.00, 38.13, 52.44, 110.92, 120.37, 141.10, 156.79 and 161.78; mass spectrum, *m/z* 366.2 and 268.2 $(M)^+$ (theoretical 366.2 and 368.2); mass spectrum (APCI), *m/z* 367.1747 and 369.1723 $(M + H)^+$ ($C_{19}H_{32}N_2Br$ requires 367.1749 and 369.1728).

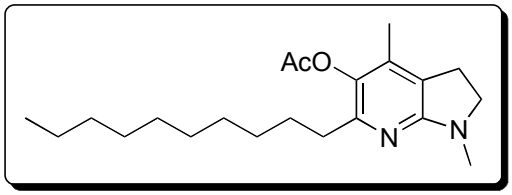

1,4-Dimethyl-6-decyl-1*H*-pyrrolo[2,3-*b*]pyridin-5-yl Acetate (3.7). To a solution of 43.0 mg (0.12 mmol) of **3.25** in 1 mL of THF was added 17.4 μL (0.12 mmol) of tetramethylethylenediamine (TMEDA) at –78 °C followed by 146.3 μL (0.23 mmol, 1.6 M in hexanes) of *n*-BuLi. After 30 min, 28.7 μL (0.26 mmol) of trimethoxy boron was added and the resulting mixture was stirred for another 1 hr. To the reaction mixture was slowly added 54.2 μL (0.26 mmol, 32 wt%) of peracetic acid and the solution was then warmed to 0 °C over 30 min. The mixture was diluted by 5 mL of H_2O and extracted with three 5-mL of EtOAc. The combined organic layer was washed with brine, dried ($MgSO_4$) and the solvent was concentrated under diminished pressure. The resulting oil was dissolved in 2 mL of CH_2Cl_2 at 0 °C, followed by the addition of 97.9 μL (0.70 mmol) of triethylamine, 1.4 mg (0.01 mmol) of DMAP and 33.1 μL (0.35 mmol) of acetic anhydride. The reaction was stirred at room temperature for 1 hr and quenched by the addition of 2 mL of sat aq NH_4Cl. The solution was then extracted with three 5-mL of EtOAc. The combined organic layer was washed with brine, dried ($MgSO_4$) and the solvent was concentrated under diminished pressure. The residue was purified by flash chromatography on a silica gel column (20 × 1.7 cm). Elution with 100:1 hexanes–ethyl acetate gave **3.7** as a yellow oil: yield 28 mg

(68%); silica gel TLC R_f 0.15 (3:7 EtOAt–hexanes); ^{1}H NMR ($CDCl_3$) δ 0.86 (t, 3H, J = 6.8 Hz), 1.24-1.28 (m, 16 H), 1.60 (quint, 2H, J = 7.6 Hz), 1.92 (s, 3H), 2.28 (s, 3H), 2.44 (t, 2H, J = 8.0 Hz), 2.82 (t, 2H, J = 8.4 Hz), 2.87 (s, 3H) and 3.41 (t, 2H, J = 8.4 Hz); ^{13}C NMR ($CDCl_3$) δ 12.88, 14.10, 20.54, 22.66, 24.62, 28.68, 29.33, 29.50, 29.58, 28.63, 31.89, 32.49, 33.31, 52.82, 120.08, 134.68, 136.50, 149.65, 161.17 and 169.91; mass spectrum, *m/z* 346.3 $(M)^+$ (theoretical 246.3); mass spectrum (APCI), *m/z* 347.2696 $(M + H)^+$ ($C_{21}H_{35}N_2O_2$ requires 347.2699).

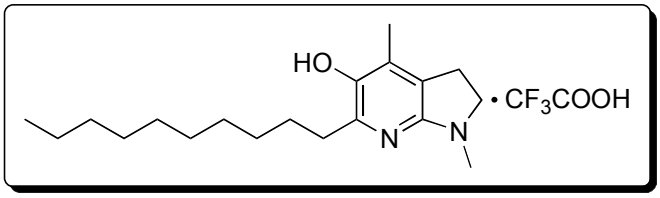

1,4-Dimethyl-6-decyl-1*H*-pyrrolo[2,3-*b*]pyridin-5-ol and its trifluoroacetic acid salt (3.6). To a solution of 19.0 mg (54.8 μmol) of **3.7** in 1 mL of CH_2Cl_2 was added 165 μL (165 μmol, 1.0 M in hexanes) of DIBAL-H at –78 °C. The reaction mixture was stirred at the same temperature for 1 h before 2 mL of sat aq sodium potassium tartrate was added slowly. The reaction mixture was slowly warmed to room temperature over 30 min. The solution was extracted with three 5-mL ethyl acetate. The combined organic layer was washed with brine, dried ($MgSO_4$) and concentrated under diminished pressure to give the crude product as a yellow oil: silica gel TLC R_f 0.16 (1:9 MeOH–CH_2Cl_2). The residue was then

dissolved in 1 mL of CH_3CN and 1% aq TFA, frozen and lyophilized. The crude product was purified by Prepex C_8 reversed phase semi-preparative (250 mm x 10 mm) HPLC column using a gradient of methanol and water. Linear gradients were employed using 1:4 methanol/water → 4:1 methanol/water over a period of 20 min, and then 4:1 methanol/water → methanol over a period of 40 min, at a flow rate of 3.5 mL/min (monitoring at 260 nm); Fractions containing the desired product eluted at 28.2 min, and were collected, frozen, and lyophilized to give **3.6** as a light yellow solid: yield 13.0 mg (76%); ^{1}H NMR (CD_3CN) δ 0.89 (t, 3H, J = 6.8 Hz), 1.27-1.31 (m, 16H), 1.54 (quint, 2H, J = 7.6 Hz), 2.13 (s, 3H), 2.70 (t, 2H, J = 8.0 Hz), 2.99 (t, 2H, J = 8.4 Hz), 3.06 (s, 3H) and 3.72 (t, 2H, J = 8.4 Hz); ^{13}C NMR ($CDCl_3$) δ 13.0, 13.4, 22.4, 24.4, 27.3, 28.6, 28.9, 29.00, 29.04, 29.3, 29.3, 31.6, 32.4, 53.1, 117.3, 126.1, 132.1, 140.4, 141.5 and 152.1; mass spectrum, *m/z* 304.3 $(M)^+$ (theoretical 304.3); mass spectrum (APCI), *m/z* 305.2590 $(M + H)^+$ ($C_{19}H_{33}N_2O$ requires 305.2593).

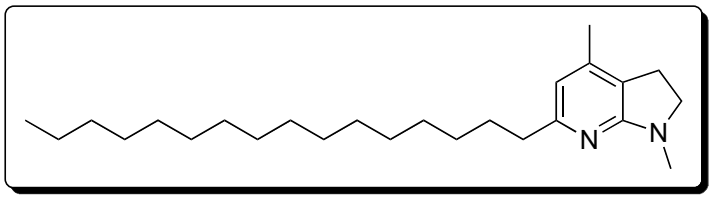

1,4-Dimethyl-6-hexadecyl-2,3-dihydro-1*H*-pyrrolo[2,3-*b*]pyridine (3.26). To a solution of 277 mg (1.71 mmol) of **3.12** in 5 mL of THF was added 1.71 mL (2.73 mmol, 1.6 M in hexanes) of *n*-BuLi followed by 518 μL (1.79 mmol) of 1-

bromononane at –78 °C. The reaction mixture was slowly warmed to room temperature and stirred for another 16 h. The reaction mixture was quenched by the addition of 10 mL of sat aq NH_4Cl at 0 °C. The mixture was extracted with EtOAc. The combined organic layer was washed with brine, dried ($MgSO_4$) and concentrated under diminished pressure. The residue was purified by flash chromatography on a silica gel column (25.4 × 3.2 cm). Elution with 10:1 hexanes–ethyl acetate gave the product **3.26** as a white solid: yield 330 mg (52%); mp 43–45 °C; silica gel TLC R_f 0.25 (8:1:1 hexanes–ethyl acetate–MeOH); ^{1}H NMR ($CDCl_3$) δ 0.88 (t, 3H, J = 7.2 Hz), 1.25-1.31 (m, 28H), 1.66 (quint, 2H, J = 7.6 Hz), 2.08 (s, 3H), 2.55 (t, 2H, J = 8.0 Hz), 2.80 (t, 2H, J = 8.4 Hz), 2.90 (s, 3H), 3.38 (t, 2H, J = 8.4 Hz) and 6.13 (s, 1H); ^{13}C NMR ($CDCl_3$) δ 14.1, 18.0, 22.7, 24.4, 29.38, 29.38, 29.57, 29.62, 29.65, 29.68, 29.72, 29.72, 29.72, 29.72, 29.72, 29.72, 28.0, 32.0, 33.2, 38.1, 52.4, 112.4, 118.2, 141.0, 159.1 and 163.7; mass spectrum, *m/z* 372.3 (M^+) (theoretical 372.4); mass spectrum (APCI), *m/z* 373.3574 $(M + H)^+$ ($C_{25}H_{45}N_2$ requires 373.3583).

5-Bromo-1,4-dimethyl-6-hexadecyl-2,3-dihydro-1*H*-pyrrolo[2,3-*b*]-pyridine (3.27). To a solution of 278 mg (0.75 mmol) of **3.26** in 4 mL of chloroform was

added 108 mg (0.38 mmol) of 1,3-dibromo-5,5-dimethylhydantoin in portions at 0 °C. The reaction mixture was stirred at 0 °C for 30 min. The reaction was quenched by the addition of 5 mL of sat aq $NaHCO_3$. The mixture was extracted with chloroform and the combined organic layer was washed with brine and dried over $MgSO_4$. The concentrated residue was purified by flash chromatography on a silica gel column (20 × 1.7 cm). Elution with 100:1 hexanes–ethyl acetate gave **3.27** as a white solid: yield 331 mg (98%); mp 49–50 °C; silica gel TLC R_f 0.78 (8:1:1 hexanes–ethyl acetate–methanol); ^{1}H NMR ($CDCl_3$) δ 0.88 (t, 3H, J = 7.2 Hz), 1.25-1.31 (m, 28H), 1.66 (quint, 2H, J = 7.6 Hz), 2.08 (s, 3H), 2.55 (t, 2H, J = 8.0 Hz), 2.80 (t, 2H, J = 8.4 Hz), 2.90 (s, 3H), 3.38 (t, 2H, J = 8.0 Hz) and 6.13 (s, 1H); ^{13}C NMR ($CDCl_3$) δ 14.13, 19.49, 22.69, 25.22, 28.68, 29.38, 29.57, 29.61, 29.65, 29.68, 29.71, 29.71, 29.71, 29.71, 29.71, 29.71, 31.9, 33.0, 38.1, 52.4, 110.92, 120.33, 141.07, 156.79 and 161.78; mass spectrum, *m/z* 451.3 and 453.2 $(M + H)^+$ (theoretical 451.3 and 453.3); mass spectrum (APCI), *m/z* 451.2680 and 453.2697 $(M + H)^+$ ($C_{25}H_{44}N_2Br$ requires 451.2688 and 453.2667).

1,4-Dimethyl-6-hexadecyl-1*H*-pyrrolo[2,3-*b*]pyridin-5-yl Acetate (3.9). To a solution of 43.5 mg (0.10 mmol) of **3.27** in 1 mL of THF was added 14.2 μL (0.10

mmol) of tetramethylethylenediamine (TMEDA) at –20 °C followed by 119 μL (0.19 mmol, 1.6 M in hexanes) of *n*-BuLi. After 30 min, 23.4 μL (0.21 mmol) of trimethoxy boron was added and the resulting mixture was stirred for another 1 hr. To the reaction mixture was slowly added 44.1 μL (0.21 mmol, 32 wt%) of peracetic acid and the solution was then warmed to 0 °C over 30 min. The mixture was diluted by 5 mL of H_2O and extracted with three 5-mL portions of EtOAc. The combined organic layer was washed with brine, dried ($MgSO_4$) and the solvent was concentrated under diminished pressure. The resulting oil was dissolved in 2 mL of CH_2Cl_2 at 0 °C, followed by the addition of 79.6 μL (0.57 mmol) of triethylamine, 1.2 mg (0.01 mmol) of DMAP and 27.0 μL (0.29 mmol) of acetic anhydride. The reaction was stirred at room temperature for 1 hr and quenched by the addition of 2 mL of sat aq NH_4Cl. The solution was then extracted with three 5-mL of EtOAc. The combined organic layer was washed with brine, dried ($MgSO_4$) and the solvent was concentrated under diminished pressure. The residue was purified by flash chromatography on a silica gel column (20 × 1.7 cm). Elution with 100:1 hexanes–ethyl acetate gave **3.9** as a yellow oil: yield 15.0 mg (37%); silica gel TLC R_f 0.20 (3:7 EtOAt–hexanes); ^{1}H NMR ($CDCl_3$) δ 0.86 (t, 3H, J = 6.8 Hz), 1.23-1.28 (m, 28H), 1.60 (quint, 2H, J = 7.6 Hz), 1.93 (s, 3H), 2.28 (s, 3H), 2.44 (t, 2H, J = 8.0 Hz), 2.82 (t, 2H, J = 8.0 Hz), 2.87 (s, 3H) and 3.41 (t, 2H, J = 8.0 Hz); ^{13}C NMR ($CDCl_3$) δ 12.88, 14.10, 20.54, 22.67, 24.62, 28.69, 29.35, 29.51, 29.59 29.64, 29.68, 29.68, 29.68, 29.68,

29.68, 29.68, 29.68, 31.91, 32.50, 33.32, 52.82, 120.08, 134.68, 136.50, 149.66, 161.18 and 169.91; mass spectrum, *m/z* 430.3 $(M)^+$ (theoretical 430.4); mass spectrum (APCI), *m/z* 431.3637 $(M + H)^+$ ($C_{27}H_{47}N_2O_2$ requires 431.3638).

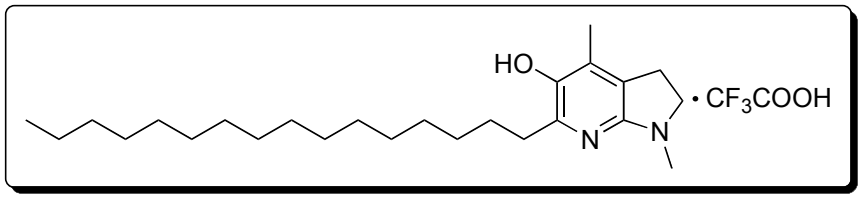

1,4-Dimethyl-6-hexadecyl-1*H*-pyrrolo[2,3-*b*]pyridin-5-ol and its trifluoroacetic acid salt (3.8). To a solution of 15.0 mg (34.8 μmol) of **3.9** in 1 mL of CH_2Cl_2 was added 105 μL (105 μmol, 1.0 M in hexanes) of DIBAL-H at –78 °C. The reaction mixture was stirred at the same temperature for 1 h before 2 mL of sat aq sodium potassium tartrate was added slowly. The reaction mixture was slowly warmed to room temperature over 30 min. The solution was extracted with three 5-mL portions of ethyl acetate. The combined organic layer was washed with brine, dried ($MgSO_4$) and concentrated under diminished pressure to give the crude product as a yellow oil: silica gel TLC R_f 0.22 (1:9 MeOH–CH_2Cl_2). The residue was then dissolved in 1 mL of CH_3CN and 1% aq TFA, frozen and lyophilized. The crude product was purified on a Prepex C_8 reversed phase semi-preparative (250 mm x 10 mm) HPLC column using a gradient of methanol and water. Linear gradients were employed using 1:4 methanol/water → 4:1 methanol/water over a period of 20 min, and then 4:1 methanol/water →

methanol over a period of 40 min, at a flow rate of 3.5 mL/min (monitoring at 260 nm); Fractions containing the desired product eluted at 37.5 min, and were collected, frozen, and lyophilized to give **3.8** as a light yellow solid: yield 11.0 mg (82%); ^{1}H NMR (CD_3CN) δ 0.89 (t, 3H, J = 6.4 Hz), 1.27-1.36 (m, 28H), 1.55 (quint, 2H, J = 7.2 Hz), 2.13 (s, 3H), 2.70 (t, 2H, J = 8.0 Hz), 3.00 (t, 2H, J = 8.4 Hz), 3.06 (s, 3H) and 3.73 (t, 2H, J = 8.4 Hz); ^{13}C NMR ($CDCl_3$) δ 13.00, 13.39, 22.40, 24.41, 27.23, 28.61, 28.71, 28.99, 29.06, 29.07, 29.21, 29.30, 29.33, 29.36, 29.39, 29.39, 29.39, 31.64, 32.39, 53.11, 117.30, 126.16, 131.92, 140.24, 141.44 and 152.06; mass spectrum, *m/z* 388.3 $(M)^+$ (theoretical 388.3); mass spectrum (APCI), *m/z* 389.3526 $(M + H)^+$ ($C_{25}H_{45}N_2O$ requires 389.3532).

REFERENCES

1. (a) *Free Radicals*; Pryor, W. A. Eds.; McGraw-Hill: New York, 1966. (b) Koppenol, W. H. *Free Radical Biol. Med.* **1990**, *9*, 67.

2. (a) *Radical Ions*; Kaiser, E. T., Kevan, L. Eds.; Interscience: New York, 1968. (b) Halliwell, B. Lancet **1994**, *34*, 721

3. *Inorganic Chemistry*, Bowser, J. R. Eds.; Brooks/Cole Publishing: Pacific Grove, 1993.

4. Isied, S. S. *Prog. Inorg. Chem.* **1984**, *32*, 443.

5. *Free Radicals in Biology and Medicine*; Halliwell, B., Gutteridge, J. M. C. Eds.; Clarendon Press: Oxford, 1989.

6. Dröge, W. Physiol. Rev. **2002**, *82*, 47.

7. Halliwell, B. *Am. J. Med.* **1991**, *91*, 14S.

8. Chabot, F.; Mitchell, J. A. Gutteridge, J. M.; Evans, T. W. *Eur. Respir. J.* **1998**, *11*, 745.

9. Pham-Huy, L. A.; He, H. Pham-Huy, C. *Int. J. Biomed. Sci.* **2008**, *4*, 89.

10. Bohorun, T.; Soobrattee, M. A. Luximon-Ramma, V.; Aruoma, O. I. *Internet J. Med.* **2006**, *1*, 1.

11. Valko, M.; Izakovic, M.; Mazur, M.; Rhodes, C. J.; Telser, J. *Mol. Cell Biochem.* **2004**, *266*, 37.

12. Valko, M.; Moncola, J.; Cronin, M. D. *Int. J. Biochem. Cell Biol.* **2007**, *39*, 44.

13. Willcox, J. K.; Ash, S. L.; Catignani, G. L.. *Crit. Rev. Food Sci. Nutr.* **2004**, *44*, 275.

14. Pacher, P.; Beckman, J. S.; Liaudet, L. *Physiol. Rev.* **2007**, *87*, 315.

15. Genestra, M. *Cell. Signal.* **2007**, *19*, 1807.

16. Halliwell, B. *Biochem. Soc. Trans.* **2007**, *35*, 1147.

17. Young, I.; Woodside, J. *J. Clin. Pathol.* **2001**, *54*, 176.

18. Valko, M.; Rhodes, C. J.; Moncol, J.; Izakovic, M. *Chem. Biol. Interact.* **2006**, *160*, 1.

19. Valko, M.; Morris, H.; Cronin, M. T. D. *Curr. Med. Chem.* **2005**, *12*, 1161.

20. Pharthasarathy, S.; Santanam, N.; Ramachandran, S.; Meilhac, O. *J. Lipid Res.* **1999**, *40*, 2143.

21. Finkel, T. *Curr. Opin. Chem. Biol*. **2003**, *15*, 247.

22. Finkel, T.; Serrano, M.; Blasco, M. A. *Nature* **2007**, *448*, 767.

23. Barnham, K. J.; Masters, C. L.; Bush, A. I. *Nat. Rev. Drug Discov.* **2004**, *3*, 205.

24. Lu, T.; Pan, Y.; Kao, S.-Y.; Li, C.; Kohane, I.; Chan, J.; Yankner, B. A. *Nature* **2004**, *429*, 883.

25. Balaban, R. S.; Nemoto, S.; Finkel, T. *Cell* **2005**, *120*, 483.

26. Chance, B.; Sies, H.; Boveris, A. *Physiol. Rev*. **1979**, *59*, 527.

27. Stadtman, E. R. *J. Free Radical Res*. **2006**, *40*, 1250.

28. Yamazaki, I. in *Free Radicals in Biology*; Pryor, W. Eds.; Academic Press: New York, 1977.

29. Kirkinezos, I.; Moraes, C. T. *Semin. Cell Dev. Biol.* **2001**, *12*, 449.

30. *Free Radicals and Oxidation Phenomena in Biological Systems*; Roberfroid, M., Calderon, P. B. Eds.; Marcel Dekker, New York, 1994.

31. Floyd, R. A.; Lewis, C. A. *Biochemistry* **1983**, *22*, 2645.

32. Braughler, J. M.; Duncan, L. A.; Chase, R. L. *J. Biol. Chem.* **1986**, *261*, 10282.

33. Halliwell, B.; Gutteridge, J. M. C. *Arch. Biochem. Biophys.* **1986**, *246*, 501.

34. Aruoma, O. I.; Halliwell, B. *Biochem. J*. **1987**, *241*, 273.

35. Minotti, G. *Chem. Res. Toxicol*. **1993**, *6*, 134.

36. Mountzouris, J. A.; Hurley, J. H. in *Bioorganic Chemistry: Nucleic acids*, Hecht, S. M., Ed.; Oxford University Press: New York, 1996.

37. (a) Lin, A. J.; Cosby, L. A.; Shasky, C. W.; Sartorelli, A. C. *J. Med. Chem*. **1972**, *15*, 1247. (b) Wilson, I.; Wardman, P.; Lin, T. S.; Sartorelli, A. C. *J. Med. Chem*. **1986**, *29*, 1381. (c) Abdella, R. J.; Fisher, J. *Environ. Health Prespec.* **1985**, *64*, 3.

38. (a) Sato, S.; Iwaizumi, M.; Handa, K.; Tamura, Y. *Gann*. **1977**, *68*, 603. (b) Bachur, N. R.; Gordon, S. L.; Gee, M. V. *Cancer Res*. **1978**, *38*, 1745.

39. Kovacic, P.; Becvar, L. E. *Curr. Pharmaceut. Des.* **2000**, *6*, 143.

40. Ross, W. A.; Glaubiger, D. L.; Kohn, K. W. *Biochim. Biophys. Acta* **1978**, *519*, 23.

41. Pan, S.-S.; Pedersen, L.; Bachur, N. R. *Mol. Pharmacol.* **1981**, *19*, 184.

42. Hertzberg, R. P.; Dervan, P. B. *Biochemistry* **1984**, *23*, 3949.

43. Garnier-Suillerot, A. in *Anthracycline and Anthracenedione-Based Anticancer Agents*, Lown, J. W., Eds.; Elsevier: Amsterdam, 1988.

44. Traatjes, D.; Fenick, D. J.; Guadiano, G.; Koch T. H. *Curr. Pharmaceut. Des.* **1998**, *4*, 203.

45. Tomasz, M.; Palom, Y. *Pharmacol. Ther.* **1997**, *76*, 73.

46. Cummings, J.; Spanswick, V. J.; Tomasz, M.; Smyth, J. F. *Biochem. Pharmacol.* **1998**, *56*, 405.

47. (a) Moore, H. W.; Czerniak, R. *Med. Res. Rev.* **1981**, *1*, 249. (b) Moore, H. W. *Science* **1977**, *197*, 527.

48. Pan, S. S.; Gonzalez, H. *Mol. Pharmacol.* **1990**, *37*, 966.

49. Kovacic, P., Amez, J. R., Ryan, M. D. *Redox Chemistry and Interfacial Behavior of Biological Molecules*, Dryhurst, G., Niki, K. Eds.; Plenum Press: New York, 1988.

50. Gantchev, T. G.; Hunting, D. G. *Biochem. Biophys. Res. Commun.* **1997**, *237*, 24.

51. Brown, J. M. *Cancer Res.* **1999**, *59*, 5863.

52. (a) Daniels, J. S.; Gates, K. S. *J. Am. Chem. Soc.* **1996**, *118*, 3380. (b) Patterson, L. H.; Taiwo, F. A. *Biochem. Pharmacol.* **2000**, *60*, 1933. (c) Kotandeniya, D.; Ganley, B.; Gates, K. S. *Bioorg. Med. Chem. Lett.* **2002**, *12*, 2325. (d) Laderoute, K. L.; Wardman, P.; Rauth, M. *Biochem. Pharmacol.* **1988**, *37*, 1487.

53. Sies, H. *Exp. Physiol.* **1997**, *82*, 291.

54. Donaldson, M. S. *Nutr. J.* **2004**, *3*, 19.

55. Burton, G. W.; Ingold, K. U. *Acc. Chem. Res.* **1986**, *19*, 194.

56. (a) Frei, B.; Stoker, R.; England, K.; Ames. B. N. Adv. Exp. Med. Biol. 1990, 264, 155. (b) *Sulfur-Centered Reactive Intermedieates in Chemistry and Biology*; Chatgilialoglu, C.; Asmus, K.-D., Eds.; Plenum Press: New York, 1990. (c) Nakazawa, H.; Ichinori, K.; Shinozaki, Y.; Okino, Hori, S. *Am. J. Physiol.* **1988**, *255*, H213.

57. Sauberlich, H. E. *Annu. Rev. Nutr.* **1994**, *14*, 371.

58. (a) DiMascio, P.; Devasagayam, T. P. A.; Kaiser, S.; Sies, H. *Biochem. Soc. Trans.* **1990**, *18*, 1054. (b) Olson, J. A. *J. Nutr. Sci. Vitaminol.* **1993**, *39*, S57.

59. (a) Torel, J.; Cillard, J.; Cillard, P. *Phytochemistry* **1986**, *25*, 383. (b) Bors, W.; Heller, W.; Michel, C.; Sara, M. *Adv. Exp. Med.* **1990**, *264*, 165. (c) Sichel, G.; Corsaro, C.; Scalia, M.; Dibilio, A.; Bonomo, R. *Free Radical Biol. Med.* **1991**, *11*, 1.

60. (a) Takeshige, K.; Takayanagi, R.; Minakami, S. *Biochem. J.* **1980**, *192*, 861. (b) Stocker, R.; Bowry, V. W.; Frei, B. *Proc. Natl. Acad. Sci. U.S.A.* **1991**, *88*, 1646. (c) *Free Radical Chain Reactions*; Huyser, E. S. Eds.; Wiley-Interscience: New York, 1970.

61. (a) Parnetti, L; Senin, U; Mecocci, P. *Drugs* **1997**, *53*, 752. (b) McDaniel, D.; Neudecker, B.; Dinardo, J.; Lewis, J.; Maibach, H. *J. Cosmet. Dermatol.* **2005**, *4*, 167.

62. *Bleomycin Chemotherapy*; Sikic, B. I., Rozencweig, M., Carter, S. K., Eds.; Academic: Orlando, FL, 1985.

63. Umezawa, H.; Suhara, Y.; Takita, T.; Maeda, K. *J. Antibiot*. **1966**, *19A*, 210.

64. Takita, T.; Muraoka, Y.; Fujii, A.; Maeda, K.; Umezawa, H. *J. Antibiot*. **1972**, *25*, 755.

65. Takita, T.; Muraoka, Y.; Nakatani, T.; Fujii, A.; Naganawa, H. *J. Antibiot*. **1978**, *31*, 801.

66. Boger, D. L.; Colletti, S. L.; Honda, T.; Menezes, R. F. *J. Am. Chem. Soc.* **1994**, *116*, 5647.

67. *Anticancer Drugs: Reactive Metabolism and Drug Interactions*; Powis, G. Eds.; Academic Press: Orlando, Florida, 1985.

68. (a) Kuwahara, J.; Sugiura, Y. *Proc. Natl. Acad. Sci. U.S.A.* **1988**, *85*, 2459. (b) Bailly, C.; Waring, M. J. *J. Am. Chem. Soc.* **1995**, *117*, 7311.

69. (a) Carter, B. J.; deVroom, E.; Long, E. C.; van der Marel, G. A.; van Boom, J. H.; Hecht, S. M. *Proc. Natl. Acad. Sci. U.S.A.* **1990**, *97*, 9373. (b) Holmes, C. E.; Carter, B. J.; Hecht, S. M. *Biochemistry* **1993**, *32*, 4293. (c) Hecht, S. M. *Bioconjugate Chem.* **1994**, *5*, 513. (d) Hecht, S. M. In *The Many Faces of RNA*.; Eggleston, D. S., Prescott, C. D., Pearson, N. D., Eds.; Academic Press: San Diego, **1998**, pp 3–17. (e) Thomas, C. J.; Chizhov, A. O.; Leitheiser, C. J.; Rishel, M. J.; Konishi, K.; Tao, Z.-F.; Hecht, S. M. *J. Am. Chem. Soc*. **2002**, *124*, 12926.

70. (a) Abraham, A. T.; Lin, J.-J.; Newton, D. L.; Rybak, S.; Hecht, S. M. *Chem. Biol*. **2003**, *10*, 45. (b) Tao, Z.-F.; Konishi, K.; Keith, G.; Hecht, S. M. *J. Am. Chem. Soc*. **2006**, *128*, 14806.

71. (a) Ishida, R.; Takahashi, T. Biochem. *Biophys. Res. Commun.* **1975**, *66*, 1432. (b) Sausvile, E. A.; Peisach, J.; Horwitz, S. B. *Biochem. Biophys. Res. Commun.* **1976**, **73**, 814. (c) Sausville, E. A.; Peisach, J.; Horwitz, S. B. *Biochemistry* **1987**, *17*, 2740. (d) Sausville, E. A.; Peisach, J.; Horwitz, S. B. *Biochemistry* **1987**, *17*, 2746.

72. (a) Enrenfeld, G. M.; Murugesan, N.; Hecht, S. M.; Chang, C.; Basus, V. J.; Oppenheimer, N. J. *Biochemistry* **1985**, *24*, 81. (b) Ehrenfeld, F. M.; Shipley, J. B.; Heimbrook, D. C.; Sugiyama, H.; Long, E. C.; van Boom, J. H.; van der

Marel, G. A.; Oppenheimer, N. J.; Hecht, S. M. *Biochemistry* **1987**, *26*, 931.

73. (a) Chang, C.; Meares, C. F. *Biochemistry* **1982**, *21*, 6332. (b) Chang, C.; Meares, C. F. *Biochemistry* **1984**, *23*, 2268. (c) Saito, I.; Morii, T.; Sugiyama, H.; Matsurra, T.; Meares, C. F.; Hecht, S. M. *J. Am. Chem. Soc.* **1989**, *111*, 2307.

74. (a) Enrenfeld, G. M.; Murugesan, N.; Hecht, S. M. *Inorg. Chem.* **1984**, *23*, 1496. (b) Burger, R. M.; Freedman, J. H.; Horwitz, S. B.; Peisach, J. *Inorg. Chem.* **1984**, *23*, 2215.

75. (a) Aoyagi, Y.; Suguna, H.; Murugesan, N.; Ehrenfeld, G. M.; Chang, L.-H.; Ohgi, T.; Shekhani, M. S.; Kirkup, M. P. Hecht, S. M. *J. Am. Chem. Soc.* **1982**, *104*, 5237. (b) Oppenheimer, N. J.; Chang, C.; Chang, L.-H.; Ehrenfeld, F.; Rodriguez, L. O.; Hecht, S. M. *J. Biol. Chem.* **1982**, *257*, 1606.

76. (a) Boger, D. L.; Cai, H. *Angew. Chem., Int. Ed.* **1999**, *38*, 448. (b) Sugiyama, H.; Ehrenfeld, G. M.; Shipley, J. P.; Kilkuskie, R. E.; Chang, L.-H.; Hecht, S. M. *J. Nat. Prod.* **1985**, *48*, 869.

77. Sugiura, Y.; Suzuki, T. *J. Biol. Chem.* **1982**, *257*, 10544.

78. Kuwahara, J.; Sugiura, Y. *Proc. Natl. Acad. Sci. U.S.A.* **1988**, *85*, 2459.

79. Carter, B. J.; Murty, V. S.; Reddy, K. S.; Wang, S.-N.; Hecht, S. M. *J. Biol. Chem.* **1990**, *265*, 4193.

80. Hecht, S. M. In *Cancer Chemotherapeutic Agents*; Foye, W. O., Ed.; American Chemical Society: Washington, DC, **1995**; p 369.

81. Kilkuskie, R. E.; Suguna, H.; Yellin, B.; Murugesan, N.; Hecht, S. M. *J. Am. Chem. Soc*. **1985**, *107*, 260.

82. Guajardo, R. J.; Hudson, S. E.; Brown, S. J.; Mascharak. P.K. *J. Am. Chem. Soc*. **1993**, *115*, 7971.

83. Oppenheimer, N. J.; Rodriguez, L. O.; Hecht, S. M. *Proc. Natl. Acad. Sci. U.S.A.* **1979***, 76*, 5616.

84. Akkerman, M. A. J.; Neijman, E. W. J. F.; Wijmenga, S. S.; Hilbers, C. W.; Bermel, W. *J. Am. Chem. Soc.* **1990**, *112*, 7462.

85. Chapuis, J.C.; Schmaltz, R. M.; Tsosie, K. S.; Belohlavek, M.; Hecht, S. M. *J. Am. Chem. Soc.* **2009**, *131*, 2438.

86. Brahim, S.; Abid, K.; Kenani, A. *Cell Biol. Int*. **2008**, *32*,171.

87. Brahim, S.; Prévotat, L.; Yatouji, S.; Merino, D.; Cortier, M.; Rebe, C. Micheau, O. ; Kenani, A.; Bettaieb, A. *Biochem. Pharmacol*., **2007**, *74*, 1445.

88. (a) Lin, S. Y.; Grollman, A. P. *Biochemistry* **1981**, *20*, 7589. (b) Skai, T. T.; Riodan, J. M.; Glickson, J. D. *Biochemistry* **1982**, *21*, 805. (c) Riordan, J. M.; Sakai, T. T. *J. Med. Chem.* **1983**, *26*, 884. (d) Chien, M.; Grollman, A. P.; Horwitz, S. B. *Biochemistry* **1977**, *16*, 3641.

89. Hamamichi, N.; Natrajan, A.; Hecht. S. M. *J. Am. Chem. Soc.* **1992**, *114*, 6278.

90. (a) Zuber, G.; Quada, J. C., Jr.; Hecht, S. M. *J. Am. Chem. Soc.* **1998**, *120*, 9368. (b) Kane, S. A.; Natrajan, A.; Hecht, S. M. *J. Biol. Chem.* **1994**, *269*, 10899.

91. Thomas, C. J.; McCormick, M. M.; Vialas, C.; Tao, Z.-F.; Leitheiser, C. J.; Rishel, M. J.; Xu, X.; Hecht, S. M. *J. Am. Chem. Soc.* **2002**, *124*, 3875.

92. (a) Otsuka, M.; Masuda, T.; Haupt, A.; Ohno, M.; Shiraki, T.; Sugiura, Y.; Maeda, K. *J. Am. Chem. Soc.* **1990**, *112*, 838. (b) Owa, T.; Haupt, A.; Otsuka, M.; Kobayashi, S.; Nobuo, T.; Itai, A.; Ohno, M. *Tetrahedron* **1992**, *48*, 1193.

93. Muraoka, Y.; Saito, S.; Nogami, T.; Umezawa, K.; Takita, T.; Takeuchi, T.; Umezawa, H.; Sakata, N.; Hori, M.; Takahashi, K.; Ekimoto, H.; Minamide, S.; Nishikawa, K.; Kuramochi, H.; Motegi, A.; Fukuoka, T.; Fukuoka, T.; Nakatani, T.; Fujii, A.; Matsuda, A. In *Horizons on Antibiotic Research*; Davis, B. D., Ichikawa, T., Maeda, K., Mitscher, L. A., Eds.; Japan Antibiotic Research Association: Tokyo, 1988.

94. Boger, D. L.; Menezes, R. F.; Dang, Q.; Yang, W. *Bioorg. Med. Chem. Lett.* **1992**, *2*, 162.

95. Carter, B. J.; Reddy, K. S.; Hecht, S. M. *Tetrahedron* **1991**, *47*, 2463.

96. Leitheiser, C. J.; Smith, K. L.; Rishel, M. J.; Hashimoto, S.; Konishi, K.; Thomas, C. J.; Li, C.; McCormick, M. M.; Hecht, S. M. *J. Am. Chem. Soc.*

2003, *125*, 8218.

97. Boger, D. L.; Ramsey, T. M.; Cai, H.; Hoehn, S. T.; Stubbe, J. *J. Am. Chem. Soc.* **1998**, *120*, 9139.

98. Owa, T.; Haupt, A.; Otsuka, M.; Kovayashi, S.; Tomioka, N.; Itai, A.; Ohno, M.; Shiraki, T.; Uesugi, M.; Sugiura, Y.; Maeda, K. *Tetrahedron* **1992**, *48*, 1193.

99. Boger, D. L.; Ramsey, T. M.; Cai, H.; Hoehn, S. T.; Stubbe, J. *J. Am. Chem. Soc.* **1998**, *120*, 9149.

100. Rishel, M. J.; Thomas, C. J.; Tao, Z.-F.; Vialas, C.; Leitheiser, C. J.; Hecht, S. M. *J. Am. Chem. Soc*. **2003**, *125*, 10194.

101. Ma, Q.; Xu, Z.; Schroeder, B. R.; Sun, W.; Wei, F.; Hashimoto, S.; Kazuhide, K.; Leitheiser, C. J.; Hecht, S. M. *J. Am. Chem. Soc.* **2007**, *129*, 12439.

102. Iitaka, Y.; Nakamura, H.; Nakatani, T.; Muraoka, A.; Fujii, A.; Takita, T.; Umezawa, H. *J. Antibiot.* **1987**, *31*, 1070.

103. Takita, T.; Muraoka, Y.; Nakatani, T.; Fukii, A.; Iitaka, Y.; Umezawa, H. *J. Antibiot.* **1987**, *31*, 1073.

104. (a) Stubbe, J.; Kozarich, J. W. *Chem. Rev.* **1987**, *87*, 1107. (b) Shipley, J. B.; Hecht, S. M. *Chem. Res. Toxicol.* **1988**, *1*, 25. (c) Claussen, C. A.; Long, E. C. *Chem. Rev.* **1999**, *99*, 2797.

105. (a) Brown, S. J.; Hudson, S. E.; Olmstead, M. M.; Mascharak, P. K. *J. Am. Chem. Soc.* **1989**, *111*, 6446. (b) Tan, J. D.; Hudson, S. E.; Brown, S. J.; Olmstead, M. M.; Mascharak, P. K. *J. Am. Chem. Soc.* **1992**, *114*, 3841. (c) Farinas, E.; Tan, J. D.; Baidya, N.; Mascharak, P. K. *J. Am. Chem. Soc.* **1993**, *115*, 2996. (d) Farinas, E. T.; Tan, J. D.; Mascharak, P. K. *Inorg. Chem.* **1996**, *35*, 2637.

106. (a) Wu, W.; Vanderwall, D. E.; Stubbe, J.; Kozarich, J. W.; Turner, C. J. *J. Am. Chem. Soc.* **1994**, *116*, 10843. (b) Lui, S. M.; Vanderwall, D. E.; Wu, W.; Tang, X.-J.; Turner, C. J.; Kozarich, J. W. Stubbe, J. *J. Am. Chem. Soc.* **1997**, *119*, 9603.

107. Boger, D. L.; Ramsey, T. M.; Cai, H.; Hoehn, S. T.; Stubbe, J. *J. Am. Chem. Soc.* **1998**, *120*, 9139.

108. (a) Dabrowiak, J. C.; Greenaway, F. T.; Longo, W. E.; van Husen, M.; Crooke, S. T. *Biochem. Biophys. Acta* **1978**, *517*, 517. (b) Xu, R. X.; Nettesheim, D.; Otvos, J. D.; Petering, D. H. *Biochemistry* **1994**, *33*, 907.

109. Boger, D. L.; Teramoto, S.; Cai, H. *Bioorg. Med. Chem.* **1996**, *4*, 179.

110. Boger, D. L.; Ramsey, T. M.; Cai, H. *Bioorg. Med. Chem.* **1996**, *4*, 195.

111. (a) Akkerman, M. A. J.; Neijman, E. W. J. F.; Wijmenga, S. S.; Hilbers, C. W.; Bermel, W. *J. Am. Chem. Soc.* **1990**, *112*, 7462. (b) Lehman, T. E.; Ming, L.-J.; Rosen, M. E.; Que, L. Jr. *Biochemistry* **1997**, *36*, 2807.

112. (a) Sugiura, Y.; Suzuki, T.; Otsuka, M.; Kobayashi, S.; Ohno, M.; Takita, T.; Umezawa, H. *J. Biol. Chem.* **1983**, *258*, 1328. (b) Kittaka, A.; Sugano, Y.; Otsuka, M.; Ohno, M. *Tetrahedron* **1988**, *44*, 2821. (c) Kenani, A.; Bailly, C.; Helbecque, N.; Catteau, J.-P.; Houssin, R.; Bernier, J.-L.; Henichart, J.-P. *Biochem. J.* **1988**, *253*, 497. (d) Kenani, A.; Bailly, C.; Houssin, R.; Henichart, J.-P. *Anticancer Drugs* **1994**, *5*, 199.

113. Boger, D. L.; Teramato, S.; Zhou, J. *J. Am. Chem. Soc.* **1995**, *117*, 7344.

114. (a) Hecht, S. M. *Acc. Chem. Res.* **1986**, *19*, 383. (b) Natrajan, A., Hecht, S. M. In *Molecular Aspects of Anticancer Drug-DNA Interactions*; Neidle, S., Waring, M. J., Eds.; MacMillan Press: London, 1994. (c) Hecht, S. M. *J. Nat. Prod.* **2000**, *63*, 158.

115.Ciriolo, M. R.; Magliozzo, R. S.; Peisach, J. *J. Biol. Chem.* **1987**, *262*, 6290.

116. Mahmutoglu, I.; Kappus, H. *Biochem. Pharmacol.* **1987**, *36*, 3677.

117.(a) Sugiura, Y.; Kikuchi, T. *J. Antibiot.***1979**, *31*, 1310. (b) Burger, R. M.; Horwitz, S. B.; Peisach, J.; Wittenberg, J. B. *J. Biol. Chem.* **1979**, *254*, 1229. (c) Kuramochi, H. Takahashi, K.; Takita, T.; Umezawa, H. *J. Antibiot.* **1981**, *34*, 576. (d) Burger, R. M.; Peisach, J.; Horwitz, S. B. *J. Biol. Chem.* **1981**, *256*, 11636.

118. Giloni, L.; Takeshita, M.; Johnson, F.; Iden, C.; Grollman, A. *J. Biol. Chem.* **1981**, *256*, 8608.

119. (a) Sugiyama, H.; Xu, C.; Murugesan, N.; Hecht, S. M. *J. Am. Chem. Soc.* **1985**, *107*, 4104. (b) Sugiyama, H.; Xu, C.; Murugesan, N.; Hecht, S. M. *Biochemistry* **1988**, *27*, 58. (c) Rabow, L. E.; Stubbe, J.; Kozarich, J. W.;

Geralt, J. A. *J. Am. Chem. Soc.* **1990**, *112*, 3203.

120. Morgan, M. M.; Hecht, S. M. *Biochemistry* **1994**, *33*, 10286.

121. Dix, D. J.; Lin, P.-N.; McKenzie, A. R.; Walden, W. E.; Theil, E. C. *J. Mol. Biol.* **1993**, *231*, 230.

122. Poddevin, D.; Orlowski, S.; Belehradek, J., Jr.; Mir, L. M. *Biochem. Pharmacol.* **1991**, *42*, S67.

123. Duff, R. J.; Vroom, E.; Geluck, A.; Hecht, S. M.; van der Marcel, G. A.; van Boom, J. H. *J. Am. Chem. Soc.* **1993**, *115*, 3350.

124. Packer, L. *NATO ASI Ser., Ser. A* **1993**, *23*, 147.

125. (a) Burton, G. W.; Ingold, K. U. *Acc. Chem. Res.* **1986**, *19*, 194. (b) Bielski, B. H. J.; Cabelli, D. E. *Int. J. Radiat. Biol.* **1991**, *59*, 291. (c) Cadenas, E.; Merenyi, G.; Lind, J. *FEBS Lett.* **1989**, *253*, 235.

126. Stryer, L.; *Biochemistry*, 4th edition, W H Freeman and Company: New York, pp. 691–700.

127. (a) Azen, S. P.; Qian, D.; Mack, W. J. *Circulation* **1996**, *94*, 2369. (b) Stephens, N. G.; Parsons, A.; Schofield, P. M.; Kelly, F.; Cheeseman, K.; Mitchinson, M. J. *Lancet* **1996**, *347*, 781. (c) Boaz, M.; Smetana, S.; Weinstein, T. *Lancet* **2000**, *356*, 1213. (d) Rapola, J. M.; Virtamo, J.; Ripatti, S. *Lancet* **1997**, *349*, 1715.

128. (a) Paolisso, G.; DiMaro, G, Galzerano D. *Am. J. Clin. Nutr.* **1994**, *59*, 1291. (b) Reaven, P. D.; Herold, D. A.; Barnett, J.; Edelman, S. *Diabetes Care.* **1995**, *18*, 807.

129. (a) Meydani, M. *Nutr. Rev.* **2001**, *59*, S75. (b) Masiki, K. H.; Losonczy, K. G.; Izmirlian, G.; Foley, D. J.; Ross, G. W.; Petrovitch, H.; Havlik, R.; White, L. R. *Neurology* **2000**, *54*, 1265.

130. (a) Yu, W.; Sanders, B. G.; Kline, K.; *Cancer Res.* **2003**, *63*, 2483. (b) You, H.; Yu, W.; Munoz-Medellin, D.; Brown, P. H.; Sanders, B. G.; Kline, K. *Mol. Carcin.* **2002**, *33*, 228. (c) Brigelius-Flohe, R.; Kelly, F. J.; Salonen, J. T.; Neuzil, J.; Zingg, J. M.; Azzi, A. *Am. J. Clin. Nutr.* **2002**, *76*, 703.

131. (a) *Oxidants, antioxidants, and free radicals*; Baskin, S. I., Salem, H. Eds.;

Taylor & Francis, Philadelphia, 1997. (b) Niki, E.; Yoshida, Y.; Saito, Y.; Noguchi, N. *Biochem Biophys. Res. Commun.* **2005**, *338*, 668. (c) Nicolescu, A. C.; Azvorin, S. I.; Turro, N. J.; Reynolds, J. N.; Thatcher, G. R. J. *Chem. Res. Toxicol.* **2002**, *15*, 985. (d) Maillard, B.; Ingold, K. U.; Scaiano, J. C. *J. Am. Chem. Soc.* **1983**, *105*, 5095. (e) Burton, G. W.; Ingold, K. U. *Acc. Chem. Res.* **1986**, *19*, 194.

132. (a) Burton, G. W.; Doba, T.; Gabe, E. J.; Hughes, L.; Lee, F.; Prasad, L.; Ingold, K. U. *J. Am. Chem. Soc.* **1985**, *107*, 7053. (b) Burton, G. W.; Ingold, K. U. *J. Am. Chem. Soc.* **1981**, *103*, 6472. (c) Bowry, V. R.; Ingold, K. U. *Acc. Chem. Res.* **1999**, *32*, 27. (e) Ingold, K. U. *Acc. Chem. Res.* **1969**, *2*, 1.

133. Liebler, D. C. *Crit. Rev. Toxicol.* **1993**, *23*, 147.

134. (a) Watanabe, A.; Noguchi, N.; Fujisawa, A.; Kodama, T.; Tamura, K.; Cynshi, O.; Niki, E. *J. Am. Chem. Soc.* **2000**, *122*, 5438. (b) Pratt, D. A.; DiLabio, G. A.; Brigati, G.; Pedulli, G. F.; Valgimigli, L. *J. Am. Chem. Soc.* **2001**, *123*, 4625. (c) Valgimigli, L.; Brigati, G.; Pedulli, G. F.; DiLabio, G. A.; Mastragostino, M.; Arbizzani, C.; Pratt, D. A. *Chem. Eur. J.* **2003**, *9*, 4997. (d) Foti, M. C.; Johnson, E. R.; Vinqvist, M. R.; Wright, J. S.; Barclay, L. R. C.; Ingold, K. U. *J. Org. Chem.* **2002**, *67*, 5190.

135. (a) Mukai, K.; Okabe, K.; Hosose, H. *J. Org. Chem.* **1989**, *54*, 557. (b) Barclay, L. R. C.; Vinqvist, M. R.; Mukai, K.; Itoh, S.; Morimoto, H. *J. Org. Chem.* **1993**, *58*, 7416. (c) Brownstein, S.; Burton, G. W.; Hughes, L.; Ingold, K. U. *J. Org. Chem*. **1989**, *54*, 560. (d) Noguchi, N.; Iwaki, Y.; Takahashi, M.; Komuro, E.; Kato, Y.; Tamura, K.; Cynshi, O.; Kodama, T.; Niki, E. *Arch. Biochem. Biophys*. **1997**, *342*, 236. (e) Tamura, K.; Kato, Y.; Ishikawa, A.; Kato, Y.; Himoro, M.; Yoshida, M.; Takashima, Y.; Suzuki, T.; Kawabe, Y.; Cynshi, O.; Kodama, T.; Niki, E.; Shimizu, M. *J. Med. Chem.* **2003**, *46*, 3083. (f) Lucarini, M.; Pedrielli, P.; Pedulli, G. F.; Valgimigli, L.; Gigmes, D.; Tordo, P. *J. Am. Chem. Soc*. **1999**, *121*, 11546. (g) Hussain, H. H.; Babic G.; Durst, T.; Wright, J. S.; Flueraru, M.; Chichirau, A.; Chepelev, L. L. *J. Org. Chem.* **2003**, *68*, 7023.

136. (a) Wayner, D. D. M.; Lusztyk, E.; Ingold, K. U.; Mulder, P. *J. Org. Chem.* **1996**, *61*, 6430. (b) Lucarini, M.; Pedrielli, P.; Pedulli, G. F.; Cabiddu, S.; Fattuoni, C. *J. Org. Chem.* **1996**, *61*, 9263. (c) Brigati, G.; Lucarini, M.; Mugnaini, V.; Pedulli, G. F. *J. Org. Chem.* **2002**, *67*, 4828.

137. Wright, J. S.; Pratt, D. A.; DiLabio, G. A.; Bender, T. P.; Ingold, K. U. *Cancer Detect. Prev.* **1998**, *22*, 204.

138. Wijtmans, M.; Pratt, D. A.; Valgimigli, L.; DiLabio, G. A.; Pedulli, G. F.; Porter, N. A. *Angew. Chem. Int. Ed.* **2003**, *42*, 4370.

139. (a) Wijtmans, M.; Pratt, D. A.; Valgimigli, L.; DiLabio, G. A; Pedulli, G. F.; Porter, N. A. *Angew. Chem. Int. Ed.* **2003**, *42*, 4370. (b) Wijtmans, M.; Pratt, D. A.; Brikhorst, J.; Serwa, R.; Valgimigli, L.; Pedulli, G. F.; Porter, N. A. *J. Org. Chem.* **2004**, *69*, 9215.

140. (a) Nam, T.-G; Rector, C. L.; Kim, H.-Y; Sonnen, A. F.-P.; Meyer, R.; Nau, W. M.; Atkinson, J.; Rintoul, J.; Pratt, D. A.; Porter, N. A. *J. Am. Chem. Soc.* **2007**, *129*, 10211. (b) Serwa, R.; Nam, T.-G; Rector, C. L.; Valgimigli, L.; Culbertson, S.; Rector, C.; Jeong, B.-S.; Pratt, D. A.; Porter, N. A. *Chem. Eur. J.* **2010**, *16*, 14106–14114. (c) Lu, J.; Khdour, O. K.; Armstrong, J. S.; Hecht, S. M. *Bioorg. Med. Chem.* **2010**, *18*, 7628–7638. (d) Nam, T.-G; Ku, J.-M.; Park, H.-G; Porter, N. A.; Jeong, B.-S. *Org. Biomol. Chem.* **2011**, *9*, 1749–1755.

141. (a) Niki, E.; Kawakami, A.; Saito, M; Yamamoto, Y.; Tsutiya, J.; Kamiya, Y. *J. Biol. Chem.* **1985**, *260*, 2191. (b) Constantinides, P. P.; Tustian, A.; Kessler, D. R. *Adv. Drug Deliv. Rev.* **2004**, *56*, 1243.

142. Takita, T.; Umezawa, Y.; Saito, S.; Morishima, H.; Naganawa, H.; Umezawa, H.; Tsuchiya, T.; Miyatake, T.; Kageyama, S.; Umezawa, S.; Muraoka, Y.; Suzuki, M.; Otsuka, M.; Narita, M.; Kobayashi, S.; Ohno, M. *Tetrahedron Lett.* **1982**, *23*, 521.

143. Aoyagi, Y.; Katano, K.; Suguna, H; Primeau, J.; Chang, L.-H.; Hecht, S. M. *J. Am. Chem. Soc.* **1982**, *104*, 5537.

144. Merrifield, R. B. *J. Am. Chem. Soc.* **1963**, *85*, 2149.

145. (a) Norberg, T.; Lüning, B.; Tejbrant, J. *Methods Enzymol.* **1994**, *247*, 87. (b) Kihlberg, J.; Elofsson, M.; Salvador, L. A. *Methods Enzymol.* **1997**, *289*, 221.

146. Seeberger, P. H.; Hasse, W.-C. *Chem. Rev.* **2000**, *100*, 4349.

147. (a) Nefzi, A.; Ostresh, J. M.; Houghten, R. A. *Chem. Rev.* **1997**, *97*, 449. (b) Franzén, R. G. *J. Comb. Chem.* **2000**, *2*, 195.

148. Amblard, M.; Fehrentz, J.-A.; Martinez, J; Subra, G. *Peptide Synthesis and Applications*, Howl, J. Eds.; Humana Press: New Jersey, 2005.

149. (a) Kent, S. B. H. *Annu. Rev. Biochem.* **1988**, *57*, 957. (b) Barany, G.; Kneib-Cordnier, N.; Mullen, D. G.; Int. *J. Peptide Protein Res.* **1987**, *1987*, 705.

150. (a) Atherton, E.; Fox, H.; Harkiss, D.; Sheppard, R. C. *J. Chem. Soc., Chem. Commun.* **1987**, 539. (b) Carpino, L. A., Han, G. Y. *J. Org. Chem.* **1972**, *37*, 3404.

151. Leitheiser, C. J.; Rishel, M. J.; Wu, X.; Hecht, S. M. *Org. Lett.* **2000**, *2*, 3397.

152. (a) Smith, K. L.; Tao, Z.; Hashimoto, S.; Leitheiser, C.; Wu, X.; Hecht, S. M. *Org. Lett.* **2002**, *4*, 1079. (b) Tao, Z.-F.; Leitheiser, C. J.; Smith, K. L.; Hashimoto, S.; Hecht, S. M. *Bioconjugate Chem.* **2002**, *13*, 426. (c) Cagir, A. Tao, Z.-F.; Sucheck, S. J.; Hecht, S. M. *Bioorg. Med. Chem.* **2003**, *11*, 5179.

153. Yoshioka, T.; Hara, T.; Takita, T.; Umezawa, H. *J. Antibiot.* **1974**, *27*, 356.

154. Levin, M. D.; Subrahamanian, K.; Katz, H.; Smith, M. B.; Burlett, D. J.; Hecht, S. M. *J. Am. Chem. Soc.* **1980**, *102*, 1452.

155. Ohgi, T.; Hecht, S. M. *J. Org. Chem.* **1981**, *46*, 1232.

156. Narita, M.; Otsuka, M.; Kobayashi, S.; Ohno, M.; Umezawa, Y.; Morishima, H.; Saito, S. *Tetrahedron Lett.* **1982**, *23*, 525.

157. Dipardo, R. M.; Bock, M. G. *Tetrahedron Lett.* **1983**, *24*, 4805.

158. (a) Owa, T.; Haupt, A.; Otsuka, M.; Kobayashi, S.; Tomioka, N.; Itai, A.; Ohno, M.; Shiraki, T.; Uesugi, M.; Sugiura, Y.; Maeda, K. *Tetrahedron* **1992**, *48*, 1193. (b) Boger, D. L.; Menezes, R. F. *J. Org. Chem.* **1992**, *57*, 4331.

159. (a) Evans, D. A.; Bartroli, J.; Shih, T. L. *J. Am. Chem. Soc*. **1981**, *103*, 2127. (b) Evans, D. A.; Nelson, J. V.; Vogel, E.; Taber, T. R. *J. Am. Chem. Soc*. **1981**, *103*, 3099.

160. Nahm, S.; Weinreb, S. M. *Tetrahedron Lett.* **1981**, *22*, 3815.

161. Fehrentz, J.A.; Castro, B. *Synthesis* **1983**, 676.

162. Ager, D. J.; Babler, S.; Froen, D. E.; Laneman, S. A.; Pantaleone, D. P.; Prakan, I.; Zhi, B. *Org. Process Res. Dev*. **2003**, 7, 369.

163. Nishi, T.; Sakurai, M.; Sato, S.; Kataoka, M.; Morisawa, Y. *Chem. Pharm. Bull*. **1989**, 37, 2200.

164. Guerlavais, V.; Carroll, P. J.; Joullié, M. M. *Tetrahedron: Asymmetry* **2002**, *13*, 675.

165. Chhabra, S. R.; Khan, A. N.; Bycroft, B. W. *Tetrahedron Lett*. **1998**, *39*, 3585.

166. Chhabra, S. R.; Khan, A. N.; Bycroft, B. W. *Tetrahedron Lett*. **2000**, *41*, 1099.

167. O'Sullivan, M. C.; Zhou, Q.; Li, Z.; Durham, T. B.; Rattendi, D.; Lane, S.; Bacchi, C. J. *Bioorg. & Med. Chem.* **1997**, *5*, 2145.

168. Kaiser, E.; Colescott, R. L.; Bossinger, C. D.; Cook, P. J. *Anal. Biochem.* **1970**, *34*, 595.

169. Carpino, L. A. *J. Am. Chem. Soc.* **1993**, *115*, 4397.

170. Carpino, L. A.; El-Faham, A.; Minor, C. A.; Albericio, F. *J. Chem. Soc., Chem. Commun.* **1994**, 201.

171. Pearson, D. A.; Blanchette, M.; Baker, M. L.; Guindon, D. A. *Tetrahedron Lett.* **1989**, *30*, 2739.

172. Akiyama, Y.; Ma. Q.; Edgar, E.; Laikhter, A.; Hecht, S. M. *J. Am. Chem. Soc*. **2008**, *130*, 9650.

173. Giroux, R.; Hecht, S. M. *J. Am. Chem. Soc*. **2010**, *132*, 16987.

174. Abraham, A. T.; Zhou, X.; Hecht, S. M. *J. Am. Chem. Soc*. **2001**, *123*, 5167.

175. Henze, K.; Martin, W. *Nature* **2003**, *426*, 127.

176. McBride, H. M.; Neuspiel, M.; Wasiak, S.; *Curr. Biol.* **2006**, *16*, R551.

177. Gardner, A.; Boles, R. G. *Curr. Psychiatry Review* **2005**, *1*, 255.

178. Lesnefsky, E. J. *J. Mol. Cell. Cardiol.* **2001**, *33*, 1065.

179. Kirkinezos, I.; Moraes, C. T. *Semin. Cell Dev. Biol.* **2001**, *12*, 449.

180. Zhang, Y.; Marcillat, O.; Giulivi, C.; Ernster L.; Davies, D. J. A. *J. Biol. Chem.* **1990**, *265*, 16330.

181. Lu, J.; Cai, X.; Hecht, S. M. *Org. Lett.* **2010**, *12*, 5189–5191.

182. Murase, H.; Moon, J.-H; Yamauchi, R.; Kato, K.; Kunieda, T.; Yoshikawa, T.; Terao, J. *Free Radic. Biol. Med.* **1998**, *24*, 217.

183. Jotwani, P.; Singh, J.; Anand, N. *Ind. J. Chem.* **1988**, *27B*, 166.

184. (a) Duan, J.; Zhang, L. H.; Dolbier, W. J., Jr. *Synlett* **1999**, 1245; (b) Mal, P.; Lourderaj, U.; Venugopalan, P. P.; Moorthy, J. N.; Sathyamurthy, N. *J. Org. Chem.* **2003**, *68*, 3446.

185. Alam, A.; Takaguchi, Y.; Ito, H.; Yoshida, T.; Tsuboi, A. *Tetrahedron*, **2005**, *6*, 1909.

186. Anderson, K. W.; Ikawa, T.; Tundel, R. E.; Buchwald, S. L. *J. Am. Chem. Soc.*, **2006**, *128*, 10694.

187. (a) Yang, J. S.; Liau, K. L.; Li, C. Y.; Chen, M. Y. *J. Am. Chem. Soc.* **2007**, *129*, 13183. (b) Papageorgiou G.; Corrie, J. E. T. *Tetrahedron*, **2007**, *63*, 9668. (c) Zhang, Q.; Peng, Y.; Wang, X. I.; Keenan, S. M.; Arora, S.; Welsh, W. J. *J. Med. Chem.* **2007**, *50*, 749.

188. (a) Pap, E. H. W.; Drummen, G. P.; Winter, V. J.; Kooij, T. W. A.; Rijken, P. J.; Wirtz, K. W. A.; Op den Kamp, J. A.; Hage, W. J.; Post, J. A. *FEBS lett.* **1999**, *453*, 278. (b) Drummen, G. P.; van Liebergen, L. C.; Op den Kamp, J. A.; Post, J. A. *Free Rad. Biol. Med.* **2002**, *33*, 473.

189. Miccadei, S.; Kyle, M. E.; Gilfor, D.; Farber, J. L. *Arch. Biochem. Biophys.* **1988**, *265*, 311.

190. (a) Tirmenstein, M. A.; Nichlls-Grzemski, F. A.; Zhang, J. G.; Fariss, M. W. *Chem.-Biol. Interact.* **2000**, *127*, 201. (b) Armstrong, J. S.; Whiteman, M.; Rose, P.; Jones, D. P. *J. Biol. Chem.* **2003**, *278*, 49079.

191. Hayes, J. D.; McLellan, L. *Free Radical Res.* **1999**, *31*, 273.

192. Arce, P. M.; Khdour, O. M.; Goldschmidt, R.; Armstrong, J. S.; Hecht, S. M. *ACS Med. Chem. Lett.* **2011**, *ASAP*.

193. Gao, Y.; Zhang, Q.; Xu, J. *Synth. Commun.* **2004**, *34*, 909.

194. McBride, L. J.; Kierzek, R.; Beaucage, S. L.; Caruthers, M. H. *J. Am. Chem. Soc.* **1986**, *108*, 2040.